Identification of novel cytosolic binding partners of the neural cell adhesion molecule NCAM and functional analysis of these interactions

DISSERTATION

zur

Erlangung des Doktorgrades (Dr. rer. nat.)

der

Mathematisch-Naturwissenschaftlichen Fakultät

der

Rheinischen Friedrich-Wilhelms-Universität Bonn

vorgelegt von

HILKE JOHANNA WOBST

aus

Leer

Bonn, August 2014

Angefertigt mit Genehmigung der Mathematisch-Naturwissenschaftlichen Fakultät

der Rheinischen Friedrich-Wilhelms-Universität Bonn

1. Gutachter: Frau Prof. Dr. Brigitte Schmitz (em.)

2. Gutachter: Herr Prof. Dr. Jörg Höhfeld

Tag der Promotion: 14.11.2014

Erscheinungsjahr: 2014

Aus dieser Dissertation hervorgegangene Veröffentlichungen

Artikel in Fachzeitschriften

Homrich M[1], Wobst H[1], Laurini C, Sabrowski J, Schmitz B, Diestel S (2014): Cytoplasmic domain of NCAM140 interacts with ubiquitin-fold modifier-conjugating enzyme-1 (Ufc1). Exp Cell Res 324 (2), 192-199.
([1]: geteilte Erstautorenschaft)

Wobst H, Förster S, Laurini C, Sekulla A, Dreiseidler M, Höhfeld J, Schmitz B, Diestel S (2012): UCHL1 regulates ubiquitination and recycling of the neural cell adhesion molecule NCAM. The FEBS Journal 279 (23), 4398-4409.

Poster

Wobst H, Sekulla A, Laurini C, Schmitz B, Diestel S (2011): Protein macroarray: A new approach to identify cytosolic NCAM binding partners. 9. Meeting der Neurowissenschaftlichen Gesellschaft Deutschland, Göttingen, Deutschland.

Wobst H, Faraidun H, Sekulla A, Dreiseidler M, Höhfeld J, Schmitz B, Diestel S (2012): UCHL1 regulates ubiquitination and recycling of the neural cell adhesion molecule NCAM. 63. Mosbacher Kolloquium, Mosbach, Deutschland.

Eingeladene Vorträge

Wobst H, Leshchyns'ka I, Schmitz B, Diestel S, Sytnyk V (2013): The neural cell adhesion molecule (NCAM): molecular mechanism of its transport to the cell surface during neuronal differentiation. 2nd Cell Architecture in Development and Disease Symposium, Lowy Research Center, UNSW, Sydney, Australien.

Abstract

The neural cell adhesion molecule (NCAM) plays an important role during brain development and in adult brain. NCAM functions through interactions with several proteins leading to intracellular signal transduction pathways ultimately causing cellular proliferation, differentiation, migration, survival, and neuritogenesis. This thesis aimed for the identification of novel, yet unknown intracellular interaction partners of NCAM to further understand the mechanisms underlying NCAM's role in the brain.

Purified intracellular domains of human NCAM180 or NCAM140 were applied onto a protein macroarray containing 24000 expression clones of human fetal brain. Using this approach, several novel potential interaction partners were detected, including ubiquitin carboxyl-terminal hydrolase isozyme L1, ubiquitin-fold modifier-conjugating enzyme 1, and kinesin light chain 1 (KLC1). KLC1 is part of kinesin-1, a motor protein that transports cargoes towards the plus end of microtubules in axons and dendrites. As the transport mechanism of NCAM in neurons is still unknown, the potential role of kinesin-1 in NCAM trafficking was specifically interesting and analyzed in detail herein.

The interaction of NCAM and KLC1 was verified in mouse brain tissue by co-immunoprecipitation. Co-localization studies in Chinese Hamster Ovary (CHO) cells overexpressing NCAM and kinesin-1 and in primary hippocampal neurons revealed an overlap of NCAM with subunits of kinesin-1.

Functional studies showed that significantly more NCAM was delivered to the cell surface in NCAM and kinesin-1 overexpressing CHO cells. This effect was inhibited by excess of free full-length intracellular domain of NCAM as well as by several shorter peptides thereof. This showed that the intracellular domain of NCAM is required for the transport of NCAM to the cell surface. Further studies were carried out in primary cortical neurons. Whereas the kinesin-1 dependent transport of NCAM seemed to be mediated constitutively in CHO cells, the amount of cell surface NCAM significantly increased only after antibody-stimulated NCAM endocytosis in primary cortical neurons. In agreement, co-localization of internalized NCAM and KLC1 was observed in these neurons.

Finally, an 8 amino acid sequence within the intracellular domain of NCAM was identified in an ELISA to be sufficient to directly interact with KLC1. The KLC1-binding region within NCAM overlaps with the domain responsible for binding to p21-activated kinase 1 (PAK1) which was shown to compete with KLC1 for binding to NCAM in a pull-down assay. This competition may provide a regulatory mechanism for the interaction between NCAM and

KLC1 and could potentially be involved in the detachment of NCAM from KLC1 after delivery to the cell surface.

Knowledge of the exact transport mechanism of NCAM will contribute to an advanced understanding of the underlying mechanisms of its functions during brain development and in adult brain.

Table of content

Table of content I

List of figures IV

List of tables V

List of abbreviations VI

List of units IX

1. Introduction 1

1.1. Cell adhesion molecules 1

1.1.1. NCAM isoforms 3
1.1.2. Posttranslational modifications of NCAM 5
1.1.3. NCAM expression 6
1.1.4. NCAM functions 7
1.1.5. NCAM interactions 8
1.1.5.1. Homophilic interactions 8
1.1.5.2. Heterophilic extracellular interactions 8
1.1.5.3. Heterophilic intracellular interactions 9
1.1.6. Trafficking of NCAM 11

1.2. Motor proteins and the intracellular transport 12

1.2.1. Myosins, dyneins, and kinesins 12
1.2.2. Kinesin-1 13

1.3. Aim of the thesis 14

2. Material 15

2.1. Commercial chemicals 15

2.2. Equipment 17

2.3. Working materials 18

2.4. Kits and standards 18

2.5. Antibodies and peptides 19

2.6. Bacterial strains, cell lines, and primary neurons 21

2.7. Plasmids 21

2.8. Enzymes 23

2.9. Solutions, media, and buffers 23

2.9.1. General buffers 23
2.9.2. Buffers and solutions for bacterial culture 23
2.9.3. Buffers and solutions for cell culture 24
2.9.4. Buffers for molecular biology (DNA-analysis) 24
2.9.5. Buffers and solutions for protein biochemistry 24
2.9.5.1. Buffers and solutions for recombinant protein expression and purification 24
2.9.5.2. Buffers and solutions for the protein macroarray 25
2.9.5.3. Solutions for SDS-polyacrylamide gel electrophoresis (SDS-PAGE) 25
2.9.5.4. Solutions for silver and Coomassie Blue staining of polyacrylamide gels 25
2.9.5.5. Solutions for Western blotting and immunological detection of proteins 26

2.9.5.6. Solutions for co-immunoprecipitation (co-IP) 26
2.9.5.7. Solutions for preparation of the cytosolic fraction of mouse brain tissue and *trans*-Golgi network (TGN) isolation 26
2.9.5.8. Buffers and solutions for enzyme linked immunosorbent assay (ELISA) 26

3. Methods 27

3.1. Molecular biology 27
3.1.1. Heat shock transformation 27
3.1.2. Plasmid isolation from *E. coli* cultures 27
3.1.3. Agarose gel electrophoresis 27
3.1.4. Restriction analysis and purification of cDNA 28
3.1.5. Photometric nucleic acid determination 28
3.1.6. Ligation 28

3.2. Protein-biochemical methods 28
3.2.1. Expression of recombinant proteins in *E. coli* 28
3.2.2. Lysis of bacteria 29
3.2.3. Recombinant protein purification 29
3.2.3.1. Purification of His-tagged hNCAM180ID by Ni-NTA affinity chromatography 29
3.2.3.2. Purification of GST-tagged hNCAM140ID by glutathione affinity chromatography 30
3.2.4. Concentration and fluorescent labeling of hNCAM180ID and hNCAM140ID 30
3.2.5. Protein macroarray 31
3.2.6. Determination of protein concentrations 31
3.2.7. SDS-PAGE 32
3.2.8. Silver staining of polyacrylamide gels 33
3.2.9. Coomassie staining of polyacrylamide gels 33
3.2.10. Western Blot (semi-dry) 33
3.2.11. Immunological detection of proteins on nitrocellulose or PVDF membranes 33
3.2.12. Removal of antibodies for re-probing of Western blots (stripping) 34
3.2.13. Co-IP 34
3.2.14. Isolation of TGN organelles 35
3.2.15. Preparation of the cytosolic fraction of mouse brain tissue 35
3.2.16. ELISA 35
3.2.17. Pull-down assay 36

3.3. Cell culture and immunofluorescence 36
3.3.1. PDL coating of glass coverslips for cell culture 36
3.3.2. CHO cells 37
3.3.2.1. Cell culture of CHO cells 37
3.3.2.2. Transfection of CHO cells 37
3.3.2.3. Immunofluorescence labeling of CHO cells 37
3.3.3. Primary neurons 38
3.3.3.1. Cultures of hippocampal and cortical neurons 38
3.3.3.2. Immunofluorescence labeling of endogenous proteins of cultured hippocampal neurons 38
3.3.3.3. Transfection and immunofluorescence labeling of cultured cortical neurons 38
3.3.4. Immunofluorescence acquisition and quantification 39
3.3.5. Statistical analyzes of immunofluorescence experiments 39

4. Results 40

4.1. Identification of potential interaction partners of hNCAM180ID and hNCAM140ID by protein macroarray 40
4.1.1. Expression and purification of hNCAM180ID 40
4.1.2. Expression and purification of hNCAM140ID 41

4.1.3. Detection and identification of potential interaction partners of hNCAM180ID and hNCAM140ID by protein macroarray 44

4.2. Verification of the interaction of NCAM and KLC1 46

4.2.1. Investigation of the interaction of NCAM and KLC1 47

4.2.1.1. Co-IP of NCAM and KLC1 from mouse brain lysate 47

4.2.1.2. Co-localization of intracellular NCAM and kinesin-1 in CHO cells 47

4.2.1.3. Co-localization of endogenous NCAM and KLC1 or KIF5A in primary hippocampal neurons 48

4.2.2. Investigation of the presence of NCAM and kinesin-1 in TGN organelles 50

4.2.2.1. Detection of NCAM, KLC1, and KIF5A in mouse brain TGN organelles by Western blot 51

4.2.2.2. Detection of co-localization of NCAM and KIF5A in TGN organelles in primary hippocampal neurons 52

4.2.3. Functional studies 53

4.2.3.1. Influence of kinesin-1 on the delivery of NCAM to the cell surface in CHO cells 53

4.2.3.2. Influence of kinesin-1 on the delivery of NCAMΔCT to the cell surface in CHO cells 55

4.2.3.3. Influence of peptides derived from NCAM-ID on the kinesin-1 dependent delivery of NCAM to the cell surface in CHO cells 57

4.2.3.4. Investigation of the functional role of kinesin-1 in the delivery of NCAM to the cell surface in primary cortical neurons 59

4.2.4. Localization of the KLC1-binding site within the NCAM-sequence and investigation of potential competition partners 61

4.2.4.1. Identification of the KLC1-binding site within NCAM by ELISA 62

4.2.4.2. Investigation of a potential competition between KLC1 and PAK1 for binding to NCAM by pull-down assay 63

5. Discussion 65

5.1. Identification of potential interaction partners by protein macroarray 65

5.1.1. Evaluation of the reliability of the protein macroarray results based on the quality of hNCAM180ID and hNCAM140ID probes 65

5.1.2. Interpretation of the protein macroarray results 66

5.2. Investigation of the interaction of NCAM and KLC1 67

5.2.1. Confirmation of the interaction of NCAM and KLC1 by co-IP 67

5.2.2. Interaction domains of NCAM and KLC1 67

5.2.3. Co-localization studies in CHO cells and primary neurons 69

5.2.4. Investigation of the presence of NCAM and kinesin-1 in TGN organelles 70

5.3. Functional studies in CHO cells and primary cortical neurons 71

5.4. Potential transport mechanisms of NCAM by kinesin-1 72

5.4.1. Kinesin-1 may influence the transport of newly synthesized and endocytosed NCAM 72

5.4.2. How could kinesin-1 increase the amount of cell surface NCAM? 76

5.4.3. Potential regulatory mechanisms mediating detachment of NCAM from kinesin-1 79

5.5. Conclusion and future studies 80

6. Summary 82

References 84

Appendix 96

List of figures

Fig. 1: The three main isoforms of NCAM 4
Fig. 2: Heterophilic interactions and posttranslational modifications of NCAM 11
Fig. 3: Schematic model of kinesin-1 and kinesin light chain 1 13
Fig. 4: Analysis of the purification fractions and the concentrate of hNCAM180ID 41
Fig. 5: Analysis of the purification fractions and the concentrate of hNCAM140ID 43
Fig. 6: Co-IP of KLC1 and NCAM from mouse brain lysate 47
Fig. 7: Immunofluorescence analysis of a CHO cell overexpressing NCAM and GFP-KLC1/KHC1 48
Fig. 8: Immunofluorescence analysis of a hippocampal neuron co-labeled with antibodies against NCAM and KLC1 or KIF5A 50
Fig. 9: Western blot analysis of brain homogenate (BH), soluble proteins (cytosol), *trans*-Golgi network (TGN) organelles, and Golgi membranes for NCAM, KIF5A, KLC1, and TGN38 51
Fig. 10: Immunofluorescence analysis of a hippocampal neuron co-labeled with antibodies against NCAM, KIF5A, and γ-adaptin 53
Fig. 11: Functional analysis of the influence of kinesin-1 on the delivery of NCAM to the cell surface in CHO cells 55
Fig. 12: Functional analysis of the influence of kinesin-1 on the delivery of NCAMΔCT to the cell surface in CHO cells 56
Fig. 13: Functional analysis of the influence of peptides derived from NCAM-ID on the kinesin-1 dependent delivery of NCAM to the cell surface in CHO cells 59
Fig. 14: Functional analysis of the influence of KLC1 or kinesin-1 on the delivery of NCAM and NCAMΔCT to the cell surface in primary cortical neurons 60
Fig. 15: Immunofluorescence analysis of cortical neurons overexpressing NCAM and KLC1 and detection of internalized and surface NCAM after NCAM-triggering 61
Fig. 16: Identification of the KLC1-binding site within NCAM by ELISA 62
Fig. 17: Investigation of a potential competition between KLC1 and PAK1 for binding to NCAM by pull-down assay 64
Fig. 18: Schematic model illustrating potential transport mechanisms of NCAM by kinesin-1 74
Fig. 19: Schematic model of a hypothesized transport mechanism of NCAM by kinesin-1 after NCAM endocytosis 77

List of tables

Tab. 1: Commercial chemicals 15
Tab. 2: Equipment 17
Tab. 3: Working materials 18
Tab. 4: Kits and standards 18
Tab. 5: Antibodies and peptides 19
Tab. 6: Bacterial strains, cell lines, and primary neurons 21
Tab. 7: Plasmids 21
Tab. 8: Enzymes 23
Tab. 9: Protease inhibitors for bacterial culture 25
Tab. 10: Composition of self-prepared gels for SDS-PAGE 32
Tab. 11: List of selected potential (upper part of the table) and already known (lower part) interaction partners of hNCAM180ID and hNCAM140ID identified in the protein macroarray 45
Tab. 12: Absorbance values of ELISA experiments investigating the KLC1-binding site within NCAM 63

List of abbreviations

ACEC	Animal Care and Ethics Committee
ANOVA	Analysis of variance
AP-2	Adaptor protein complex-2
ApoER2	Apolipoprotein E receptor 2
APP	Amyloid-ß precursor protein
APS	Ammonium persulfate
ATCC	American Type Culture Collection
ATP	Adenosine triphosphate
BDNF	Brain-derived neurotrophic factor
bFGF	Basic fibroblast growth factor
BH	Brain homogenate
Bis	Bis(2-hydroxyethyl)amino
BLAST	Basic Local Alignment Search Tool
BSA	Bovine serum albumin
CAMKII	Calcium-calmodulin-dependent protein kinase II
CAMs	Cell adhesion molecules
Caytaxin	Cayman ataxia protein
CHL1	Close homologue of L1
CHO	Chinese Hamster Ovary
Co-IP	Co-immunoprecipitation
CRMP-2	Collapsin response mediator protein-2
CSPGs	Chondroitin sulfate proteoglycans
CT	Cytoplasmic tail
C-terminus/-terminal	Carboxy-terminus/-terminal
CV	Column bed volumes
CY	CyDye
DIV	Day(s) *in vitro*
DMEM	Dulbecco`s modified Eagles`s medium
DMSO	Dimethylsulfoxide
DTT	Dithiothreitol
E	Elution fraction
E. coli	*Escherichia coli*
e.g.	*exempli gratia,* for example
e-cadherin	Epithelial cadherin
ECM	Extracellular matrix
ED	Extracellular domain
EDTA	Ethylenediaminetetraacetic acid
EGF	Epidermal growth factor
EGTA	Ethyleneglycoltetraacetic acid
ELISA	Enzyme linked immunosorbent assay
E-P-selectin	Selectins expressed by vascular endothelium
ER	Endoplasmatic reticulum
et al.	*et alii/aliae*, and others
FAK	Focal adhesion kinase
FBS	Fetal bovine serum
FGFR1	Fibroblast growth factor receptor 1
Fig.	Figure
FNIII	Fibronectin type III domain
FT	Flow-through
Fyn	Src-related nonreceptor tyrosine kinase $p59^{fyn}$
Gadkin	Gamma-A1-adaptin and kinesin interactor
GAP-43	Growth associated protein-43
GDNF	Glial cell line-derived neurotrophic factor
GFP	Green fluorescent protein

GFRα	GDNF family receptor α
GPI	Glycosylphosphatidylinositol
GSH	Glutathione
GST	Glutathione-S-transferase
His	Histidine
hNCAM	Human NCAM
hNCAMΔCT	Human NCAM with deleted intracellular domain
hNCAM140ID	Intracellular domain of human NCAM isoform 140
hNCAM180	Human NCAM isoform 180
hNCAM180ID	Intracellular domain of human NCAM isoform 180
hNCAM-ED	Extracellular domain of human NCAM
hNCAM-ID	Intracellular domain of human NCAM
HNK-1	Human natural killer antigen 1
HOMO buffer	Homogenisation buffer
HSPGs	Heparin sulfate proteoglycans
Id.	Identity
ID	Intracellular domain
i.e.	*id est*, that is
IF	Immunfluorescence
Ig	Immunoglobulin
IgCAMs	Immunoglobulin-like cell adhesion molecules
IgG	Immunoglobulin subclass G
IgSF	Immunoglobulin superfamily
IP	Immunoprecipitate
IPTG	Isopropyl β-D-1-thiogalactopyranoside
JIPs	C-Jun N-terminal kinase (JNK)-interacting proteins
KHC	Kinesin heavy chain
Kidins220/ARMS	Kinase D-interacting substrate of 220 kDa/ankyrin repeat-rich membrane spanning
KLC	Kinesin light chain
LANP	Leucine-rich acidic nuclear protein
LB	Luria Bertani medium
L-selectin	Selectins expressed by leukocytes
LSM	Laser scanning microscope
MAP	Mitogen-activated protein
MAP1A	Microtubule associated protein 1A
MCAK	Mitotic centromere-associated kinesin
MOPS	2-(N-Morpholino)-Propansulfonsäure
MSD1	Muscle specific domains 1
n-cadherin	Neural cadherin
NCAM	Neural cell adhesion molecule
NCAM-ID	Intracellular domain of NCAM
NF-κB	Nuclear factor-kappaB
NgCAM	Neuron-glia cell adhesion molecule
Ni-NTA	Nickel-nitrilotriacetic acid
N-terminus/-terminal	Amine-terminus/-terminal
OD	Optical density
OPD	O-phenylenediamine dihydrochloride
P	Pellet
PAK1	P21-activated kinase 1
PBS	Phosphate buffered saline
PBS-EW	Equilibration and wash buffer
PBST	Phosphate buffered saline with Tween
PCR	Polymerase chain reaction
PDGF	Platelet-derived growth factor
PDL	Poly-D-lysine

PFA	Paraformaldehyde
PIPES	Piperazine-1,4-bis(2-ethanesulfonic acid)
PKCβ	Protein kinase C β
PLCγ	Phospholipase C-γ-1
PMSF	Phenylmethanesulfonyl fluoride
POD	Peroxidase
PP1 / PP2A	Serine/threonine-protein phosphatase 1/2 A
PrP^c	Cellular prion protein
PSA	Polysialic acid
P-selectin	Selectins expressed by platelets
PVDF	Polyvinylidene difluoride
r	Pearson's correlation coefficient
Rab	Rat sarcoma (Ras)-related proteins in brain
ROK-α	RhoA-binding kinase- α
RPTPα	Receptor protein tyrosine phosphatase α
RT	Room temperature
RV	Rabies virus
SD	Standard deviation
SDS	Sodium dodecyl sulfate
SDS-PAGE	SDS-polyacrylamide gel electrophoresis
SEC	Secreted exon
SEM	Standard error of the mean
SKIP	SifA and kinesin-interacting protein
ST8SiaII	Sialyltransferase 8 sia II
ST8SiaIV	Sialyltransferase 8 sia IV
Tab.	Table
TAG-1	Transient axonal glycoprotein-1
TBS	Tris buffered saline
TBST	Tris buffered saline with Tween
TEMED	N,N,N‘,N‘,-Tetramethylethylendiamine
TGN	*Trans*-Golgi network
TNGT	Elution buffer
TOAD-64	Turned on after division-64
TPR	Tetratricopeptide repeat
Tris	Tris(hydoxymethyl)methylaminelamine
Triton X-100	Tolyethylene glycol p-(1,1,3,3-tetramethylbutyl)-phenyl ether
Tween® 20	Polyoxyethylene (20) sorbitan monolaurate
Uba5	Ubiquitin-activating enzyme 5
UCHL1	Ubiquitin C-terminal hydrolase isozyme 1
Ufc1	Ubiquitin-fold modifier-conjugating enzyme 1
Ufm1	Ubiquitin-fold modifier 1
UV	Ultraviolet
v/v	Volume per volume
VASE	Variable alternative-spliced exon
ve-cadherin	Vascular endothelial cadherin
W	Washing fraction
w/v	Weight per volume
WB	Western Blot
wt	Wild type

List of units

°C	Degree Celsius
µ	Micro (10^{-6})
µg	Microgram
µl	Mircoliter
µm	Micrometer
µM	Micromolar
cm^2	Square centimeter
g	Gram
h	Hour(s)
kb	Kilo base pairs
kDa	Kilodalton
l	Liter
m	Milli (10^{-3})
M	Concentration of solution in mol/l
mA	Milliampere
mg	Milligram
min	Minute(s)
ml	Milliliter
mM	Millimolar
mm	Millimeter
n	Nano (10^{-9})
ng	Nanogram
nm	Nanometer
rpm	Rotations per minute
sec	Second(s)
U	Enzyme units
V	Volt
x g	Standard gravity as unit for acceleration

1. Introduction

1.1. Cell adhesion molecules

Cell adhesion is crucial for the development and maintenance of tissue structures and multicellular organs. In mammals, several families of cell adhesion molecules (CAMs), which are typically transmembrane glycoproteins, mediate interactions on the cellular surface or between two opposing surfaces (Gumbiner, 1996). They are involved in cell-cell adhesion to ensure adequate communication and also the binding between cells and extracellular matrix (ECM) proteins. Furthermore, CAMs are known to trigger intracellular events and to be involved in cellular processes, such as migration, differentiation, proliferation, and cell death (Rojas & Ahmed, 1999). Especially in the nervous system, CAMs play a pivotal role in development, maturation, and regeneration. They have been shown to be involved in migration and differentiation of neurons, neurite outgrowth, axon fasciculation, regulation of synaptogenesis, synapse plasticity, and activation of signaling pathways (Cavallaro & Dejana, 2011; Togashi *et al.*, 2009; Hansen *et al.*, 2008; Walsh & Doherty, 1997). Therefore, CAMs "*not only maintain tissue integrity but also may serve as biosensors that modulate cell behavior in response to the surrounding microenvironment*" (Cavallaro & Dejana, 2011). Four major classes of CAMs have been identified: cadherins, selectins, integrins, and the immunoglobulin (Ig)-like superfamily.

Cadherins are single-pass transmembrane proteins that facilitate cell-cell recognition and adhesion by mostly homophilic *cis*- and *trans*-interactions in a Ca^{2+}-dependent manner. Nowadays, at least 80 mammalian members of the cadherin superfamily are known. The superfamily includes classic cadherins, which were the first to be identified, and non-classic cadherins, such as desmogleins, desmocollins, and protocadherins (Cavallaro & Dejana, 2011). Classic cadherins are named according to their major expression in specific tissues, for example, e-cadherin (epithelial cadherin in epithelial cells), n-cadherin (neural cadherin in the nervous system), and ve-cadherin (vascular endothelial cadherin in the endothelia). All cadherins contain at least two extracellular domains (ED) for cell-cell interactions and moreover, classic cadherins contain a highly conserved intracellular domain (ID). With the ID they are able to interact with a group of defined cytoplasmatic proteins, the catenins (Harris & Tepass, 2010). Catenins coordinate the cadherin-mediated adherens junction dynamics and signaling. Beneath the functions in cell adhesion, morphogenesis, cytoskeletal organization, and cell migration, cadherin dysfunctions have been implicated in pathological processes such as cancer (Cavallaro & Dejana, 2011; Jeanes *et al.*, 2008; Wheelock & Johnson, 2003; Angst *et al.*, 2001).

The **selectin** family includes three closely related cell-surface molecules, which are expressed by leukocytes (L-selectin), platelets (P-selectin), and vascular endothelium (E- and P-selectin). Selectins are composed of a characteristic ED that contains an amino-terminal lectin domain, an epidermal growth factor (EGF)-like domain, two to nine short consensus repeat units, and further a transmembrane domain, and a short ID (Kansas, 1996). Interestingly, selectin function is uniquely restricted to the vascular system, in contrast to most other CAMs, which function in a broad variety of tissues throughout the body (Tedder *et al*., 1995). The lectin-domain binds partly Ca^{2+}-dependent fucosylated and sialylated glycoprotein ligands on other cells and mediates adhesion of leucocytes and platelets to vascular surfaces. Thereby, selectins are involved in constitutive lymphocyte homing, and in chronic and acute inflammation processes. Lack of selectins or selectin-ligands leads to recurrent bacterial infections and persistent diseases (Ley, 2003; McEver, 2002).

Integrins are a superfamily of transmembrane αβ-heterodimers that are expressed in a wide range of cells, whereupon most cells express several integrins. In humans, 18 α- and 8 β-subunits are known, generating so far 24 known heterodimers. This diversity widens the variety of extracellular matrix ligands, cell-surface and soluble ligands, which bind to integrins (Takada *et al.* 2007; Hynes, 1992). Through binding to extracellular ligands (fibronectin, vitronectin, collagen, and laminin) as well as to cytoskeletal components (actin microfilaments) and intracellular signaling molecules, integrins serve as a linker between the extracellular and intracellular environments. Ligand binding leads to signal transmission into the cell (outside-in signaling) and, conversely, the extracellular ligand binding affinity is regulated by intracellular signals (inside-out signaling; Luo *et al.*, 2007; Takada *et al.*, 2007). The binding of extracellular ligands triggers a large set of signal transduction pathways that modulate cell behaviors such as adhesion, proliferation, survival or apoptosis, morphology, polarity, motility, and differentiation, mostly through effects on the cytoskeleton (Luo *et al.*, 2007; Takada *et al.*, 2007; Hynes, 1992).

The **Ig-like** cell adhesion molecules constitute the Ig superfamily (IgSF), which is one of the largest families of related proteins in vertebrates. In humans, approximately 765 members of the IgSF are known (Brümmendorf & Lemmon, 2001). Their common structural and name giving attribute are one or more extracellular Ig-like domains, which are characterized by two cysteines separated by 55 to 75 amino acids (Springer, 1990; Williams & Barclay, 1988). The Ig-like domains are composed of 70-110 amino acids arranged in a sandwich of two sheets of anti-parallel β-strands, which are usually stabilized by at least one disulfide bond at its centre. Most of the proteins of the IgSF are glycosylated transmembrane proteins with short IDs. Additionally, Ig-like cell adhesion molecules (IgCAMs) often contain at least one

fibronectin type III domain (FNIII) and may contain other extracellular modules (Walmod *et al.* 2007; Springer, 1990). IgCAMs mediate cell-cell and cell-ECM interactions through homophilic and heterophilic binding to a variety of ligands in a Ca^{2+}-independent manner (Williams & Barclay, 1988). Thus, they are not only responsible for cell adhesion, but can also affect intracellular signaling. IgCAMS have a crucial role in immune and inflammatory responses, embryonic development, and the development and maintenance of the nervous system (Barclay, 2003; Rougon & Hobert, 2003; Springer, 1990). In the brain, IgCAMs have been implicated as key players in axonal growth and guidance (Tessier-Lavigne & Goodman, 1996). The first IgCAM to be characterized in the brain was the neural cell adhesion molecule NCAM (Jørgensen & Bock, 1974).

1.1.1. NCAM isoforms

NCAM was the first adhesion molecule that was shown to be able to mediate adhesion of cells in the retina of chicken embryos (Thiery *et al.*, 1977; Rutishauser *et al.*, 1976). Three main isoforms of human NCAM exist, which are named after their apparent molecular weight: NCAM180, NCAM140, and NCAM120. NCAM180 and NCAM140 are transmembrane isoforms with IDs of different length, whereas NCAM120 is anchored to the membrane by glycosylphosphatidylinositol (GPI; Fig. 1).

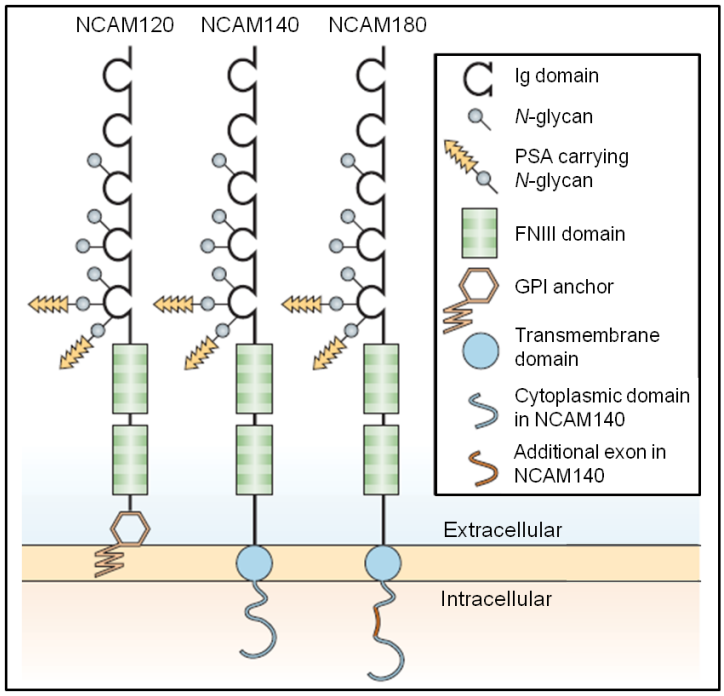

Fig. 1: The three main isoforms of NCAM

The extracellular domains of the three main isoforms of NCAM consist of five Ig-like domains and two FNIII domains. The Ig-like domains contain six *N*-glycosylation sites; two of them in the IgV domain may be modified with polysialic acid (PSA). NCAM120 is anchored to the membrane by glycosylphosphatidylinositol (GPI). The transmembrane isoforms NCAM140 and NCAM180 differ in 261 additional amino acids in the ID of NCAM180 resulting from alternatively splicing of exon 18 (modified after Kleene & Schachner, 2004).

The isoforms result from alternative splicing of the transcript of a single gene (Owens *et al.*, 1987), which is located on chromosome 11 in humans and is composed of 26 exons distributed over approximately 85 kb (Colwell *et al.*, 1992). Exons 0-14 code for the five extracellular Ig-like domains (IgI-V) and for the FNIII-modules. Exon 15 contains a stop codon, resulting in the GPI-anchored isoform NCAM120 (Cunningham *et al.*, 1987). Exon 16 encodes the transmembrane segment, and exons 17-19 encode the cytoplasmic part of the molecule. Exon 18 is specific for NCAM180, leading to an insert of 261 amino acids. Apart from the main isoforms, many more isoforms exist because of exclusion or inclusion of six small exons into the original transcript. The variable alternative-spliced exon (VASE) is located between exon 7 and 8 and leads to insertion of ten additional amino acids within the fourth Ig-like domain. This short sequence is known to have an inhibitory effect on neurite outgrowth (Lahrtz *et al.*, 1997; Liu *et al.*, 1993; Doherty *et al.*, 1992; Walsh *et al.*, 1992) and furthermore has been predicted to be related to psychiatric disorders as shown also for the secreted exon (SEC; Vawter *et al.*, 2000, 1999). SEC is positioned between exon 12 and 13 and contains a stop codon, leading to a truncated ED of NCAM, which is secreted into the extracellular space (Gower *et al.*, 1988; Bock *et al.*, 1987). The further known exons are the three muscle specific domains 1 (MSD1a-c) and the so-called AAG, which are only inserted

in cell types other than neurons and are likely to have modulatory effects, for example on the interactions with extracellular binding partners of NCAM (Soroka *et al.*, 2010; Kiselyov et at., 2005; Kasper *et al.*, 1996).

1.1.2. Posttranslational modifications of NCAM

The variety of NCAM is not only given by the isoforms, but also by posttranslational modifications. In total, NCAM contains six *N*-glycosylation sites (see Fig. 1; Albach *et al.*, 2004), whose glycosylation pattern is spatially and temporally regulated (Sasaki & Endo, 1999; Schwarting *et al.*, 1987).

NCAM is unique among adhesion molecules in being glycosylated with polysialic acid (PSA; Finne *et al.*, 1983; Hoffman *et al.*, 1982). PSA is a large homopolymer of negatively charged α-2,8-linked sialic acid molecules that can be attached to two *N*-glycosylation sites in the IgV-domain of NCAM by two polysialyltransferases named sialyltransferase 8 sia IV (ST8SiaIV) and sialyltransferase 8 sia II (ST8SiaII; Angata *et al.*, 1998; Kojima *et al.*, 1996; Mühlenhoff *et al.*, 1996; Nelson *et al.*, 1995). PSA-NCAM expression is most prominent during embryogenesis in growing axons and migrating cells with up to 30 % of the mass of NCAM being attributed to PSA. It is progressively reduced as the brain develops (Chuong & Edelman, 1984). However, in adult brain, it remains expressed in regions where PSA-NCAM is known to be involved in synaptic plasticity and generation of neurons, such as the adult dentate gyrus of the hippocampus (Bonfanti *et al.*, 1992), the olfactory bulb (Rousselot *et al.*, 1995; Bonfanti *et al.*, 1992), and the hypothalamo-neurohypophyseal system (Theodosis *et al.*, 1991). The presence of PSA on NCAM has been shown to decrease NCAM-dependent cell adhesion. PSA-chains build a large negatively charged hydration shell around NCAM, which affects homophilic *trans*-binding (binding between NCAM molecules expressed on neighboring cells) as well as *cis*-binding, *i.e.* the binding between NCAM molecules or between NCAM and other molecules on the same cell surface leading to the inhibition of homophilic clustering within the plane of a membrane, or inhibition of heterophilic interactions (Storms & Rutishauser, 1998; Hoffman & Edelman; 1983; Sadoul *et al.*, 1983). On the other hand, NCAM without PSA significantly inhibits NCAM-mediated neurite outgrowth (Doherty *et al.*, 1990). Thus, PSA seems to be the factor to change NCAM function from a plasticity-promoting (through signaling pathways) to a stability-promoting protein (through direct adhesive interactions; Rønn *et al.*, 2000). Enzymatic removal of PSA confirmed the role of PSA-NCAM in cell migration, neurite outgrowth, branching, and pathfinding *in vivo* and *in vitro* (Muller *et al.*, 1996; Ono *et al.*, 1994; Tang *et al.*, 1994). Interestingly, it was shown that ectopic NCAM expression in neural stem cells favors neurogenesis *in vivo* independently of its polysialylation (Boutin *et al.*, 2009). But, importantly, simultaneous genetic ablation of both polysialyltransferases in mice leads to a lethal phenotype likely due to uncontrolled homo- and/or heterophilic interactions. In triple knock-out mice additionally lacking NCAM, this

phenotype was rescued showing mild defects as observed in NCAM-knock-out mice (see 1.1.4; Weinhold *et al.*, 2005), further demonstrating the role of PSA in controlling NCAM functions.

Another functionally important glycan is the human natural killer antigen 1 (HNK-1), which was detected at five possible *N*-glycosylation sites of NCAM (Albach *et al.*, 2004). Beyond that, NCAM can express *O*-linked HNK-1 attached to the MSD1-region (Walsh *et al.*, 1989).

The transmembrane isoforms of NCAM can further be posttranslationally modified by palmitoylation of two to four highly conserved intracellular cysteine residues. The palmitoylation serves as a second anchor to the plasma membrane and is possibly organizing the remaining cytoplasmatic tail for the interactions with other molecules that are important in NCAM-mediated signaling (Little *et al.*, 1998). Apart from that, Niethammer and coworkers showed palmitoylation of NCAM140 being essential for the association with cholesterol- and sphingolipid-rich microdomains, the so-called detergent-resistant microdomains or lipid rafts, ultimately enabling NCAM-mediated signal transduction and neurite outgrowth (Niethammer *et al.*, 2002; Little *et al.*, 1998).

Moreover, the cytoplasmatic domains of NCAM180 and NCAM140 can be phosphorylated at serine and threonine residues (Sorkin *et al.*, 1984). For example, the phosphorylation of at least one threonine residue has been described to be important for NCAM-mediated activation of the transcription factor nuclear factor-kappaB (NF-κB; Little at al., 2001). NCAM has been shown to become phosphorylated on serine or threonine residues upon stimulation of differentiation (Matthias & Horstkorte, 2006). Just recently, phosphorylation of serine 774 of NCAM has been shown to be involved in NCAM-mediated neurite outgrowth (Pollscheit *et al.*, 2012). Apart from being phosphorylated at serine and threonine, NCAM180 has been shown to be tyrosine phosphorylated on Y734. The tyrosine phosphorylation is predicted to have an inhibitory effect on neurite outgrowth (Diestel *et al.*, 2004).

NCAM has also been shown to be mono-ubiquitylated, which is proposed to represent a signal for endocytosis (Diestel *et al.*, 2007).

1.1.3. NCAM expression

Despite its name, NCAM is not only expressed in the nervous system but also by several cell types in many other tissues as, for example, skeletal and heart muscles (Andersson *et al.*, 1993; Gaardsvoll *et al.*, 1993), the digestive system (Esni *et al.*, 1999; Sakamoto *et al.*, 1994) and on natural killer cells (Lanier *et al.*, 1991). Several studies revealed also a deregulation

of NCAM expression and/or modification with PSA in several different cancer tissues (Campodónico et a., 2010; Zecchini & Cavallaro, 2010; Lehembre *et al.*, 2008; Novotny *et al.*, 2006; Trouillas *et al.*, 2003; Tezel *et al.*, 2001; Lantuéjoul *et al.* 2000, 1998; Kameda *et al.*, 1999; Sasaki *et al.*, 1998; Fogar *et al.*, 1997).

In the brain, NCAM is expressed by neurons and glial cells, and the expression level is temporally and spatially regulated as well as isoform specific. NCAM expression starts during initial stages of embryogenesis, peaks in early postnatal life, and is continued in adulthood. Interestingly, NCAM180 is mainly expressed in neurons and NCAM120 in glial cells, whereas NCAM140 is found on both cell types (Noble *et al.*, 1985). NCAM180 is primarily expressed on differentiated neurons and postsynaptic membranes and accumulates at sites of neurite to neurite contacts to stabilize them by association with the cytoskeleton (Sytnyk *et al.*, 2002; Persohn *et al.*, 1989; 1987; Pollerberg *et al.*, 1987, 1986). NCAM140 occurs mainly in growth cones of developing neurons at the time of target search and on pre- and postsynaptic membranes (Persohn *et al.*, 1989). Thus, initiation of cell-cell contacts leads to downregulation of the expression of NCAM140 and upregulation of NCAM180 expression (Pollerberg *et al.*, 1987, 1986, 1985).
NCAM120 is mainly expressed in lipid rafts (Krämer *et al.*, 1999), as typical for GPI-anchored proteins and also described for palmitoylated NCAM140 (Niethammer *et al.*, 2002; Little *et al.*, 1998).

1.1.4. NCAM functions

During embryogenesis and in the adult brain, NCAM is not only involved in cell adhesion, but in several signal transduction processes that ultimately lead to cell migration, neurite outgrowth, axonal growth, and fasciculation (Hinsby *et al.*, 2004; Chazal *et al.*, 2000; Cremer *et al.*, 1997; Doherty *et al.*, 1990). Furthermore, NCAM is involved in synaptic formation and plasticity thus being important for learning and memory function of the brain (Panicker *et al.*, 2003; Cremer *et al.*, 1997). NCAM deficient mice display increased lateral ventricle size (Wood *et al.*, 1998), a significant smaller olfactory bulb and deficits in hippocampal-/amygdala-dependent learning. Apart from that, the mice are healthy and fertile (Cremer *et al.*, 1994). Thus, it is assumable that other CAMs are able to compensate for the absent NCAM. In humans, the increase of soluble NCAM in affected brain regions and cerebrospinal fluid has been linked to schizophrenia and correlates with the progression of the illness (Vawter *et al.*, 2001, 1998; van Kammen *et al.* 1998; Poltorak *et al.*, 1997, 1995). Furthermore, the NCAM encoding gene has been identified to be relevant in schizophrenia (Schizophrenia Working Group of Psychiatric Genomics Consortium, 2014; Greenwood *et al.*, 2012). NCAM's functions are regulated by transcriptional and posttranscriptional/posttranslational modifications, as described above (see 1.1.1 and 1.1.2).

Whereas the degree of NCAM polysialylation is drastically reduced during development (Chuong & Edelman, 1984), the expression of the VASE exon increases (Small & Akeson, 1990). In brain areas retaining PSA-NCAM expression in adulthood (Rousselot *et al.*, 1995; Bonfanti *et al.*, 1992; Theodosis *et al.*, 1991), VASE is not expressed (Small & Akeson, 1990). This inverse expression also accounts for the change from NCAM promoting plasticity to a stability-promoting protein (Rønn *et al.*, 2000).

1.1.5. NCAM interactions

1.1.5.1. Homophilic interactions

NCAM is involved in homophilic *cis*- and *trans*-interactions (Hoffman & Edelman, 1983; Rutishauser *et al.*, 1982). Which Ig-like domains mainly participate in these interactions and the exact mechanisms have been highly discussed over years (Atkins *et al.*, 2001, 1999; Jensen *et al.*, 1999; Ranheim *et al.*, 1996; Rao *et al.*, 1994, 1993, 1992; Zhou *et al.*, 1993). Kiselyov and coworkers concluded a *cis*-interaction between the first and second Ig-like domain of NCAM as described by Kasper *et al.* being the most likely scenario (Kiselyov *et al.*, 2005; Kasper *et al.*, 2000). Apart from that, three *trans*-interactions were found: binding between IgII and IgIII ("flat zipper"), between IgI and IgIII and between IgII and IgII ("compact zipper") of NCAM molecules on opposing cell surfaces. A two-dimensional zipper is given by the combination of the compact and flat zippers ("compact flat double zipper"), producing homophilic NCAM adhesion complexes involving several NCAM molecules. The physiological relevance was shown by the inhibition of NCAM homophilic binding by peptides corresponding to the above-mentioned contacts, leading to decreased NCAM-mediated neurite outgrowth (Kiselyov *et al.*, 2005; Soroka *et al.*, 2003). Additionally, homophilic interactions are influenced by the PSA modification of NCAM (see 1.1.2) and the inclusion of the VASE exon. PSA-chains build a voluminous hydration shell around NCAM and inhibit the homophilic binding ability (Sadoul *et al.*, 1983). Although located in IgIV, expression of the VASE exon within NCAM leads to an enhanced homophilic affinity to cells which also express NCAM with VASE compared to cells expressing NCAM without VASE (Chen *et al.*, 1994).

1.1.5.2. Heterophilic extracellular interactions

NCAM is also able to bind heterophilically to other molecules. Extracellular binding partners are, for example, other members of the IgSF, such as the transient axonal glycoprotein-1 (TAG-1) and L1. The interaction with L1 occurs between carbohydrates expressed on L1 and a lectin homology motif in the IgIV domain of NCAM. This most probable *cis*-interaction induces phosphorylation of tyrosine and serine residues of L1 and ultimately causes neurite outgrowth (Heiland *et al.*, 1998; Horstkorte *et al.*, 1993).

Another NCAM binding partner is adenosine triphosphate (ATP), which binds directly to the second FNIII domain of NCAM (Kiselyov *et al.*, 2003). Interestingly, NCAM has been shown to have ecto-ATPase activity. The binding of ATP to NCAM inhibits cellular aggregation and neurite outgrowth induced by homophilic NCAM *trans*-interaction most likely by structural alterations of NCAM's extracellular part (Skladchikova *et al.*, 1999, Dzhandzhugazyan & Bock, 1997) or indirect inhibition of the interaction between NCAM and the fibroblast growth factor receptor 1 (FGFR1; Kiselyov *et al.*, 2003), as described below.

Furthermore, NCAM binds to several components of the ECM such as heparin (Cole & Glaser, 1986), collagen (Probstmeier *et al.*, 1989), laminin (Grumet *et al.*, 1993), some chondroitin sulfate proteoglycans (CSPGs), and heparin sulfate proteoglycans (HSPGs) including agrin, neurocan, and phosphacan (Margolis *et al.*, 1996; Storms *et al.*, 1996). In 2003, Paratcha and coworkers showed that NCAM can function as a signaling receptor for members of the glial cell line-derived neurotrophic factor (GDNF) ligand family and associates with the GDNF family receptor α (GFRα; Paratcha *et al.*, 2003). Furthermore, PSA-NCAM is involved in regulating the effects of the brain-derived neurotrophic factor (BDNF; Vutskits *et al.*, 2001) and the platelet-derived growth factor (PDGF; Zhang *et al.*, 2004).

Further known binding partners are P- and L-selectin (Needham & Schnaar, 1993), the receptor for rabies virus (RV; Thoulouze *et al.*, 1998), and the cellular prion protein (PrP^{c}) that recruits NCAM180 and NCAM140 to lipid rafts ultimately enhancing neurite outgrowth according to Santuccione and coworkers (Santuccione *et al.*, 2005). But the probably most important heterophilic extracellular interaction partner of NCAM is the FGFR1, an IgSF receptor tyrosine kinase. The binding occurs between NCAM's FNIII domains and the IgII and IgIII domains of the FGFR1 and leads to phosphorylation of the receptor ultimately causing neurite outgrowth (Kiselyov *et al.*, 2003; Saffell *et al.*, 1997; Williams *et al.*, 1994). Interestingly, ATP is suspected to have a regulatory role through competing with FGFR1 for the binding to NCAM (Kiselyov *et al.*, 2003).

1.1.5.3. Heterophilic intracellular interactions

The transmembrane isoforms of NCAM have also been demonstrated to exhibit a number of direct and indirect interactions with various intracellular proteins. The first identified intracellular binding partner of NCAM was the cytoskeletal linker-protein spectrin. Initially, a highly affinity binding between NCAM180 and spectrin was detected (Pollerberg *et al.*, 1987; 1986). Later, also NCAM140 was shown to bind directly to spectrin, however less efficient than NCAM180, and even NCAM120 appeared to interact indirectly with spectrin via lipid rafts (Leshchyns'ka *et al.*, 2003). The same study revealed an association of NCAM180 and NCAM140 with activated protein kinase C β (PKCβ) via spectrin in dependency of the FGFR1 activation. The formation of the PKCβ-spectrin-NCAM complex was shown to be

implicated in NCAM-mediated neurite outgrowth (Leshchyns'ka *et al.*, 2003). Additionally, the NCAM/spectrin complex plays an important role at nascent synapses (Sytnyk *et al.*, 2002) and the maintenance of the structural integrity of postsynaptic densities (Puchkov *et al.*, 2011).

Beggs *et al.* described an interaction between NCAM140 and the src-related nonreceptor tyrosine kinase $p59^{fyn}$ (Fyn; Beggs *et al.*, 1997). It has not been clarified yet, if Fyn and NCAM interact directly or indirectly, but the activation of Fyn depends on its dephosphorylation by the receptor protein tyrosine phosphatase α (RPTPα) which interacts directly with the ID of NCAM140 (Bodrikov *et al.*, 2005). Therefore, RPTPα serves as a linker between NCAM140 and Fyn. Additionally, the focal adhesion kinase (FAK) has been co-immunoprecipitated with NCAM140, but is believed to interact indirectly with NCAM by binding to Fyn (Beggs *et al.*, 1997). Through Fyn and FAK, NCAM is able to activate the mitogen-activated protein (MAP)-kinase pathway stimulating neurite outgrowth (Kolkova *et al.*, 2000; Schmid *et al.*, 1999).

A further molecule shown by immunoprecipitation to bind to NCAM140 is the growth associated protein-43 (GAP-43) that serves as a linker between NCAM and actin (He & Meiri, 2002; Meiri *et al.*, 1998) and may act as a switch between NCAM140 and NCAM180 mediated neurite outgrowth (Korshunova *et al.*, 2007).

More major cytoskeletal proteins have been identified to interact with NCAM180 and NCAM140: α- and β-tubulin that form the microtubules, as well as α-actinin. Interestingly, β-actinin, tropomyosin, the microtubule associated protein 1A (MAP1A), and the rhoA-binding kinase-α (ROK-α) preferentially bind to NCAM180 (Büttner *et al.*, 2003). Büttner and coworkers were able to identify even more binding partners for NCAM180 and NCAM140 by ligand affinity chromatography when focusing on signaling molecules: phospholipase Cγ (PLCγ), leucine-rich acidic nuclear protein (LANP, a phosphatase inhibitor), turned on after division-64 (TOAD-64, a protein involved in axonal growth, interacts only with NCAM180), syndapin (a protein involved in vesicle trafficking), and the serine/threonine-protein phosphatase PP1 and PP2A (Büttner *et al.*, 2005).

Apart from that, Miñana *et al.* showed the association of both transmembrane NCAM isoforms with clathrin and α-adaptin, which is a component of adaptor protein complex-2 (AP-2), and confirmed NCAM being endocytosed via a clathrin-dependent pathway (Miñana *et al.*, 2001). Interestingly, it has also been shown that NCAM co-immunoprecipitates with caveolin, the principal component of the caveolae (He & Meiri, 2002). Subsequently, it has been shown that NCAM is also endocytosed by the calveolae-dependent pathway (Diestel *et al.*, 2007).

Recently, p21-activated kinase 1 (PAK1) was identified as new intracellular interaction partner for NCAM and the interaction is also implicated in neurite outgrowth (Li *et al.*, 2013).

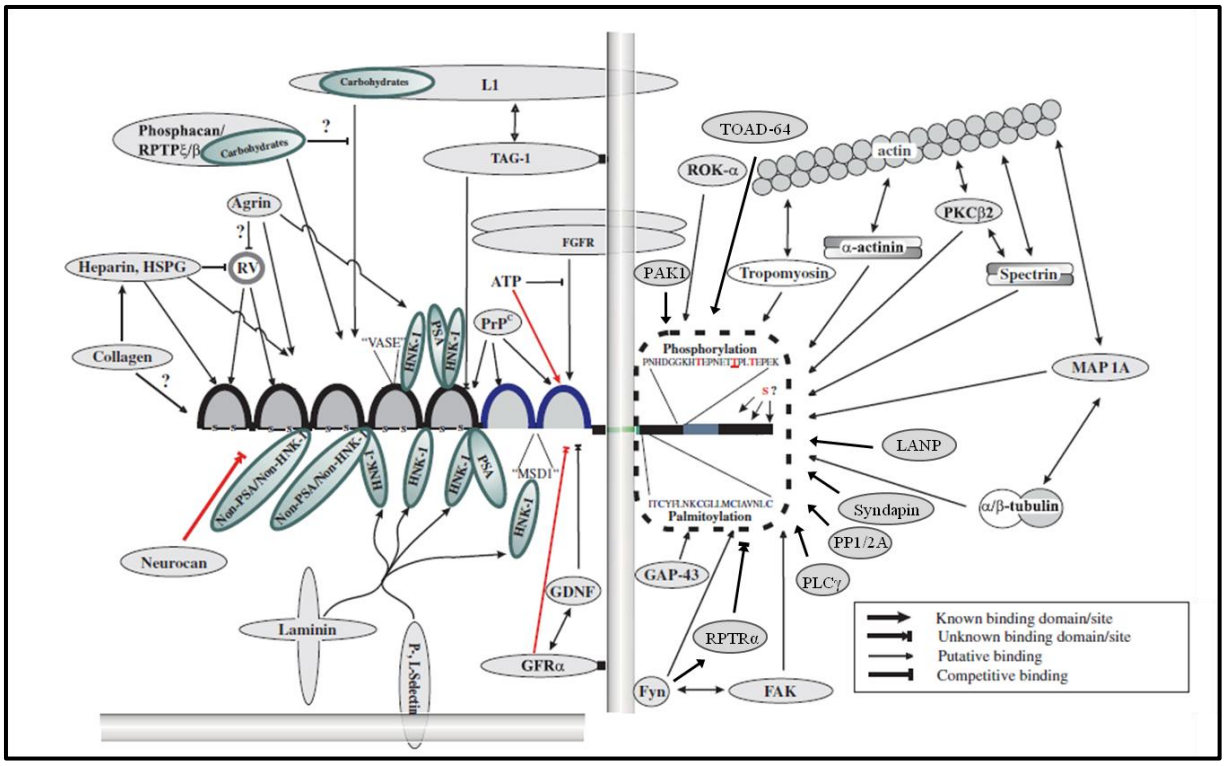

Fig. 2: Heterophilic interactions and posttranslational modifications of NCAM

Shown are most interaction partners described in the text above. Modifications with carbohydrates are shown in green. The actual type of glycosylation identified at the individual *N*-glycosylation sites varies between species. Putative threonine phosphorylation sites in the intracellular domain of NCAM are shown in red (the most likely site is underlined). “S ?” indicates unknown serine phosphorylation sites. Potential palmitoylation sites in the cytoplasmatic part of NCAM are shown in blue. Interactions known to affect homophilic NCAM interactions are shown with red arrows. Question marks indicate putative interactions. Abbreviations and references are given in the text (modified after Walmod *et al.*, 2004).

1.1.6. Trafficking of NCAM

The biosynthesis of NCAM was investigated by Lyles and coworkers three decades ago in cultured fetal neuronal cells of the rat (Lyles *et al.*, 1984a, b). They showed that NCAM is as expected synthesized in the endoplasmatic reticulum (ER) as two polypeptides with a molecular weight of approximately 186 kDa and 136 kDa (Lyles *et al.*, 1984b). Initially four to five high mannose cores are attached to NCAM, which are processed approximately 20 to 30 minutes after synthesis in the *trans*-Golgi compartment into more complex glycans which are also sialylated and polysialylated. Approximately 35 minutes after synthesis, NCAM appears at the cell surface where it is phosphorylated (Lyles *et al.*, 1984a). The biosynthesis of NCAM decreases drastically during maturation of the mice brain, with a 350-fold turnover decline from embryonic day 17 to postnatal day 25 and a steady state expression of 50 % of the level of postnatal day 12 beginning at postnatal day 40 (Linnemann *et al.*, 1985; Jacque *et al.*, 1976).

Miñana and coworkers showed NCAM being endocytosed from the plasma membrane in astrocytes (Miñana *et al.*, 2001). Recent studies confirmed NCAM’s endocytosis and

revealed that NCAM is subsequently recycled to the plasma membrane, whereas only a small amount of NCAM becomes lysosomally degraded. Endocytic vesicles were observed in somata, neurites, and growth cones of cortical neurons in a developmentally regulated manner, potentially implying that endocytosis of NCAM140 may predominantly play a role in immature neurons, whereas internalization of NCAM180 may be more important in more developed neurons (Diestel *et al.*, 2007). Mono-ubiquitination of NCAM serves as a signal for endocytosis, even though further studies revealed that other NCAM endocytosis signals must exist additionally (Diestel *et al.*, 2007; Diestel, unpublished data, Institute of Nutrition and Food Science, Department of Human Metabolomics, University of Bonn, Germany).

Only very little evidence existed on the intracellular transport of NCAM. In chick retinal ganglion cells, NCAM180 and NCAM140, but not NCAM120, were shown to be transported by the fast axonal transport (Garner *et al.*, 1986; Nybroe *et al.*, 1986). Furthermore, in organotypic slice cultures from postnatal hypothalami it has been shown that PSA-NCAM reaches the surface of neurons and astrocytes via the constitutive pathway, independently of Ca^{2+} entry and increased neuronal activity (Pierre *et al.*, 2001). However, the exact transport mechanism of newly synthesized and/or endocytosed NCAM remained still unknown.

1.2. Motor proteins and the intracellular transport

Intracellular transport of protein complexes, membranous organelles, and other cargoes is essential for cellular function, morphogenesis, and survival. In neurons, proteins expressed in the cell body need to be transported and properly distributed to dendrites, axons, and nerve terminals to maintain neuronal function and viability (Salinas *et al.*, 2008; Chevalier-Larsen & Holzbaur, 2006; Hirokawa & Takemura, 2003). Three large superfamilies of motor proteins facilitate the intracellular transport using cytoskeletal filaments for the movement: myosins, dyneins, and kinesins.

1.2.1. Myosins, dyneins, and kinesins

Myosins move along actin filaments and are responsible for the transport of cargoes within short distances, as for example within regions of actin filament networks near the plasma membrane. Long-distance transport as between the nucleus and the plasma membrane is mediated by kinesins and dyneins, which move along microtubules in dependency on ATP (Hirokawa & Takemura, 2003; Hirokawa, 1998). Dyneins transport their cargo from the periphery to the cell body (retrograde; Schroer *et al.*, 1989; Paschal & Vallee, 1987), whereas kinesins act in the opposite direction by moving anterograde from the cell body to the synapses (Hirokawa *et al.*, 1991; Vale *et al.*, 1985).

1.2.2. Kinesin-1

Kinesin-1 was the first member of the kinesin superfamily to be identified. Kinesin-1 transports cargoes fast with an average velocity of 0.6–0.8 µm s^{-1} from the cell body to the synapses along microtubules in neuronal axons and dendrites (Brady, 1985; Vale *et al.*, 1985). Mammalian kinesin-1 (formerly kinesin family 5, KIF5) is assembled from three kinesin heavy chains (KHCs: KIF5A, KIF5B, KIF5C) and four kinesin light chains (KLCs: KLC1, KLC2, KLC3, KLC4). The KHCs and KLCs form homodimer, which can associate in all possible combinations resulting in a functional kinesin-1 heterotetramer (Rahman *et al.*, 1998; Xia *et al.*, 1998; Niclas *et al.*, 1994; Cabeza-Arvelaiz *et al.*, 1993). The KHCs build the amine (N)-terminal globular motor domain at the head region of kinesin-1 that uses ATP hydrolysis to energize the movement along microtubules. The tail domain consists of the carboxy (C)-terminus of the KHCs that regulates the ATPase and microtubule binding activity, and of two KLCs (Yang *et al.*, 1990). KLCs contain an N-terminal α-helical domain that associates with the KHC stalk and six tetratricopeptide repeat (TPR) motifs, which mediate cargo attachment (Diefenbach *et al.*, 1998, Hirokawa *et al.*, 1989). Additionally, KLCs are involved in the regulation of KHC activity (Hirokawa 1998; Verhey *et al.*, 1998; Hirokawa *et al.*, 1989).

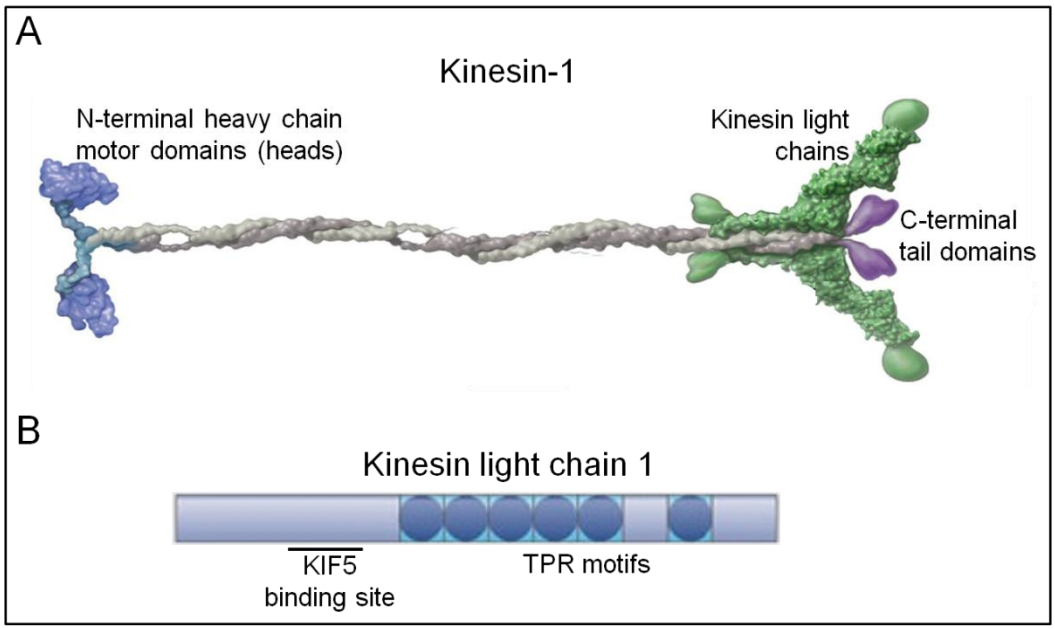

Fig. 3: Schematic model of kinesin-1 and kinesin light chain 1

(A) Kinesin-1 motor domains are shown in blue, heavy chain tail domains in purple and kinesin light chains in green (modified after Vale, 2003). **(B)** Domain structure of kinesin light chain 1 containing six tetratricopeptide repeat (TPR) motifs and the KIF5 binding site (modified after Hirokawa & Takemura, 2005).

Amongst others, kinesin-1 is known to transport neuronal transmembrane proteins such as apolipoprotein E receptor 2 (ApoER2; Verhey *et al.*, 2001), amyloid-ß precursor protein (APP; Lazarov *et al.*, 2005; Kamal *et al.*, 2000), Calsyntenin-1/alcadein (Araki *et al.*, 2007;

Konecna *et al.*, 2006), the cytosolic Cayman ataxia protein (Caytaxin; Aoyama *et al.*, 2009), and Kinase D-interacting substrate of 220 kDa/ankyrin repeat-rich membrane spanning (Kidins220/ARMS; Bracale *et al.*, 2007). Most of these interaction partners bind directly to the TPR domains of KLC1, although partly c-Jun N-terminal kinase (JNK)-interacting proteins (JIPs) are involved, which bind to KLCs and connect vesicles containing, for example, ApoER2 to kinesin-1 (Verhey *et al.*, 2001). A possible interaction of NCAM's ID and KLC1 was especially interesting as although NCAM has already been described decades ago as being transported by the fast axonal transport in chicken retinal ganglion neurons (Garner *et al.*, 1986; Nybroe *et al.*, 1986), the exact mechanism of its transport remained still unknown.

1.3. Aim of the thesis

This thesis aimed for the identification of novel potential interaction partners of NCAM and functional analyzes of these interactions to further understand the mechanisms underlying NCAM's functions in the brain. NCAM has been implicated in neural development and maintenance of the adult nervous system. NCAM initiates intracellular signal transduction pathways ultimately leading to cell migration, differentiation, plasticity, and survival through homophilic and heterophilic interactions with several proteins. To broaden knowledge about the role of heterophilic interactions on NCAM's functions, yet unknown intracellular interaction partners of human NCAM180 and NCAM140 should be identified using a protein macroarray screening. Potential interaction partners should subsequently be verified by alternative approaches such as co-immunoprecipitation, immunofluorescence staining for co-localization studies, and enzyme linked immunosorbent assay. Functions of verified interactions should be investigated with various methods adjusted to the respective interaction partner to gain further insight into the functions of NCAM interactions underlying the role of NCAM in the brain.

2. Material

Experiments were carried out in the laboratory of Prof. Dr. Brigitte Schmitz (emer., Institute of Animal Sciences, Department of Biochemistry, University of Bonn, Germany), since 2013 laboratory of PD Dr. Simone Diestel (Institute of Nutrition and Food Science, Department of Human Metabolomics, University of Bonn, Germany), and Dr. Vladimir Sytnyk (School of Biotechnology and Biomolecular Sciences, University of New South Wales, Sydney, NSW, Australia). Variations in buffer compositions and methods, which were performed in both laboratories, are highlighted as exponents ([1]: laboratory of Prof. Dr. Brigitte Schmitz and PD Dr. Simone Diestel; [2]: laboratory of Dr. Vladimir Sytnyk) and/or in italic letters in parentheses.

2.1. Commercial chemicals

Tab. 1: Commercial chemicals

Chemical	Source
Acetic acid, 96 %	Merck, Darmstadt (GER); Ajax FineChem, Taren Point, NSW (AUS)
Acetone	Ajax FineChem, Taren Point, NSW (AUS)
Agar	Difco, Detroit, MI (USA)
Agarose	Roche, Grenzach-Whylen (GER)
Ammonium persulfate (APS)	Merck, Darmstadt (GER)
Aprotinin	Sigma-Aldrich, Steinheim (GER)
B-27	Life Technologies™, Carlsbad, CA (USA)
Basic fibroblast growth factor (bFGF)	Life Technologies™, Carlsbad, CA (USA)
β-mercaptoethanol	Merck, Darmstadt (GER); Sigma-Aldrich, Castle Hill, NSW (AUS)
Boric acid (H_3BO_3)	Merck, Darmstadt (GER)
Bovine serum albumin (BSA)	Solarbio Science & Technology Co., Beijing (CHN)
Bromophenol blue	Merck, Darmstadt (GER); Sigma-Aldrich, Castle Hill, NSW (AUS)
Calcium chloride ($CaCl_2$)	Ajax FineChem, Taren Point, NSW (AUS)
Citric acid	Ajax FineChem, Taren Point, NSW (AUS)
Developer for X-ray films	Kodak, Rochester, NY (USA)
Dimethylsulfoxide (DMSO)	Sigma-Aldrich, Castle Hill, NSW (AUS)
Disodium hydrogen phosphate * 2 H_2O (Na_2HPO_4 * 2 H_2O)	Merck, Darmstadt (GER); Ajax FineChem, Taren Point, NSW (AUS)
Dithiothreitol (DTT)	Sigma-Aldrich, Taufkirchen (GER); Castle Hill, NSW (AUS)
Donkey serum	Sigmal-Aldrich, Castle Hill, NSW (AUS)
Dulbecco`s modified Eagles`s medium (DMEM, with 4.5 g Glucose/L)	PAA Laboratories, Morningside, QLD (AUS)
DYOMICS DY-633	Fluorophore Dyomics, Jena (GER)
EDTA-free protease inhibitor cocktail	Roche Applied Science, Castle Hill, NSW (AUS)
Ethyleneglycoltetraacetic acid (EGTA)	Sigma-Aldrich, Castle Hill, NSW (AUS)
Ethanol, 96 %	KMF Laborchemie, Lohmar (GER); Ajax FineChem, Taren Point, NSW (AUS)
Ethidium bromide	Sigma-Aldrich, Steinheim (GER)

Chemical	Source
Ethylenediaminetetraacetic acid (EDTA)	Merck, Darmstadt (GER)
Fetal bovine serum (FBS)	PAA Laboratories, Morningside, QLD (AUS)
Fixing solution for X-ray films	Kodak, Rochester, NY (USA)
FluorPreserve™ reagent	Calbiochem (Merck), Darmstadt (GER)
Formaldehyde, 37 %	Merck, Darmstadt (GER)
Gentamicin/Amphotericin B	Life Technologies™, Carlsbad, CA (USA)
GlutaMAX™	Life Technologies™, Carlsbad, CA (USA)
Glutathione (GSH) superflow	Qiagen, Hilden (GER)
Glycerol	Ajax FineChem, Taren Point, NSW (AUS)
Ham's F-12	PAA Laboratories, Morningside, QLD (AUS)
Hydrochloric acid (HCl)	KMF OptiChem, Lohmar (GER); Ajax FineChem, Taren Point, NSW (AUS)
Hydrogen peroxide (H_2O_2), 30 %	Sigma-Aldrich, Castle Hill, NSW (AUS)
Imidazole	Sigma-Aldrich, Steinheim (GER)
Isopropanol	KMF OptiChem, Lohmar (GER)
Isopropyl β-D-1-thiogalactopyranoside (IPTG)	Biomol, Hamburg (GER)
Leupeptin	Sigma-Aldrich, Steinheim (GER)
L-Glutathione, reduced	Sigma-Aldrich, Steinheim (GER)
Lipofectamine™ 2000	Invitrogen, Mount Waverly, VIC (AUS)
Magnesium chloride ($MgCl_2$)	Ajax FineChem, Taren Point, NSW (AUS)
Methanol	Merck, Darmstadt (GER); Ajax FineChem, Taren Point, NSW (AUS)
N,N,N',N',-Tetramethylethylendiamine (TEMED)	Sigma-Aldrich, Steinheim (GER)
Neurobasal® A medium	Life Technologies™, Carlsbad, CA (USA)
Nickel sulfate	Sigma, Taufkirchen (GER)
Nickel-nitrilotriacetic acid (Ni-NTA) agarose	Qiagen, Hilden (GER)
NuPAGE® Antioxidant, 200 x	Invitrogen, Mount Waverly, VIC (AUS)
NuPAGE® MOPS SDS running buffer, 20 x	Invitrogen, Mount Waverly, VIC (AUS)
O-phenylenediamine dihydrochloride (OPD)	Perbio Science, Parkdale, VIC (AUS)
Paraformaldehyde (PFA)	Sigma-Aldrich, Castle Hill, NSW (AUS)
Pepstatin A	Sigma-Aldrich, Steinheim (GER)
Phenylmethanesulfonyl fluoride (PMSF)	Sigma-Aldrich, Steinheim (GER); Castle Hill, NSW (AUS)
Piperazine-1,4-bis(2-ethanesulfonic acid) (PIPES)	Sigma-Aldrich, Castle Hill, NSW (AUS)
Poly-D-lysine (PDL)	Sigma-Aldrich, Castle Hill, NSW (AUS)
Ponceau-S	Sigma-Aldrich, Steinheim (GER)
Potassium chloride (KCl)	Merck, Darmstadt; Ajax FineChem, Taren Point, NSW (AUS)
Potassium dihydrogen phosphate (KH_2PO_4)	Merck, Darmstadt (GER); Ajax FineChem, Taren Point, NSW (AUS)
Protein A/G-agarose beads	Santa Cruz Biotechnology, Inc., Santa Cruz, CA (USA)
Protein A-agarose beads	Santa Cruz Biotechnology, Inc., Santa Cruz, CA (USA)
Rotiphorese® Gel 40, 40 %	Roth, Karlsruhe (GER)
S.O.C. medium	Invitrogen, Mount Waverly, VIC (AUS)
Silver nitrate ($AgNO_3$)	Merck, Darmstadt (GER)
Skim milk powder	Coles, Randwick, NSW (AUS)
Sodium azide (NaN_3)	Sigmal-Aldrich, Castle Hill, NSW (AUS)
Sodium bicarbonate ($NaHCO_3$)	Ajax FineChem, Taren Point, NSW (AUS)

Chemical	Source
Sodium carbonate (Na_2CO_3)	Ajax FineChem, Taren Point, NSW (AUS)
Sodium chloride (NaCl)	Merck, Darmstadt (GER); Ajax FineChem, Taren Point, NSW (AUS)
Sodium diphosphate ($Na_4P_2O_7$)	Sigma Aldrich, Castle Hill, NSW (AUS)
Sodium dodecyl sulfate (SDS)	Roth, Karlsruhe (GER)
Sodium fluoride (NaF)	Sigma Aldrich, Castle Hill, NSW (AUS)
Sodium hydoxide (NaOH)	T.J. Baker, Deventer (NL); Ajax FineChem, Taren Point, NSW (AUS)
Sodium orthovanadate (Na_3VO_4)	Sigma-Aldrich, Castle Hill, NSW (AUS)
Sodium thiosulfate ($Na_2S_2O_3$)	Merck, Darmstadt (GER)
Sucrose	BDH Prolabo, Murarrie, QLD (AUS)
Tris(hydoxymethyl)aminomethane (Tris)	Merck, Darmstadt (GER); Ajax FineChem, Taren Point, NSW (AUS)
Tris-Glycine buffer, 10 x	Bio-Rad Laboratories, Regents Park, NSW (AUS)
Tolyethylene glycol p-(1,1,3,3-tetramethylbutyl)-phenyl ether (Triton X-100)	Serva, Heidelberg (GER); Bio-Rad Laboratories, Regents Park, NSW (AUS)
Trypsin-EDTA	Life Technologies™, Carlsbad, CA (USA)
Tryptone	Difco, Detroit, MI (USA)
Polyoxyethylene (20) sorbitan monolaurate (Tween® 20)	BDH Prolabo, Murarrie, QLD (AUS)
Yeast	Difco, Detroit, MI (USA)

2.2. Equipment

Tab. 2: Equipment

Equipment	Source
Agarose gel electrophoresis Mini-Sub® Cell GT system	Bio-Rad, Hercules, CA (USA)
Aida™ Array Compare software	Raytest, Straubenhardt (GER)
Aida™ Image Analyzer software version 4.24	Raytest, Straubenhardt (GER)
Chemiluminescence-system MicroChemi 4.2	DNR Bio-Imaging Systems (GER)
Confocal laser scanning microscope (LSM510)	Nikon Corporation, Tokyo (JPN)
Electrophoresis system Mini-Protean 3	Bio-Rad, Hercules, CA (USA)
ELISA reader POLARstar Omega	BMG Labtech, Mornington, VIC (AUS)
ELISA reader Titertek PLUS MS2	ICN Biomedicals GmbH, Meckenheim (GER)
Microsoft Office 2007	Microsoft Corporation, Redmond, WA (USA)
GraphPad Prism 6	GraphPad, San Diego, CA (USA)
ImageJ software, version 1.43	National Institutes of Health, Bethesda, MD (USA)
Licor ODYSSEY Infrared Imaging System Scanner	LI-COR Biosciences GmbH, Bad Homburg (GER)
LSM510 software	Nikon Corporation, Tokyo (JPN)
Mini-Cell Electrophoresis system XCell SureLock®	Invitrogen, Mount Waverly, VIC (AUS)
Neon® Transfection System	Life Technologies™, Carlsbad, CA (USA)
Oil Plan Apo VC 60x objective (numerical aperture 1.4)	Nikon Corporation, Tokyo (JPN)
Slot blot apparatus PR 600	Hoefer Inc., Holliston, MA (USA)
Spectrophotometer SmartSpec™ Plus	Bio-Rad, Hercules, CA (USA)

Equipment	Source
Technical data sheet “Scoring Template for Macroarrays”	Source Bioscience ImaGenes, Berlin (GER)
Trans-Blot® Semi Dry Transfer Cell	Bio-Rad, Hercules, CA (USA)
Ultraviolet (UV)-transilluminator Uvsolo	Biometra, Göttingen (GER)
XK-16 column	Pharmacia Biotech, Uppsala (SWE)

2.3. Working materials

Tab. 3: Working materials

Material	Source
24-well plates	Greiner bio-one, Frickenhausen (GER)
30 kDa cut-off columns	EMD Millipore, Cork (IRL)
50 kDa cut-off columns, Vivaspin 6®	Sartorius, Göttingen (GER)
75 cm^2 culture flasks	Greiner bio-one, Frickenhausen (GER)
96-well MICROLON® 600 plates	Greiner bio-one, Frickenhausen (GER)
CL-XPosure™ X-ray film	Thermo scientific, Rockford, IL (USA)
Filter paper for Western blots	Bio-Rad, Hercules, CA (USA)
Nitrocellulose membrane Hybond™-ECL, 0.2 µm	GE Healthcare, Freiburg (GER)
NuPAGE® Bis-Tris precast gels	Invitrogen, Mount Waverly, VIC (AUS)
Polyvinylidene difluoride (PVDF) membrane, 0.45 µm	Immobilon; Millipore, Kilsyth, VIC (AUS)
Protein macroarray Part 8, Id. 367.60.515	Source Bioscience ImaGenes, Berlin (GER)
Protein macroarray Part 9, Id. 367.56.521	Source Bioscience ImaGenes, Berlin (GER)

2.4. Kits and standards

Tab. 4: Kits and standards

Name	Source
DC-protein assay	Bio-Rad, München (GER)
DNA Clean & Concentrator Kit	Zymo Research, HISS Diagnostics, Freiburg (GER)
ECL Pro Enhanced Oxidizing reagent	Thermo scientific, Rockford, IL (USA)
ECL Western blotting reagent	Merck, Darmstadt (GER)
Fluoro Spin 681, Protein Labeling & Purification Kit	Emp Biotech, Berlin (GER)
GeneJET™ Plasmid Miniprep Kit	Fermentas, St. Leon-Rot (GER)
GeneRuler™ DNA Ladder Mix	Fermentas, St. Leon-Rot (GER)
Laemmli SDS-PAGE buffer, non-reducing, 5x	Invitrogen, Mount Waverly, VIC (AUS)
Laemmli SDS-PAGE buffer, reducing, 5x	Invitrogen, Mount Waverly, VIC (AUS)
Loading dye, 6x	Fermentas, St. Leon-Rot (GER)
Novex® Sharp Pre-stained protein standard	Invitrogen, Mount Waverly, VIC (AUS)
PageRuler™ Unstained Protein Ladder	Fermentas, St. Leon-Rot (GER)
Plasmid Midi Kit	Qiagen, Hilden (GER)
QIAquick Gel Extraction Kit	Qiagen, Hilden (GER)
SuperSignal®West Dura	Thermo Scientific, Rockford, IL (USA)
SuperSignal®West Pico	Thermo Scientific, Rockford, IL (USA)

2.5. Antibodies and peptides

Tab. 5: Antibodies and peptides

Primary antibodies	Characteristics	Source	Concentration / dilution factor / application
5B8	Mouse monoclonal antibody against human NCAM-ID	Own production. Hybridoma cells were kindly provided by R. Horstkorte, University of Halle (GER)	1.1 mg/ml; 1:4000 (WB)
Anti-His IRDye™ 800-antibodies	IRDye™800CW conjugated polyclonal rabbit antibodies against 6x Histidine (His)-tags	Rockland Immunochemicals Inc., Gilbertsville, PA (USA)	1 mg/ml; 1:10000 (macroarray)
ERIC 1	Mouse monoclonal antibody against human NCAM-ED	Santa Cruz Biotechnology Inc., Santa Cruz, CA (USA)	200 µg/ml; 1:50 (IF), 1:100 (NCAM-triggering)
GST-tag antibody	Mouse monoclonal immunoglobulin subclass G (IgG) antibody against glutathione-S-transferase (GST)-tags	Novagen (Merck KGaA), Darmstadt (GER)	1 mg/ml; 1:10000 (WB)
H28	Rat monoclonal antibody against mouse NCAM-ED	Own production. Hybridoma cells were kindly provided by R. Michalides, The Netherlands Cancer Institute, Amsterdam (NL)	1:2 (IF); 1:10 (WB)
KIF5A (clone H-75)	Rabbit polyclonal antibodies against KIF5A	Santa Cruz Biotechnology Inc., Santa Cruz, CA (USA)	200 µg/ml; 1:60 and 1:200 (IF), 1:1000 (WB)
KLC1 (clone H-75)	Rabbit polyclonal antibodies against KLC1	Santa Cruz Biotechnology Inc., Santa Cruz, CA (USA)	200 µg/ml; 1:200 (WB), 5 µg (co-IP), 0.05 µg/well (ELISA)
KLC1 (clone L2)	Mouse monoclonal antibody against KLC1	Santa Cruz Biotechnology Inc., Santa Cruz, CA (USA)	200 µg/ml; 1:50 (IF)
Non-specific IgGs	Rabbit IgGs isolated from naive sera	Santa Cruz Biotechnology Inc., Santa Cruz, CA (USA)	100 µg/ml; 5 µg (co-IP)
p61	Rat monoclonal antibody against NCAM-ID	Own production. Hybridoma cells were kindly provided in the laboratory of Dr. V. Sytnyk	1:2 (IF)
Poly NCAM1	Rabbit polyclonal antibodies against mouse NCAM-ED	Kindly provided by M. Schachner, Center for Molecular Neurobiology, University of Hamburg (GER)	1:1000 (WB)

Primary antibodies	**Characteristics**	**Source**	**Concentration / dilution factor / application**
Tetra-His antibody	Mouse monoclonal IgG antibody recognizes at least 4x His-tagged proteins / Epitope HHHH	Qiagen, Hilden (GER)	200 µg/ml; 1:8000 (WB)
TGN38 (clone M-290)	Rabbit polyclonal antibodies against mouse TGN38	Santa Cruz Biotechnology Inc., Santa Cruz, CA (USA)	200 µg/ml; 1:1000 (WB)
γ-adaptin	Mouse monoclonal antibody against γ-adaptin (IgG)	BD Biosciences, San Jose, CA (USA)	250 µg/ml; 1:50 (IF)
Secondary antibodies / NeutrAvidin	**Characteristics**	**Source**	**Concentration / dilution factor / applications**
anti-mouse-CY3	CyDye (CY)3-conjugated goat polyclonal antibodies against mouse IgG (H+L)	Jackson ImmunoResearch Laboratories Inc., West Grove, PA (USA)	1:200 (IF)
anti-mouse-CY5	CY5-conjugated goat polyclonal antibodies against mouse IgG (H+L)	Jackson ImmunoResearch Laboratories Inc., West Grove, PA (USA)	1:200 (IF)
anti-mouse-POD	Peroxidase (POD)-conjugated AffiniPure goat polyclonal antibodies against mouse IgG + IgM	Dianova, Hamburg (GER)	800 µg/ml *(400 µg/ml)*; 1:10000 (WB)
anti-rabbit-CY3	CY3-conjugated goat polyclonal antibodies against rabbit IgG (H+L)	Jackson ImmunoResearch Laboratories Inc., West Grove, PA (USA)	1:200 (IF)
anti-rabbit-POD	POD-conjugated goat polyclonal antibodies against rabbit IgG (H+L)	Jackson ImmunoResearch Laboratories Inc., West Grove, PA (USA)	1:50000 (WB)
anti-rat-DL488	DL488-conjugated goat polyclonal antibodies against rat IgG (H+L)	Jackson ImmunoResearch Laboratories Inc., West Grove, PA (USA)	1:200 (IF)
anti-rat-POD	POD-conjugated goat polyclonal antibodies against rat IgG (H+L)	Jackson ImmunoResearch Laboratories Inc., West Grove, PA (USA)	1:10000 (WB)
POD-conjugated NeutrAvidin	POD-conjugated NeutrAvidin, binds to biotin	Jackson ImmunoResearch Laboratories Inc., West Grove, PA (USA)	1:5000 (ELISA), 1:30000 (Pull-down assay)
Peptides	**Characteristics**	**Source / Reference**	**Concentration / dilution factor**
$NCAM140_{748-763}$, $NCAM140_{764-777}$, $NCAM140_{756-770}$	Biotinylated peptides corresponding to indicated amino acid sequences of mouse NCAM140	Peptide 2.0, Chantilly VA (USA; described in Li *et al.*, 2013)	10 mg/ml; 1:2000

ELISA: enzyme linked immunosorbent assay, IF: immunofluorescence,
co-IP: co-immunoprecipitation, WB: Western Blot

2.6. Bacterial strains, cell lines, and primary neurons

Tab. 6: Bacterial strains, cell lines, and primary neurons

Name	Description / Specification	Source / Reference
Escherichia coli (E. coli) BL21 (DE3)	F- ompT, hsdSB (rB-mB-) gal dcm (DE3)	Stratagene (Studier & Moffatt, 1986)
E. coli TOP10	One Shot® TOP10 competent cells	Invitrogen, Mount Waverly, VIC (AUS)
E. coli XL1-blue	recA1 endA1 gyrA96 thi-1 hsdR17 supE44 relA1 lac [F´ proAB lacIqZΔM15 Tn10 (Tetr)]	Stratagene (Stratagene, 2004)
Chinese Hamster Ovary (CHO)-K1	Chinese hamster ovary dehydrofolatreductase deficient hamster cell line. ATCC (American Type Culture Collection) CCL 61	Life Technologies™, Carlsbad, CA (USA)
Hippocampal and cortical neurons	Brain tissue from wild-type C57Bl6 mice (postnatal day 2) was extracted with the approval of the Animal Care and Ethics Committee of the University of New South Wales (ACEC Number 09/112A).	Mice were obtained from Biological Resources, University of New South Wales, Kensington, NSW (AUS).

2.7. Plasmids

Tab. 7: Plasmids

Name	Characteristics	Source / Reference
pBJG1/hNCAM140ID	pBJG1 vector was constructed by Gross *et al*., 2005; cDNA of human NCAM140ID (hNCAM140ID) was generated with the following primers: forward 5'- GGA TCC GGA TCC ATG GAC ATC ACC TGC TAC TTC CTG AAC AAG-3' and reverse 5'- CTC GAG CTC GAG TGC TTT GCT CTC GTT CTC CTT TG-3', restricted with *Bam*HI and *Xho*I and inserted in frame in the pBJG1 vector; contains 8x His-tag and kanamycin resistance gene	Kindly provided by C. Laurini, Institute of Nutrition and Food Science, Department of Human Metabolomics, University of Bonn (GER)
pBJG1/hNCAM180ID	pBJG1 vector was constructed by Gross *et al*., 2005; cDNA of human NCAM180ID (hNCAM180ID)was cloned in frame into the pBJG1 vector by *Bam*HI- and *Xho*I restricition sites; contains 8x His-tag and kanamycin resistance gene	Kindly provided by H. Faraidun (Wobst *et al.*, 2012)
pcDNA3	Contains ampicillin and G418-resistance gene	Purchased from Invitrogen, Carlsbad (USA)
pGFP	Plasmid encodes wild-type GFP from *Aequorea Victoria*; contains kanamycin resistance gene	Purchased from Clontech, Palo Alto, CA (USA)

Name	Characteristics	Source / Reference
pcDNA3.1-GFP/mKHC1	Mouse KHC1 cDNA was cloned into the pcDNA3.1 vector (Invitrogen) at the *Hind*III/*Xba*I sites; Green fluorescent protein (GFP)-tag was inserted at the 5'-terminus of the cDNA; contains ampicillin resistance gene	Kindly provided by Prof. Dr. T. Suzuki, Graduate School of Pharmaceutical Sciences, Hokkaido University (JPN; Araki *et al.*, 2007; Kawano *et al.*, 2012)
pcDNA3.1-GFP/mKLC1	Mouse KLC1 cDNA (GenBank accession number AY753300/AK031309) was cloned into the pcDNA3.1 vector (Invitrogen) at the *Hind*III/*Xba*I sites; the KLC1 used in this study has a 98% protein sequence identity to human KLC1 (Q07866); GFP-tag was inserted at the 5'-terminus of the cDNA; contains ampicillin resistance gene	
pcDNA3.1V5-His/ NCAM-ID	Rat NCAM140ID was used as template to produce fragments, which were cloned into the pcDNA3.1V5-His vector (Invitrogen). Peptide sequence of NCAM-ID$_{748-777}$ shares 99 % identity (1 amino acid diference; F→M) and NCAM-ID$_{729-750}$ and NCAM-ID$_{777-810}$ are 100 % identical with the respective hNCAM180 domains	Kindly provided in the laboratory of Dr. V. Sytnyk (Li *et al.*, 2013; Chernyshova *et al.*, 2011; Leshchyns'ka *et al.*, 2003; Sytnyk *et al.*, 2002)
pcDNA3.1V5-His/ NCAM-ID$_{748-777}$		
pcDNA3.1V5-His/ NCAM-ID$_{729-750}$		
pcDNA3.1V5-His/ NCAM-ID$_{777-810}$		
pcDNA3/hNCAM180wt	Wild type (wt) human NCAM180 cDNA was cloned in frame into the pcDNA3 vector by *Bam*HI restriction sites	Kindly provided in the laboratory of PD Dr. S. Diestel (Boutin *et al.*, 2009; Diestel *et al.*, 2005, 2004)
pCX-MCS2/hNCAMΔCT	The hNCAM with deleted cytoplasmic tail (CT; hNCAMΔCT) construct was created by PCR using pCX-MCS2/hNCAM140wt construct (Diestel *et al.*, 2007) as template, introducing a stop codon directly after the transmembrane domain; the PCR product was then introduced in the pCX-MCS2 vector; contains ampicillin resistance gene	
pGEX-4T-2	The plasmid contains the cDNA of the 26 kDa GST from *Schistosoma japonicum*, resulting in a GST-tag at the N-terminus of expressed proteins and an ampicillin resistance gene	Kindly provided by Prof. Dr. R. Horstkorte, Institute of Physiological Chemistry, Martin-Luther-University Halle-Wittenberg (GER)
pGEX-4T-2/ hNCAM140ID	The cDNA of hNCAM140ID was restricted from pcDNA3/hNCAM140ID with *Bam*HI and *EcoRI* and inserted in frame in the pGEX-4T-2 vector	Generation described in this work, vector map is provided in the appendix

2.8. Enzymes

Tab. 8: Enzymes

Name	Source
*Bam*HI	Fermentas, St. Leon-Rot (GER)
DNase	Böhringer, Mannheim (GER)
*Eco*RI	Fermentas, St. Leon-Rot (GER)
T4 DNA Ligase	Fermentas, St. Leon-Rot (GER)

2.9. Solutions, media, and buffers

All solutions, media, and buffers were prepared with ultrapure water, if not indicated otherwise.

2.9.1. General buffers

Phosphate buffered saline 1 (PBS[1])
137 mM NaCl
2.7 mM KCl
8.1 mM Na_2HPO_4
1.5 mM KH_2PO_4
pH 7.2

Phosphate buffered saline 2 (PBS[2])
137 mM NaCl
2.7 mM KCl
10 mM Na_2HPO_4
1.76 mM KH_2PO_4
pH 7.4

PBST[1]
PBS[1]
0.05 % (v/v) Tween® 20

PBST[2]
PBS[2]
0.5 % (v/v) Tween® 20

Tris buffered saline 1 (TBS[1])
20 mM Tris
137 mM NaCl
pH 7.6

Tris buffered saline 2 (TBS[2])
50 mM Tris
145 mM NaCl
pH 7.4

TBST[1]
TBS
0.5 % (v/v) Tween® 20

TBST[2]
TBS
0.1 % (v/v) Tween® 20

2.9.2. Buffers and solutions for bacterial culture

Medium for bacterial culture was autoclaved for 20 min and antibiotics added afterwards to warm medium.

Luria Bertani medium (LB) medium
10 g Tryptone
5 g Yeast extract
10 g NaCl
pH 7

LB-agar
LB media
1.5 % (w/v) Agar

Ampicillin stock
50 mg/ml, sterile filtered.
Final concentration: 50 µg/ml

Kanamycin stock
30 mg/ml, sterile filtered.
Final concentration: 30 µg/ml

2.9.3. Buffers and solutions for cell culture

Medium for CHO cells
DMEM or Ham's F-12
5 % or 10 % (v/v) FBS
10 µg/ml Gentamicin
0.25 µg/ml Amphotericin B

Medium for hippocampal neurons
Neurobasal® A medium
2 % (v/v) B-27
2 mM GlutaMAX™
2 ng/ml bFGF

2.9.4. Buffers for molecular biology (DNA-analysis)

TBE buffer
100 mM Tris
83 mM Boric acid
1 mM EDTA

TE buffer
10 mM Tris
1.3 mM EDTA

2.9.5. Buffers and solutions for protein biochemistry

2.9.5.1. Buffers and solutions for recombinant protein expression and purification

IPTG stock
100 mM IPTG, sterile filtered.
Final concentration: 1 mM

Lysis buffer for bacteria expressing His-tagged hNCAM180ID
PBS[1] (see 2.9.1)
1 % (v/v) Triton X-100
Protease inhibitors (see Tab. 9)

Lysis buffer for bacteria expressing GST-tagged hNCAM140ID
PBS[1] (see 2.9.1)
1 % (v/v) Triton-X-100
1 mM DTT
1 mM EDTA
Protease inhibitors (see Tab. 9)

Equilibration buffer
Lysis buffer
2 mM Imidazole
pH 8

Imidazole stock
1 M Imidazole

Washing buffer
50 mM NaH_2PO_4
20 mM Imidazole
300 mM NaCl
pH 8

Elution buffer
50 mM NaH_2PO_4
250 mM Imidazole
300 mM NaCl
pH 8

PBS-EW (equilibration and wash buffer)
1 x PBS[1] (see 2.9.1)
1 mM DTT
1 mM EDTA

TNGT (elution buffer)
50 M Tris, pH 8.0
0.1 M NaCl
50 mM reduced L-Glutathione
0.1 % (v/v) Triton-X-100
1 mM DTT

Tab. 9: Protease inhibitors for bacterial culture

Protease inhibitor	Stock	Dilution factor
Aprotinin	10 mg/ml in PBS[1] (see 2.9.1)	1:1000
Leupeptin	10 mg/ml in ultrapure water	1:1000
Peptstatin	1 mg/ml in 1:10 acedic acid:methanol	1:100
PMSF	100 mM in isopropanol	1:100

2.9.5.2. Buffers and solutions for the protein macroarray

Blocking buffer
Blocking buffer ODYSSEY

Blocking buffer/T
Blocking buffer ODYSSEY
50 % (v/v) PBST[1] (see 2.9.1)

Stripping buffer
2 % (v/v) SDS
65.5 mM Tris/HCl, pH 6.8
100 mM (v/v) β-Mercaptoethanol

2.9.5.3. Solutions for SDS-polyacrylamide gel electrophoresis (SDS-PAGE)

4 x Sample buffer (reducing)
260 mM Tris (pH 6.8)
40 % (v/v) Glycerine
12 % (w/v) SDS
20 % (v/v) β-mercaptoethanol
0.25 % (w/v) Bromophenol blue

Acrylamide/Bis-solution (30 %/0.8 %)
75 % (v/v) Rotiphorese® Gel 40

Tris-HCl solutions
1.5 M Tris, pH 6.8 (for stacking gel)
1.5 M Tris, pH 8.8 (for separation gel)

10 % SDS solution
10 % (w/v) SDS

10 % APS solution
10 % (w/v) APS

1 x MOPS running buffer
5 % (v/v) NuPAGE® MOPS SDS running buffer, 20 x
0.5 % (v/v) NuPAGE® Antioxidant, 200 x

10 x SDS running buffer
248 mM Tris
1.918 M Glycine
35 mM SDS

2.9.5.4. Solutions for silver and Coomassie Blue staining of polyacrylamide gels

Fixing solution for silver staining
10 % (v/v) Acetic acid
30 % (v/v) Ethanol

Washing solution for silver staining
20 % (v/v) Ethanol

Sensitizer for silver staining
0.8 mM $Na_2S_2O_3$

Silver solution for silver staining
11.8 mM $AgNO_3$
0.75 % (v/v) Formaldehyde (37 %)

Developer for silver staining
0.02 mM $Na_2S_2O_3$
0.5 % (v/v) Formaldehyde (37 %)
0.58 M Na_2CO_3

Stopping solution for silver staining
5 % (v/v) Acetic Acid

Coomassie Blue fixing & destaining solution
10 % (v/v) Acetic Acid
30 % (v/v) Ethanol

Coomassie Blue staining solution
Destaining solution
2 g/l Coomassie Brilliant Blue R-250

2.9.5.5. Solutions for Western blotting and immunological detection of proteins

Milk powder blocking buffer
1 x TBST[1] or PBS[2] (see 2.9.1)
5 % (w/v) skim milk powder

BSA blocking buffer
1 x PBS[2] (see 2.9.1)
3 % (w/v) BSA

Transfer buffer[1]
48 mM Tris
39 mM Glycine
1.3 mM SDS
20 % (v/v) Methanol

Transfer buffer[2]
25 mM Tris
192 mM Glycine
20 % (v/v) Methanol

Ponceau-S staining solution
0.2 % (w/v) Ponceau-S
3 % (v/v) Acetic acid (96 %)

Stripping buffer
0.5 M NaCl
0.2 M Glycine
pH 2.8

2.9.5.6. Solutions for co-immunoprecipitation (co-IP)

Homogenisation (HOMO) buffer
5 mM Tris (pH 7.4)
1 mM $MgCl_2$
1 mM $CaCl_2$
0.1 mM PMSF
EDTA-free protease inhibitor cocktail

Lysis buffer
50 mM Tris (pH 7.5)
150 mM NaCl
1 % (v/v) Triton X-100
1 mM Na4P2O7
1 mM NaF
2 mM Na3VO4
0.1 mM PMSF
EDTA-free protease inhibitor cocktail

2.9.5.7. Solutions for preparation of the cytosolic fraction of mouse brain tissue and *trans*-Golgi network (TGN) isolation

Sucrose-PKM buffer
100 mM KH_2PO_4 (pH 6.5)
5 mM $MgCl_2$
3 mM KCl
0.1 mM PMSF
EDTA-free protease inhibitor cocktail
0.5 M, 0.7 M, 1.1 M or 1.3 M sucrose

PEMS buffer
10 mM PIPES (pH 7.0)
1 mM EGTA
2 mM $MgCl_2$
0.25 M Sucrose
0.1 M PMSF
EDTA-free protease inhibitor cocktail

2.9.5.8. Buffers and solutions for enzyme linked immunosorbent assay (ELISA)

Sodium carbonate buffer
8 % (v/v) 0.2 M Na_2CO_3
92 % (v/v) 0.2 M $NaHCO_3$
pH 9.2

Citric buffer
48.5 % (v/v) 0.1 M Citric acid
51.5 % (v/v) 0.2 M Na_2HPO_4
pH 5.0

Detection solution
0.1 M Citric buffer (pH 5.0)
0.05 % (v/v) H_2O_2 (30 %), freshly added
9.2 mM OPD

3. Methods

3.1. Molecular biology

3.1.1. Heat shock transformation

Competent *E. coli* bacteria (XL1 Blue *(TOP10)* for DNA preparation, BL21 (DE3) for protein expression) were thawed on ice and 50 µl bacteria suspension added to 50-100 ng of plasmid DNA. In case of ligation, the complete ligation mix was used for transformation. The bacteria/DNA mixture was mixed gently and incubated on ice for 30 min. To facilitate the introduction of the DNA into the cell, a heat shock was performed at 42°C for 1 min *(45 sec)* in a water bath and samples were placed back on ice immediately for 2 min. 450 µl LB medium *(250 µl S.O.C. medium)* were added to the bacteria and the solution incubated under constant shaking (220 rpm) for 30-60 min *(1.5 h)* at 37°C. Finally, 100 and 400 µl *(50 and 200 µl)* cell suspension were spread onto pre-warmed agar plates containing the appropriate antibiotic (ampicillin or kanamycin). Plates were incubated for 16 h at 37°C.

3.1.2. Plasmid isolation from *E. coli* cultures

Plasmid isolation from 5 ml cultures (Minipreps)

5 ml LB medium containing the appropriate antibiotic (LB/antibiotic) were inocculated with a single bacteria colony and incubated overnight at 37°C under constant agitation. Plasmids were isolated from the bacteria using GeneJET™ Plasmid Miniprep Kit according to manufacturer's instructions (Fermentas). DNA was stored at -20°C.

Plasmid isolation from 50 ml or 200 ml cultures (Midipreps)

For preparation of large quantities of DNA (up to 100 µg of plasmid DNA), 50 ml (for high copy plasmids) or 200 ml (for low copy plasmids as pBJG1) LB/antibiotic were inocculated with a single colony and incubated overnight at 37°C under constant agitation. DNA was isolated by means of a Plasmid Midi Kit as described in the manufacturer's protocol (Qiagen). DNA was stored at -20°C.

3.1.3. Agarose gel electrophoresis

Gels containing 0.8 % or 1 % (w/v) agarose were prepared by boiling the appropriate amount of agarose in 50 ml TBE buffer in a microwave oven. The solution was allowed to cool down to approximately 60°C before ethidium bromide was added in a final concentration of 0.4 µg/ml. The melted agarose was poured into the gel tray containing a well comb and gel allowed to solidify. The gel tray was put into the electrophoresis apparatus, which was filled with TBE buffer until the gel was covered and subsequently the well comb was removed. Samples and molecular weight marker were mixed with loading dye and loaded into the wells

of the gel. Gel run was performed at 80 V for approximately 1 h. DNA bands were visualized using an UV-transilluminator.

3.1.4. Restriction analysis and purification of cDNA

For subcloning or analysis of cDNA-constructs, 5 µg or 200-300 ng cDNA, respectively, were mixed with the respective enzyme buffer and the enzyme according to manufacturer's protocol and adjusted with ultrapure water to a total volume of 20 µl. The samples were incubated for 1-1.5 h at 37°C.

Generation of the pGEX-4T-2/hNCAM140ID construct was done by digestion of pcDNA3/hNCAM140ID and pGEX-4T-2 with *Bam*H1 and *Eco*R1. cDNAs were digested with *Bam*H1 and subsequently purified to remove enzyme by means of the DNA Clean & Concentrator Kit according to manufacturer's instructions (Zymo Research). The cDNAs were digested with *Eco*R1 and samples subjected to agarose gel electrophoresis. To extract the cDNAs from the agarose gels, the gel area containing the respective cDNA fragment was cut out and eluted from the gel by using QIAquick Gel Extraction Kit according to manufacturer's protocol (Qiagen). After determination of the cDNA concentration, ligation of both cDNA fragments followed.

3.1.5. Photometric nucleic acid determination

The DNA was diluted 1:100 in ultrapure water and concentration was determined by its UV absorbance at 260 nm (an absorbance of 1 is equivalent to 50 µg DNA/ml) and the plasmid purity by the ratio of A260nm/A280nm using a spectrophotometer. The sample is pure, when the value is between 1.8 and 2.0.

3.1.6. Ligation

Ligation of a DNA insert and a vector was performed by using T4 DNA ligase according to manufacturer's instructions (Fermentas).

To generate the pGEX-4T-2/hNCAM140ID construct, pcDNA3/hNCAM140ID and pGEX-4T-2 were digested with *Bam*H1 and *Eco*R1 (see 3.1.4) and the products used for ligation with insert (hNCAM140ID) : vector (pGEX-4T-2) ratios of 2:1 and 3:1. Samples were incubated overnight at 16°C and afterwards heat shock transformation was performed (see 3.1.1). The correctness of the ligation product was tested by restriction analysis (see 3.1.4).

3.2. Protein-biochemical methods

3.2.1. Expression of recombinant proteins in *E. coli*

Competent BL21 (DE3) bacteria were transformed (see 3.1.1) with the expression plasmid and spread on agar plates containing the appropriate antibiotic. 5 ml LB/antibiotic were

inocculated with a single bacteria colony and incubated overnight at 37°C with constant agitation (220 rpm). Bacteria suspension was transferred into fresh LB/antibiotic in the ratio of 1:50 and incubated at 37°C under constant agitation until the culture reached the optical density $(OD)_{600}$ of 0.4-0.6. Protein expression was induced by adding IPTG (1 mM final concentration) and the culture was further incubated at 37°C for 3.5 h (hNCAM180ID) or at 20°C for 24 h (hNCAM140ID). Bacteria were collected by centrifugation (4500 x g, 10 min, 4°C). Bacteria pellets were resuspended in 12 ml PBS[1]/1 % Triton X-100 per liter bacteria culture and samples either stored at -80°C or directly lysed.

3.2.2. Lysis of bacteria

Protease inhibitors (Tab. 9) were added to the bacteria pellets resuspended in PBS[1]/1 % Triton X-100. For hNCAM140ID, EDTA and DTT at a final concentration of 1 mM each were added additionally. Lysis was done by 7-10 freezing/thawing cycles with liquid nitrogen and a warm water bath, followed by treatment with a Potter homogenizer. To reduce the viscosity of the lysate, 10 µg/ml DNase were added and incubated on ice for 2.5 h. The lysate was centrifuged (27.000 x g, 30 min, 4°C) and the supernatant collected for purification. Pellets were resuspended in PBS[1]/1 % Triton X-100 and stored at -80°.

3.2.3. Recombinant protein purification

Just before purification, lysates were centrifuged vigorously (100000 x g, 30 min, 4°C) to spin down any cell debris which otherwise could clog the chromatography columns.

3.2.3.1. Purification of His-tagged hNCAM180ID by Ni-NTA affinity chromatography

Recombinant proteins containing a poly-His-residue can be purified by Ni-NTA chromatography. NTA is linked to agarose and binds Ni^{2+}-ions, which in turn bind the His-residues of the proteins via their imidazole ring. Ni-NTA bound proteins are eluted by buffers containing high imidazole concentrations (100-250 nm). Imidazole binds also to Ni^{2+}-ions and will lead to dissociation of the His-tagged proteins.

For protein purification, a XK-16 column was packed with 15 ml Ni-NTA agarose and connected to a peristaltic pump. Purification was performed according to the Qiagen protocol (Qiagen, 2003) and all steps were done at 4°C. If the Ni-NTA was used for the first time, it was washed with ultrapure water, 0.1 M EDTA, 0.5 M NaOH, and 0.1 M nickel sulfate. Between the washing steps, 2 column bed volumes (CV) of ultrapure water were applied. Before each purification, the Ni-NTA resin was equilibrated with 4 CV of equilibration buffer. Imidazole was added to the hNCAM180ID-lysate in a final concentration of 2 mM, the lysate applied to the column and incubated with the Ni-NTA overnight circulating with a flow rate of approximately 0.5 ml/min. The next day, the flow rate was increased to 1 ml/min to collect the lysate (flow-through fraction) and the column washed with 4 CV washing buffer. Two

separate fractions of 2 CV each were collected: washing fraction 1 (W1) and washing fraction 2 (W2). Afterwards, 4 CV elution buffer were applied and the eluate also collected in fractions: elution fraction 1-3 (E1-3) of 10 ml each and a final elution fraction 4 (E4) of 30 ml. The flow-through, washing and elution samples were analyzed by SDS-PAGE and stored at -80°C. The column was washed with 4 CV each of PBS[1], ultrapure water, 0.5 M NaOH, and again ultrapure water, and stored in 30 % (v/v) ethanol at 4°C.

3.2.3.2. Purification of GST-tagged hNCAM140ID by glutathione affinity chromatography

GST or GST-tagged proteins can be purified by GSH, which is stably immobilized on agarose or sepharose. The disruption of the binding and elution of GST or GST-tagged proteins takes place by competitive excess of reduced GSH. The purification was performed with a XK-16 column packed with 6 ml GSH superflow resin, which was connected to a peristaltic pump. All steps of purification were done at 4°C and according to the Qiagen protocol for purification of GST-tagged proteins using GSH superflow cartridges (Qiagen, 2009). The resin was equilibrated with 10 CV of buffer PBS-EW. The lysate loaded to the resin and incubated overnight circulating with a flow rate of approximately 0.5 ml/min. The flow through was collected and the column washed with 10 CV of buffer PBS-EW in two washing fractions (W1 and W2) of the same volume at an approximate flow rate of 2 ml/min. Afterwards, the flow rate was reduced to 0.5 ml/min again and GST-tagged proteins were eluted with 10 CV of TNGT elution buffer, collected in four fractions: E1-3 of 6 ml each and E4 with the remaining volume of 42 ml. The flow-through, washing, and elution fractions were analyzed by SDS-PAGE followed by staining of the gel or Western blotting and stored at -80°C. The resin was cleaned with 0.1 M NaOH (at least 2 CV), and 0.1 M HCl (2 CV), and washed with 5 CV of buffer PBS-EW. The resin was reused or prepared for storage at 4°C by applying 5 CV of 20 % (v/v) ethanol.

3.2.4. Concentration and fluorescent labeling of hNCAM180ID and hNCAM140ID

A concentration of 1-15 mg/ml of pure protein was needed for protein macroarray performance. Therefore, the hNCAM180ID and hNCAM140ID eluates were concentrated using 30 kDa (EMD Millipore) and 50 kDa cut-off columns (Sartorius), respectively, according to manufacturer's instructions. The volumes of eluates were reduced by centrifugation at 2500-3000 x g at 4°C and the concentrators refilled with PBS[1]. The samples were concentrated again and the process repeated at least 3 times, until the Triton concentration was sufficiently reduced (≤ 0.01 %, according to manufacturer's protocol) and the eluates concentrated to a minimum of 1 mg/ml. For the protein macroarray, approximately 680 µg (15 nM) of hNCAM180ID and 1377 µg (14 nM) of hNCAM140ID were fluorescently labeled with DYOMICS DY-633 Fluorophore. The labeling and purification was performed according

to manufacturer's instructions using Fluoro Spin 681, Protein Labeling & Purification Kit (Emp Biotech).

3.2.5. Protein macroarray

The protein macroarray consists of two membranes which together exhibit 24000 His-tagged expression clones of human fetal brain proteins. Protein expression was carried out by the manufacturer in an *E. coli* based expression system for recombinant proteins, and proteins were immobilized on a 22 cm x 22 cm PVDF membrane surfaces. One membrane contains 2/3 (Part 8, Id. 367.60.515) and the other 1/3 (Part 9, Id. 367.56.521) of all expression clones. By incubation of fluorescently labeled hNCAM180ID (part 8) and hNCAM140ID (part 8 and 9), respectively, with the membranes and analysis of positive spots, yet unknown interaction partners of NCAM-ID were identified.

Prior to incubation with the proteins, the membranes were rinsed in 96 % ethanol for 1-2 min under constant shaking to lyse bacterial colonies followed by washing 5 times with ultrapure water. The solution was changed to PBS[1] and excess colony material was carefully wiped-off using paper tissue. After washing in PBS[1] 3 times for 5 min, all bacterial traces were removed. The membranes were incubated with 50 ml blocking buffer for 2 h under constant agitation. Subsequently, labeled NCAM was diluted in 50 ml blocking buffer/T and incubated overnight at 4°C under constant agitation and light protection. The next day, the solution was discarded and the membranes washed 4 times for 1 h with PBST[1] and 2 times for 15 min with PBS[1] protected from light. Signals were detected using the Licor ODYSSEY scanner. For removal of bound proteins, the membranes were agitated in 70°C hot stripping buffer for 30 min and washed with PBS[1] for 1 h. To determine expression levels of spotted proteins, the membranes were blocked with blocking buffer and incubated with Anti-His IRDye™ 800-antibodies in 50 ml blocking buffer/T overnight, as described above. The membranes were washed, scanned, stripped again (see above), and stored at 4°C in PBST[1] containing 0.02 % sodium azide. The resulting images were analyzed with Aida™ Image Analyzer software version 4.24 and Aida™ Array Compare software.

3.2.6. Determination of protein concentrations

Protein concentrations were determined using the DC-protein assay. First, a BSA serial dilution ranging from 0.0195 mg/ml to 5 mg/ml was prepared. 5 µl of the samples and standard dilutions were pipetted in triplicates into wells of a 96-well microtiter plate and incubated with 25 µl of a mixture of solution S and A (ratio 1:50) and 200 µl of reagent B for 15 min at room temperature (RT). The extinctions of the samples were determined at 690 nm wave length in an ELISA reader (Titertek PLUS MS2, ICN Biomedicals or POLARstar

Omega, BMG Labtech) and the protein concentration analyzed by means of the software GraphPad Prism 6.

3.2.7. SDS-PAGE

Protein samples were separated by SDS-PAGE. According to the size of proteins, separation gels contained different percentages of acrylamide (8 % or 10 %). The stacking gels always contained 4 % of acrylamide.

For electrophoresis, either NuPAGE® Bis-Tris precast gels were used with MOPS running buffer and the XCell SureLock® Mini-Cell Electrophoresis System or gels were self-prepared. For 2x1.5 mm thick gels, the separation and stacking gel ingredients were mixed as described in the table below. TEMED was added just before casting of the gels.

Tab. 10: Composition of self-prepared gels for SDS-PAGE

Solutions (ml)	8 % separation gel	10 % separation gel	4 % stacking gel
Ultrapure water	9.3	7.9	4.1
Acrylamide/Bis-solution (30 %/0.8 %)	5.3	6.7	1.0
1.5 M Tris-HCl	5.0 (pH 8.8)	5.0 (pH 8.8)	0.75 (pH 6.8)
10 % SDS-solution	0.2	0.2	0.06
10 % APS-solution	0.2	0.2	0.06
TEMED	0.012	0.008	0.006

20 ml of separation gel and approximately 6 ml of stacking gel solutions were prepared for 2x1.5 mm thick gels.

The separation gel solution was poured into the gel casting form and the top of the gel covered with isopropanol. When the gel was polymerized, isopropanol was removed, the stacking gel solution poured on top of the separation gel and the well comb inserted. After polymerization of the entire SDS-PAGE, the well comb was removed and the chamber was assembled as described by the manufacturer's protocol (Mini-PROTEAN® Electrophoresis System, Bio-Rad) using SDS running buffer.

Samples were diluted with appropriate amount of SDS sample buffer (reducing or non-reducing, see Tab. 4 and 2.9.5.3) and boiled for 5 min at 95°C *(10 min at 70°C)* when reducing conditions were set up. Samples were mixed, centrifuged and loaded into the wells of the gel. A molecular weight marker was also applied. The precast gels were run at constant 150 V and the self-prepared gels at 35 mA for approximately 30 min and then at 40 mA. The run was stopped when the blue bromophenol running front had reached the bottom of the gel. Gels were either stained or subjected to Western blotting.

3.2.8. Silver staining of polyacrylamide gels

Silver staining has a detection limit of 10-50 ng of protein and is thereby a very sensitive method for staining of proteins separated by SDS-PAGE. Ag^+ binds to amino acid residues of proteins and is subsequently reduced by formaldehyde to elemental silver that appears black. All steps were performed under constant agitation. The gel was fixed with fixing solution for silver staining 3 times for 30 min and washed for 10 min in washing buffer and for 20 min in water. Then, the gel was incubated in sensitizer for 1 min and washed twice with water for 30 sec, followed by incubation in silver solution for 30 min and again washing with water for 30 sec. The gel was incubated in developer until all protein bands were visible. The reaction was stopped by immersing the gel in stopping solution.

3.2.9. Coomassie staining of polyacrylamide gels

The Coomassie dye binds with a detection limit of approximately 100 ng to amino groups of proteins as well as through van der Waals forces. After SDS-PAGE, the gels were fixed in fixing solution for Coomassie staining for 15-30 min and subsequently incubated with Coomassie Blue staining solution for 1-2 h under constant agitation. Gels were incubated in destaining solution for 1-16 h until the background of the gel appeared clear.

3.2.10. Western Blot (semi-dry)

Following electrophoresis, proteins were electroblotted onto nitrocellulose or PVDF membranes. Prior to use, PVDF membranes were activated by soaking in methanol for 45 sec and washed 2 times for 5 min with water. The gel, membrane and filter paper were equilibrated in transfer buffer[1] *(transfer buffer[2])* for 30 min at constant agitation. The blotting sandwich was assembled according to manufacturer's protocol (Bio-Rad) and proteins transferred at 1 mA/cm^2 for 1.5 h *(5 mA/cm^2 for 45 min in a pre-cooled chamber and ice on top during the transfer)*. Blots were washed once with PBS[1] *(PBS[2])*. The successful protein transfer was either monitored by using prestained molecular weight marker or by incubating in Ponceau-S staining solution for about 1 min and washing with water until protein bands were clearly visible. Staining was removed by briefly incubating the membrane in hot PBS[1].

3.2.11. Immunological detection of proteins on nitrocellulose or PVDF membranes

Membranes were blocked with milk powder or BSA blocking buffer for 1-2 h at RT. All incubation and washing steps were performed under constant agitation. Membranes were washed 3 times for 5 min in TBST[1] *(briefly with PBS[2])* and incubated with appropriate primary antibodies applied in milk powder or BSA blocking buffer overnight at 4°C. The unbound primary antibodies were removed by washing the membranes 3 times for 5 min with TBST[1] *(3 times for 10 min with PBST[2])*, followed by incubation with corresponding peroxidase

(POD)-conjugated secondary antibodies in milk powder or BSA solution for 1-2 h at RT. Membranes were washed again 3 times for 5 min with TBST[1] *(3 times for 10 min with PBST[2])* and 2 times briefly with TBS[1] *(TBS[2])*. Immunoreactive bands were visualized either by means of the chemiluminescence-system MicroChemi 4.2 and ECL Western blotting reagent or ECL Pro Enhanced Oxidizing reagent or by exposing the membranes manually to X-ray films. Super Signal® West Pico or Dura solutions were used according to manufacturer's protocols and membranes were exposed to the film for different time periods depending on the strength of the chemiluminescence signal, then the film incubated in developer for 30 sec, washed briefly in water and fixed for approximately 2 min in fixing solution. Band intensities were quantified using ImageJ Software.

3.2.12. Removal of antibodies for re-probing of Western blots (stripping)

For detection of several proteins on a Western blot, bound antibodies were stripped by shaking the membrane in stripping buffer for 2-10 min at RT, then neutralized by incubation for several minutes in 20 mM Tris-HCl (pH 8.8) and washed 3 times for 10 min with PBST[2]. Membranes were subjected to immunological detection of proteins as described above.

3.2.13. Co-IP

For co-IP experiments, the brain of a 1 day old mouse was homogenized in cold HOMO buffer containing 0.32 M sucrose using a pre-cooled Potter homogenizer on ice. Protein concentration was determined (see 3.2.6) and 1 mg of total protein was lysed with ice-cold lysis buffer for 30 min at 4°C. All following centrifugation and incubation steps were performed at 4°C. The lysates were centrifuged at 20000 x g for 15 min. Supernatants were collected and pre-cleared with 30 µl protein A/G-agarose beads for 3 h under constant gentle rotation. Samples were centrifuged for 2 min at 2000 x g and supernatants transferred into new aliquots. Approximately 5 µg of rabbit polyclonal antibodies against KLC1 or nonspecific IgG (control) were added to the samples and incubated overnight under constant gentle rotation. The next day, complexes were precipitated with 30 µl protein A/G-agarose beads applied for 3 h under constant gentle rotation. Samples were centrifuged for 2 min at 2000 x g and beads were washed 2 times with ice-cold lysis buffer and 1 time with ice-cold TBS[2]. All centrifugation steps in between the washing steps were performed at 2000 x g for 2 min. Complexes were eluted from beads with 100 µl non-reducing Laemmli buffer to detect KLC1 in Western blot. For detection of NCAM, 10 µl of 1 M DTT was added to samples, samples were boiled for 10 min at 70°C, and applied to SDS-PAGE followed by Western blot analysis.

3.2.14. Isolation of TGN organelles

Isolation of TGN organelles was performed with some modifications as described previously (Sytnyk *et al.*, 2002; Fath & Burgess, 1993). All steps were performed on ice or at 4°C. Brains from 1 to 3 day old mice were homogenized in ice-cold PKM buffer (3 ml/brain) with 0.5 M sucrose using a Potter homogenizer. Brain homogenates were centrifuged at 600 x g for 10 min. The supernatant was collected and centrifuged on a discontinuous density gradient of 0.7/1.3 M sucrose-PKM buffer at 105000 x g for 1 h. The supernatant containing the cytosol was collected and stored at -20°C. The concentrated membranes at the 0.7/1.3 M sucrose-PKM buffer interface were collected, adjusted to 1.25 M sucrose-PKM buffer, overlaid with 1.1 M and 0.5 M sucrose-PKM buffer, and centrifuged at 90000 x g for 1.5 h. The Golgi stacks were collected at the 0.5/1.1 M interface, adjusted to 0.7 M sucrose-PKM, and then centrifuged at 10000 x g for 15 min to pellet Golgi stacks. The small TGN-containing membranes remaining in the supernatant were collected by centrifugation at 259000 x g for 30 min. The membranes were resuspended in PEMS buffer. Samples of different fractions (brain homogenate, cytosol, TGN organelles, and Golgi stacks) were analyzed by Western blot.

3.2.15. Preparation of the cytosolic fraction of mouse brain tissue

Brains from 1 to 3 day old mice were homogenized in ice-cold 0.5 M sucrose-PKM buffer (3 ml/brain) using a Potter homogenizer. Brain homogenates were centrifuged at 100000 x g for 1 h at 4°C. Supernatant (cytosol) was collected and used as source for KLC1 in ELISA and pull-down assay.

3.2.16. ELISA

Rabbit polyclonal antibodies against KLC1 (1 µg/ml in sodium carbonate buffer pH 9.6, 50 µl/well) were adsorbed to the surface of wells of 96-well MICROLON 600 plates overnight at 4°C in humid atmosphere. Wells were washed 3 times for 5 min with 200 µl TBS^2 and blocked with 150 µl of 1 % BSA in TBS^2 for 1 h at 37°C. Wells were washed as described before and incubated with 50 µl/well of the cytosolic fraction of mouse brain tissue (see 3.2.15) diluted 1:10 in $TBST^2$ for 1 h at 37°C. Wells were washed 3 times for 5 min with 200 µl $TBST^2$. Increasing concentrations of chemically synthesized biotinylated peptides corresponding to amino acid sequences 748-763 ($NCAM\text{-}ID_{748\text{-}763}$), 764-777 ($NCAM\text{-}ID_{764\text{-}777}$), and 756-770 ($NCAM\text{-}ID_{756\text{-}770}$) of mouse NCAM140 diluted in $TBST^2$ (50 µl/well) were incubated for 1 h at 37°C. Wells were washed with $TBST^2$ as described above and incubated for 1 h at 37°C with POD-conjugated NeutrAvidin diluted 1:5000 in $TBST^2$ containing 1 % BSA (50 µl/well). After repeated washing with $TBST^2$ as described above, color reaction was developed with 150 µl detection solution/well containing OPD and

H_2O_2. The OD was measured at 450 nm with an ELISA reader (POLARstar Omega, BMG Labtech).

3.2.17. Pull-down assay

All steps were performed on ice or at 4°C and with ice-cold solutions. For immunopurification and immobilization of KLC1, the cytosolic fraction of mouse brain tissue (see 3.2.15) was pre-cleared with 30 µl protein A-agarose beads for 3 h under constant agitation. Samples were centrifuged at 2000 x g for 2 min and supernatants transferred into new tubes. Approximately 14 µg of polyclonal rabbit KLC1 antibodies were added and incubated overnight under constant agitation. Complexes were precipitated with 120 µl protein A-agarose beads for 7 h under rotation. Beads were washed 5 times with 2 ml $TBST^2$ and centrifuged at 2000 x g for 2 min in between the washing steps. Beads were aliquoted in four tubes and incubated with chemically synthesized biotinylated peptides NCAM-$ID_{748-763}$, NCAM-$ID_{764-777}$, and NCAM-$ID_{756-770}$ of mouse NCAM140 diluted 1:2000 in $TBST^2$ in a total volume of 1 ml. Purified PAK1 (120 x the amount of peptide, kindly provided by Iryna Leshchyns'ka; described in Li *et al.*, 2013) was added where indicated. Samples were incubated overnight under constant rotation. Beads were collected by centrifugation at 2000 x g for 2 min and washed 4 times with $TBST^2$ as described above. Proteins were eluted with 60 µl 0.2 M glycine buffer (pH 2.0) and 12 µl 1 M Tris (pH 8.0) were added immediately for neutralization. Samples of bound proteins and input material (peptides diluted 1/2000 in $TBST^2$) were applied onto a Slot blot with activated PVDF membrane (see 3.2.10 for PVDF activation) and probed for peptides with POD-conjugated NeutrAvidin (1:30000 in 1 % BSA in $TBST^2$) after blocking of the membrane (3 % BSA in $TBST^2$).

3.3. Cell culture and immunofluorescence

3.3.1. PDL coating of glass coverslips for cell culture

Coverslips were cleaned thoroughly by treatment with ultrasound for 30 min in acetone. The procedure was repeated with ethanol. Subsequently, coverslips were washed a few times with sterile ultrapure water and incubated in sterile PDL (100 µg/ml) solution at 37°C for 2 h under constant shaking. After one more washing step with sterile ultrapure water, coverslips were spread onto aluminium foil, which was sterilized with 70 % ethanol, and dried overnight under UV light in the laminar flow hood.

3.3.2. CHO cells

3.3.2.1. Cell culture of CHO cells

CHO cells were cultured in 75 cm^2 culture flasks in DMEM or Ham's F-12 containing FBS and antibiotics at 37°C, a CO_2 level of 5 %, and > 95 % relative humidity. If not indicated otherwise, the term medium refers to DMEM or Ham's F-12 supplemented with FBS and antibiotics. At a confluency of 80-90 %, cells were washed with FBS- and antibiotic-free medium and detached from the flask bottom with Trypsin-EDTA. Trypsinization was either stopped by adding medium when cells were plated on coverslips for transfection or Trypsin-EDTA-cell solution was transferred into a new flask containing medium for further cultivation.

For long time storage, cells were frozen in cryovials. Therefore, the trypsinized cells were transferred into a 15 ml tube containing medium. The cells were pelleted by centrifugation for 7 min at 180 x g. After removal of the supernatant, the cells were resuspended in 1.8 ml medium. 10 % DMSO was added, the cell suspension aliquoted into two cryovials and frozen immediately at -80°C or liquid nitrogen for long time storage. Cells were thawed by adding medium into the cryovial and transferring the cell solution into 9 ml medium in a 15 ml tube. After centrifugation (170 x g, 7 min, RT), cells were resuspended in 1 ml medium and transferred in a culture flask containing fresh medium.

3.3.2.2. Transfection of CHO cells

One day before transfection, cells were plated on PDL coated glass coverslips (see 3.3.1) in 2 cm^2-wells of a 24-well plate in medium containing 10 % FBS. The CHO cells were 90-95 % confluent the next day and then transfected with Lipofectamine™ 2000. Solutions were prepared in Eppendorf tubes. Per well, 1-1.25 µg cDNA in total (when co-transfected with the cDNA of peptides: 2-fold the amount of peptide-cDNA) was diluted in 50 µl DMEM and mixed gently. Afterwards, 2 µl Lipofectamine™ 2000 were diluted in 50 µl DMEM for each well, mixed gently and incubated for 5 min at RT. The diluted Lipofectamine™ solution was combined with the prepared cDNA solution, mixed gently, and incubated for 20 min at RT. The complexes were added to the cells on the plate. The suspensions were mixed by rocking the plate gently and cells were finally incubated in the incubator for 40-42 h under conditions as described above.

3.3.2.3. Immunofluorescence labeling of CHO cells

To label cell surface NCAM, CHO cells were placed and kept on ice until indicated otherwise to inhibit endocytosis. All antibodies were applied in DMEM containing 10 % FBS. Primary antibody against hNCAM-ED (ERIC 1; for dilution factors of antibodies see Tab. 5) was applied to living cells for 20 min. Cells were washed carefully 3 times for 5 min with ice-cold

PBS^2 and incubated with corresponding anti-mouse-CY5-conjugated secondary antibodies for 15 min protected from light. Cells were washed again with ice-cold PBS^2 as described above and fixed with 4 % PFA in PBS^2 for 15 min at RT. After one more washing step with PBS^2, cells were embedded in FluorPreserve™ reagent, if no other staining was performed. Otherwise, cells were washed 3 times for 5 min with PBS^2 at RT and permeabilized with 0.25 % Triton X-100 in PBS^2 for 5 min, followed by one washing step with PBS^2. Cells were blocked with 1 % BSA in PBS^2 for 20 min and solution changed to PBS^2. To stain intracellular NCAM, ERIC 1 antibody was applied overnight at 4°C. Cells were washed 3 times for 10 min with PBS^2 and anti-mouse-CY3-conjugated secondary antibodies applied for 45 min at RT. After another washing step with PBS^2 (3 times, 10 min), coverslips were embedded in FluorPreserve™ reagent.

3.3.3. Primary neurons

3.3.3.1. Cultures of hippocampal and cortical neurons

Cultures of hippocampal or cortical neurons were prepared from postnatal day 2 C57Bl6 mice by Dr. V. Sytnyk and maintained in Neurobasal® A medium supplemented with B-27, GlutaMAX™ and bFGF on glass coverslips coated with PDL.

3.3.3.2. Immunofluorescence labeling of endogenous proteins of cultured hippocampal neurons

Cultured hippocampal neurons were fixed with 4 % PFA in PBS^2 for 15 min. Neurons were washed with PBS^2 3 times for 5 min and cell membranes were permeabilized by incubating neurons with 0.25 % Triton X-100 in PBS^2 for 5 min. After washing once with PBS^2, neurons were blocked with 1 % BSA in PBS^2 for 20 min. All antibodies were applied in 0.1 % BSA in PBS^2. Primary antibodies were applied overnight at 4°C, neurons were washed again 3 times for 5 min, and incubated with corresponding secondary antibodies for 45 min at RT protected from light. Neurons were washed as described above and coverslips embedded in FluorPreserve™ reagent.

3.3.3.3. Transfection and immunofluorescence labeling of cultured cortical neurons

Cortical neurons were prepared from mouse brain tissue and transfected before plating using Neon® Transfection System according to the manufacturer's instructions (Life Technologies™). After 1 day *in vitro* (DIV), neurons were fixed, washed, and blocked as described above for hippocampal neurons (see 3.3.3.2), but without permeabilization of the neurons. Cell surface hNCAM180 was labeled by incubation of ERIC 1 antibody for 1 h at RT, neurons were washed 3 times for 5 min with PBS^2, and anti-mouse-CY3-conjugated

secondary antibodies applied for 45 min at RT protected from light. Neurons were washed again and coverslips embedded as described (3.3.3.2).

When NCAM endocytosis was stimulated (NCAM-triggering), neurons were transfected and cultured for 1 day before living cortical neurons were incubated with ERIC 1 antibody (2 µg/ml) for 1 h at 37°C and washed 3 times for 5 min with PBS^2. All following steps were performed at RT. Neurons were fixed with 4 % PFA in PBS^2 for 15 min. After washing as described above, neurons were blocked with 5 % donkey serum in PBS^2 for 15 min and labeled with anti-mouse-CY3-conjugated secondary antibodies applied in 1 % donkey serum in PBS^2 for 30 min to visualize cell surface NCAM. Neurons were washed again 3 times for 5 min with PBS^2 and post-fixed with 2 % PFA in PBS^2 for 5 min, washed as described, and treated with 0.25 % Triton X-100 in PBS^2 for 5 min to permeabilize membranes. Neurons were washed once with PBS^2, followed by blocking with 5 % donkey serum in PBS^2 for 20 min. Solution was changed to PBS and anti-mouse-CY5-conjugated secondary antibodies applied for 45 min to visualize cell surface and during the incubation time internalized NCAM. Coverslips were embedded in FluorPreserve™ reagent.

3.3.4. Immunofluorescence acquisition and quantification

Images of CHO cells and primary neurons were acquired at RT using confocal laser scanning microscope (LSM) 510, LSM510 software, and oil Plan Apo VC 60x objective with numerical aperture 1.4. Quantification of immunofluorescence staining and fluorescence intensities were performed with ImageJ software by manually outlining of cells and measuring mean immunofluorescence intensities within the outlines. Plot profiles were conducted with ImageJ by manually drawing a line within areas of co-localization and measurement of the intensities of the respective labeling along the line. The contrast and brightness of images of exemplary cells were further adjusted in ImageJ. Graphs were made by means of Graphpad prism 6 software.

3.3.5. Statistical analyzes of immunofluorescence experiments

All statistical analyzes were done by means of Microsoft Office Excel 2007 and GraphPad Prism version 6. Datasets with three groups were analyzed by one-way analysis of variance (ANOVA), followed by Dunnett's multiple comparison test. Analyzes of two groups were performed by unpaired t-test (two-tailed). The strength of a linear relationship between two sets of data was measured by Pearson's correlation coefficient (r). Statistical significance was assumed at $p < 0.05$.

4. Results

4.1. Identification of potential interaction partners of hNCAM180ID and hNCAM140ID by protein macroarray

For the identification of novel interaction partners of human NCAM-ID (hNCAM-ID) a protein macroarray containing 24000 expression clones of human fetal brain was performed. Therefore hNCAM180ID and hNCAM140ID were recombinantly expressed and purified by ligand chromatography. After incubation with the macroarray membrane, expression clones which bound the purified hNCAM-ID isoforms were analyzed and the interaction further investigated.

4.1.1. Expression and purification of hNCAM180ID

The ID of hNCAM180 was cloned by H. Faraidun (Faraidun, 2008) into the prokaryotic expression vector pBJG1, which contains an 8x His-tag. After overexpression in *E. coli* BL21 (DE3) bacteria, cells were lysed, centrifuged, and the soluble fraction containing hNCAM180ID was used for purification by Ni-NTA chromatography. The pellet (P) was resuspended in PBS/Triton. After preparing the column with Ni-NTA sepharose and loading the hNCAM180ID sample, the flow-through was collected, followed by multiple washing and elution steps. Purification samples were separated by SDS-PAGE followed by Western blotting and probing of the membrane with NCAM-ID specific antibody 5B8. As shown in Fig. 4 A, no signals appeared in the flow-through (FT) and washing fractions (W1/2), which confirmed a strong binding of NCAM to the Ni-NTA. The increased amount of imidazole in the elution buffer led to a disruption of the Ni-NTA/His-NCAM interaction and elution of NCAM, which was visible as 85 kDa band in the second elution fraction (E2). NCAM antibody was removed from the membrane before it was reprobed with tetra-His antibody (Data not shown), confirming the presence of the His-tag and translation of the complete construct as the tag is located at the C-terminus.

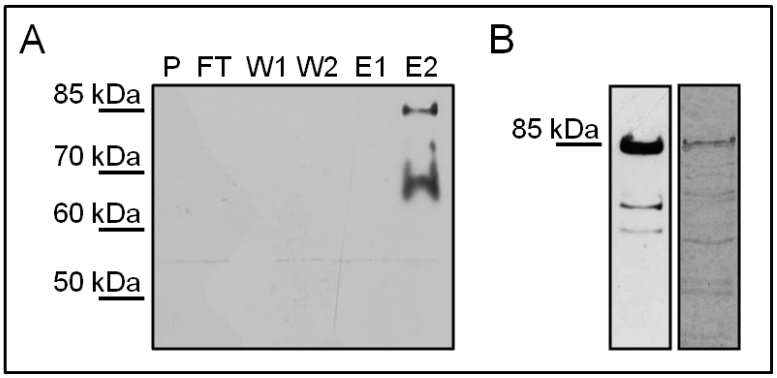

Fig. 4: Analysis of the purification fractions and the concentrate of hNCAM180ID

(A) Pellet (P), flow-through (FT), washing (W1/2), and elution fractions (E1/2) were separated by SDS-PAGE followed by Western blotting and probing with 5B8 antibody. **(B)** The hNCAM180ID concentrate was separated by SDS-PAGE followed by Western blotting and probing with 5B8 antibody (left) or silver staining of the gel (right).

For macroarray performance, a concentration of 1-15 mg/ml of pure protein was needed. Therefore, the eluted protein was concentrated to a final protein concentration of 2.22 mg/ml in PBS. The hNCAM180ID concentrate was separated by SDS-PAGE followed by Western blotting (Fig. 4 B, left panel) or silver staining (Fig. 4 B, right panel) of the gel. The Western blot confirmed the presence of hNCAM180ID with an apparent molecular weight of 85 kDa. The two lower bands may have been degradation products of the ID of hNCAM180. The silver staining showed a strong NCAM band at 85 kDa and some other weaker bands with a lower molecular weight, which may also have been degradation products of hNCAM180ID or contaminations with host bacterial proteins. Even though other proteins or degradation products were present in the concentrate, the purity of the sample was sufficient for the performance of the macroarray as hNCAM180ID was the most prominent protein and possible interactions detected by the macroarray were to be confirmed by other methods. Approximately 680 µg (15 nM) of recombinant hNCAM180ID isolated from 2.6 l bacteria culture were fluorescently labeled with DYNOMICS DYE-633.

4.1.2. Expression and purification of hNCAM140ID

The ID of hNCAM140 was initially cloned into the prokaryotic expression vector pBJG1 by C. Laurini (Institute of Nutrition and Food Science, Department of Human Metabolomics, University of Bonn, Germany), resulting in an 8x His-tagged construct. The expression of hNCAM140ID in *E. coli* BL21 (DE3) bacteria was successful, but after lysis of the bacteria the protein remained insoluble in PBS/Triton under various expression times (0-22 h) and temperatures (20°C, 30°C, and 37°C; Data not shown). High expression levels of recombinant proteins can lead to formation of insoluble aggregates, the so-called inclusion bodies, which can be solved by strong denaturants (QIAGEN, 2003). By using 8 M urea buffer, hNCAM140ID was successfully dissolved from the pellet and the supernatant used for

purification by Ni-NTA chromatography. The washing and elution fractions were separated by SDS-PAGE followed by silver staining. Two prominent protein bands appeared in the elution fractions, one with an apparent molecular weight of hNCAM140ID at 34 kDa, another at approximately 45 kDa (Data not shown).

As the relatively great amount of the contaminating protein would have been difficult to remove from the concentrate of hNCAM140ID, another approach for expression and purification of hNCAM140ID was tested. The cDNA of hNCAM140ID was subcloned in frame into the prokaryotic expression vector pGEX-4T-2, using the restriction enzymes *Bam*H1 and *Eco*R1, resulting in a GST-tagged hNCAM140ID construct. The pGEX-4T-2/hNCAM140ID plasmid was transformed into *E. coli* BL21 (DE3) bacteria and different expression times (0-24 h) and temperatures tested (20°C, 30°C, and 37°C) to optimize hNCAM140ID protein expression and solubility. Bacteria were harvested by centrifugation, resuspended in PBS/Triton, and lysed by freezing/thawing cycles with liquid nitrogen and ultrasound. After another centrifugation step, supernatants were collected and the were pellets resuspended in PBS/Triton by ultrasound. The pellet and supernatant samples were analyzed by SDS-PAGE followed by Western blotting and Ponceau-S staining. The stained membranes revealed a protein with the apparent molecular weight of GST-tagged hNCAM140ID (approximately 50 kDa) being expressed after IPTG induction and being soluble in PBS/Triton (Data not shown). As optimal conditions for a strong expression and good solubility of hNCAM140ID in PBS/Triton, an expression time of 24 h at 20°C was chosen for an expression volume of 3 l.

After centrifugation, bacteria were resuspended in PBS/Triton and lysed by freezing/thawing cycles and usage of a Potter homogenizer. The lysate was centrifuged, the pellet resuspended again in PBS/Triton, and the supernatant applied onto a column packed with GSH superflow. The flow-through, washing, and elution fractions were collected and applied onto an SDS-PAGE gel, which was stained with Coomassie Blue (Fig. 5 A). Whereas several protein bands appeared in the pellet (P), flow-through (FT), and washing fraction 1 (W1), hardly any band was present in W2, showing an efficient washing of the column in the first washing step. In the elution fractions E1, E2, and E3, clear protein bands were visible at the apparent molecular weight of GST-tagged hNCAM140ID (50 kDa) and one additional band appeared at 38 kDa. The hNCAM140ID in E1 emerged slightly below E2 and E3 due to the change from wash to elution buffer and hence a mixed buffer composition in this fraction.

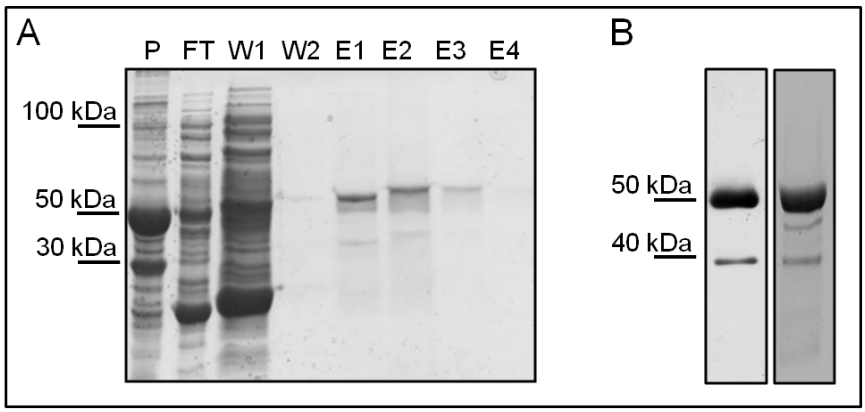

Fig. 5: Analysis of the purification fractions and the concentrate of hNCAM140ID

(A) Pellet (P), flow-through (FT), washing (W1/2) and elution fractions (E1-4) were separated by SDS-PAGE and stained by Coomassie Blue. **(B)** The hNCAM140ID concentrate was separated by SDS-PAGE followed by Western blotting and probing with 5B8 antibody (left) or Coomassie Blue staining of the gel (right).

As there was a great amount of hNCAM140ID remaining in the flow-through, purification of this fraction was repeated. The elution fractions of both purifications were pooled and concentrated to a final protein concentration of 1.7 mg/ml. The concentrate purity and presence of NCAM was tested by a Coomassie stained gel (Fig. 5 B, right panel) and a Western blot probed with 5B8 antibody (Fig. 5 B, left panel) and a GST-tag antibody (data not shown), confirming the prominent presence of GST-tagged hNCAM140ID at 50 kDa. The additional band at 38 kDa was detected by 5B8 antibody, but not with an antibody against GST (data not shown). Therefore, it was suggested to be a partially degraded hNCAM140ID construct devoid of a GST fragment. Additionally, one more light band with an apparent molecular weight of approximately 47 kDa was detected by Coomassie staining, which did neither react with 5B8 antibody nor with the antibody against GST (data not shown). Therefore it was speculated to represent a contamination with bacterial protein. Finally, the three protein bands were analyzed by mass spectrometry (data not shown), kindly performed by B. Gehrig (Institute of Biochemistry and Molecular Biology, University of Bonn, Germany), which confirmed the Western blot results with GST-tagged NCAM at 50 kDa and untagged NCAM at 38 kDa. The band at 47 kDa was identified as translation initiation factor IF-2 and GST. It was then tried to cleave the GST-tag from hNCAM140ID by an internal thrombin cleavage site inherent in the pGEX-4T-2 vector, as GST could influence the binding between NCAM and its potential interaction partners or lead otherwise to false positive signals. But even by varying the amount of thrombin cleavage units (0.16 - 0.005 U), incubation temperatures (4°C, 20°C, and 37°C), and times (2, 4, 8, and 16 h), GST could only be removed from a subset of purified hNCAM140ID (data not shown). Finally, GST-tagged hNCAM140ID was used for macroarray performance. In total, approximately 1.4 mg (14 nM) hNCAM140ID was extracted from 3 l bacterial culture and fluorescently labeled with DYNOMICS DYE-633.

4.1.3. Detection and identification of potential interaction partners of hNCAM180ID and hNCAM140ID by protein macroarray

The protein macroarray consists of two membranes (named part 8 and 9; Source Bioscience ImaGenes, Berlin) which together contain 24000 His-tagged expression clones of human fetal brain proteins. For the identification of yet unknown interaction partners of hNCAM-ID, the membranes were incubated with fluorescently labeled recombinant hNCAM180ID (part 8) or hNCAM140ID (part 8 and 9). Part 9 has previously been analyzed with hNCAM180ID by A. Sekulla (Sekulla, 2010). Signals were detected by scanning the membranes at a wavelength of 700 nm. Additionally, the expression levels of the spotted His-tagged proteins on the membrane part 8 were detected. Therefore, hNCAM180ID was stripped off of the membrane and the membrane incubated with anti-His IRDye™ 800-antibodies and scanned at a wavelength of 800 nm. The images were analyzed manually by means of the softwares Aida™ Image Analyzer and Aida™ Array Compare. First, a raster was layed on top of both membrane images to facilitate the assigning of positive signals to their exact position in the coordinate matrix and ultimately enable correct identification. Thereafter, in case of hNCAM180ID, both membrane images were overlaid, resulting in an image showing green (DYNOMIC DYE-633 labeled hNCAM180ID) and red dots (Alexa-Fluor-800 labeled His-tagged spotted proteins). Whereas the green dots showed binding of hNCAM180ID to relatively weakly expressed proteins, red dots reflected a strong expression of the spotted proteins and no or only little hNCAM180ID binding. With this approach, a relation between the strength of the binding of hNCAM180ID to the spotted protein and its expression level was given. A yellow signal appeared when hNCAM180ID bound strongly to a highly expressed protein, alike when hNCAM180ID bound weakly to a faintly expressed protein on the membrane. In case of hNCAM140ID, only signals of the bound protein were detected by scanning the membranes at a wavelength of 700 nm and the expression strength of the spotted proteins not further considered.

For each protein, the expression clones have been spotted several times on the membranes and additionally arranged in duplicates in a characteristic pattern around a guiding point. Green and yellow fluorescent signals were only considered as positive binding signals if both spots were significantly brighter than the background. The technical data sheet “Scoring Template for Macroarrays” indicated the corresponding spotting pattern, and the positions (x, y coordinates) of positive signals were related to a particular expression clone using the Source Bioscience imaGenes annotation table.

Several already known interaction partners of NCAM such as spectrin (Pollerberg *et al.*, 1986), PLCγ, and PP2A (Büttner *et al.*, 2005) were identified by the macroarray. Additionally, several other interesting yet unknown interaction partners were found. Our group focused on the verification and analysis of NCAM’s interaction with ubiquitin C-terminal hydrolase

isozyme L1 (UCHL1), ubiquitin-fold modifier-conjugating enzyme 1 (Ufc1), and KLC1. The Gene bank accession number and the frequency of the binding of the two NCAM isoforms to the proteins on the macroarray are shown in Tab. 11.

Tab. 11: List of selected potential (upper part of the table) and already known (lower part) interaction partners of hNCAM180ID and hNCAM140ID identified in the protein macroarray

Name	Gene bank accession number	Protein macroarray	
		hNCAM180ID	hNCAM140ID
Ubiquitin C-terminal hydrolase isozyme L1 (UCHL1)	P09936	1 (30), 3 %	0 (70), 0 %
Ubiquitin-fold modifier-conjugating enzyme 1 (Ufc1)	Q9Y3C8	2 (2), 100 %	8 (8), 100%
Ubiquitin-activating enzyme 5 (Uba5)	Q9GZZ9	0 (0)	4 (6), 66 %
Kinesin light chain 1 (KLC1)	Q07866	6 (18), 33 %	8 (22), 36 %
Serine/threonine-protein phosphatase 2 A (PP2A)	P30153	0 (22), 0 %	24 (46), 52 %
Spectrin α-chain (α-spectrin), brain	Q13813	0 (30), 0 %	6 (36), 16 %
Spectrin β-chain, (β-spectrin), brain 2	O15020	6 (12), 50 %	2 (12), 16 %
Phospholipase C (PLCγ)	P19174	2 (6), 33 %	0 (6), 0 %

Given are the name and Gene bank accession number of the detected proteins, and for each protein the number of clones bound to the respective isoform of hNCAM-ID, the total number of spotted clones (in parentheses), and the percentage of detected clones binding to hNCAM-IDs (binding coverage in %). Percentages are rounded down.

Although only one positive spot of 30 spotted clones of UCHL1 was detected and not both spots of a duplicate, a potential interaction between NCAM and the deubiquitinating enzyme UCHL1 was of high interest an, as NCAM has been described to become mono-ubiquitinated at the plasma membrane (Diestel *et al.*, 2007), and therefore further analyzed. The results of this analysis as well as of the analysis of Ufc1 have been published (Mirka Homrich[1], Hilke Wobst[1], Christine Laurini, Julia Sabrowski, Brigitte Schmitz, Simone Diestel: Cytoplasmic domain of NCAM140 interacts with ubiquitin-fold modifier-conjugating enzyme-1 (Ufc1). Exp Cell Res 324 (2), 192-199, 2014. ([1]: equal contribution); Hilke Wobst, Sarah Förster, Christine Laurini, Agathe Sekulla, Michael Dreiseidler, Jörg Höhfeld, Brigitte Schmitz, Simone Diestel: UCHL1 regulates ubiquitination and recycling of the neural cell adhesion molecule NCAM. The FEBS Journal 279 (23), 4398-4409, 2012). They are not in the focus of this work and, therefore, only shortly summarized here.

Mono-ubiquitination of plasma membrane proteins results in endocytosis or sorting and targeting of proteins in the endosome into the multivesicular body/lysosomal pathway

(Hicke & Dunn, 2003; Katzmann *et al.*, 2001). Deubiquitinating enzymes detach ubiquitin and thereby rescue proteins from lysosomal degradation and support their recycling to the cell surface (Schwarz & Patrick, 2012; Butterworth *et al.*, 2007; Wilkinson, 2000). We showed that NCAM180 and NCAM140 partially colocalize with UCHL1 in cell somata and neurites of primary cortical neurons and in the B35 neuroblastoma cell line. The co-overexpression of UCHL1 and hNCAM180 or hNCAM140, respectively, significantly decreased the constitutive ubiquitination of both NCAM isoforms whereas the inhibition of endogenous UCHL1 increased the ubiquitination of NCAM. Additionally, after co-overexpression with UCHL1, the lysosomal localization of NCAM180 and NCAM140 was significantly reduced and internalized NCAM was shown to partially colocalize with UCHL1. Therefore, UCHL1 is suggested to be a novel interaction partner of both NCAM transmembrane isoforms that regulates their ubiquitination and intracellular trafficking (Wobst *et al.*, 2012).

Furthermore, the protein macroarray revealed Ufc1 as potential interaction partner of both NCAM isoforms with 100 % binding coverage. Additionally, hNCAM140ID interacted with 66 % of all spotted clones of the ubiquitin-like modifier activating enzyme 5 (Uba5). An interaction of Uba5 with hNCAM180ID was not detected, as no clones expressing Uba5 were spotted on the macroarray membrane part 8, which was incubated with hNCAM180ID. Ufc1 is a specific enzyme, which conjugates the ubiquitin-fold modifier 1 (Ufm1) to target proteins, resulting in a posttranslational modification related to ubiquitination, the so-called ufmylation. Before its conjugation, Ufm1 needs to be activated by Uba5 (Komatsu *et al.*, 2004). Further investigation by our group revealed a partial co-localization of NCAM140 with Ufc1 and Ufm1 and an increased endocytosis of NCAM140 in the presence of Ufm1. These observations point out a possible ufmylation of NCAM140 and a potential novel function of Ufm1 for cell surface proteins (Homrich *et al.*, 2014).

4.2. Verification of the interaction of NCAM and KLC1

KLC1 was identified 6 times (18 spotted clones in total; 33 % binding coverage) as potential interaction partner for hNCAM180ID and 8 times (22 spotted clones in total; 6 % binding coverage) for hNCAM140ID. Due to these observations and the potentially highly interesting role of KLC1 for NCAM function(s), the interaction of NCAM and KLC1 was analyzed in detail in this thesis.

For the verification of an interaction between NCAM and KLC1, several approaches were pursued. In addition, functional studies were carried out to investigate whether NCAM transport to the cell surface might be mediated by kinesin-1, as KLC1 is a component of this motor protein. For all transfection studies cDNA of hNCAM180 was used.

4.2.1. Investigation of the interaction of NCAM and KLC1

4.2.1.1. Co-IP of NCAM and KLC1 from mouse brain lysate

First, the interaction of NCAM with KLC1 was confirmed in brain tissue by co-IP. Therefore, a brain of a 1 day old mouse was homogenized and lysed. The lysate was pre-cleared and incubated with antibodies against KLC1 or non-specific IgGs (control). Complexes were precipitated and eluted from the beads with non-reducing Laemmli buffer to detect KLC1, as KLC1 antibodies did not function under reducing conditions. For detection of NCAM, the proteins were reduced by adding DTT and boiling of the samples. Proteins were separated by SDS-PAGE followed by Western blotting and detection of the proteins with appropriate antibodies (Fig. 6). No signals were detected with KLC1 and poly NCAM1 (NCAM) antibodies in the control (IgG), whereas KLC1 was successfully precipitated from brain lysate when using KLC1 antibodies for co-IP. Analysis with poly NCAM1 antibodies showed that NCAM was co-precipitated with KLC1, suggesting an interaction of NCAM and KLC1 in mouse brain. In young mouse brain NCAM is heavily polysialylated. Therefore, the NCAM signal in Western blot appeared as a broad smear with an apparent molecular weight above 180 kDa (Hoffman *et al.*, 1982; Rothbard *et al.*, 1982). The KLC1 band was shifted above its apparent molecular weight of approximately 60 kDa to almost 80 kDa when it was analyzed by SDS-PAGE under non-reducing conditions.

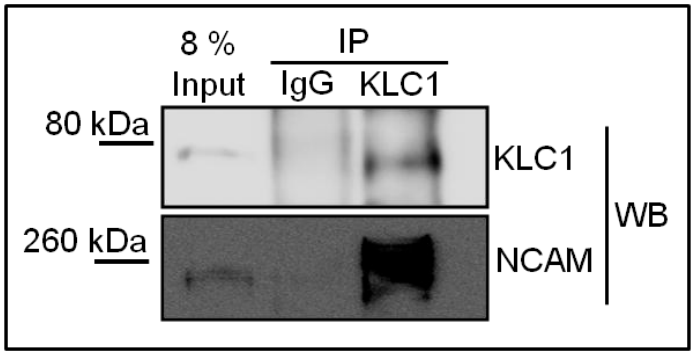

Fig. 6: Co-IP of KLC1 and NCAM from mouse brain lysate

KLC1 immunoprecipitates (IP) from brain lysate and input material (Input) were separated by SDS-PAGE and analyzed by Western blot (WB) with KLC1 and poly NCAM1 (NCAM) antibodies. Control IP with non-specific IgG antibodies served as control. Similar results were obtained in four independent experiments.

4.2.1.2. Co-localization of intracellular NCAM and kinesin-1 in CHO cells

The co-localization of NCAM and kinesin-1 would further support that the proteins interact. To get a first impression of a potential intracellular overlap of both proteins, CHO cells were transiently co-transfected with cDNAs of hNCAM180 and equal amounts of both parts of a kinesin-1 tetramer, GFP-KLC1 and GFP-KHC1 (GFP-KLC1/KHC1). Approximately 40 hours later, cell surface hNCAM180 was labeled with ERIC 1 antibody and

anti-mouse-CY5-conjugated secondary antibodies before cells were fixed, permeabilized, and stained again with ERIC 1 antibody and anti-mouse-CY3-conjugated secondary antibodies to detect total, meaning cell surface and intracellular hNCAM180. In Fig. 7, confocal images of the stained total and surface hNCAM180 and the GFP-KLC1/KHC1 fluorescence are shown separately and merged. The hNCAM180, which was not detected with NCAM antibodies applied before permeabilization of the cell is identified as intracellular hNCAM180. Yellow dots in the merged image showed strong co-localization of GFP-KLC1/KHC1 with intracellular hNCAM180, also confirmed by the graph of the immunofluorescence intensity profiles along the line.

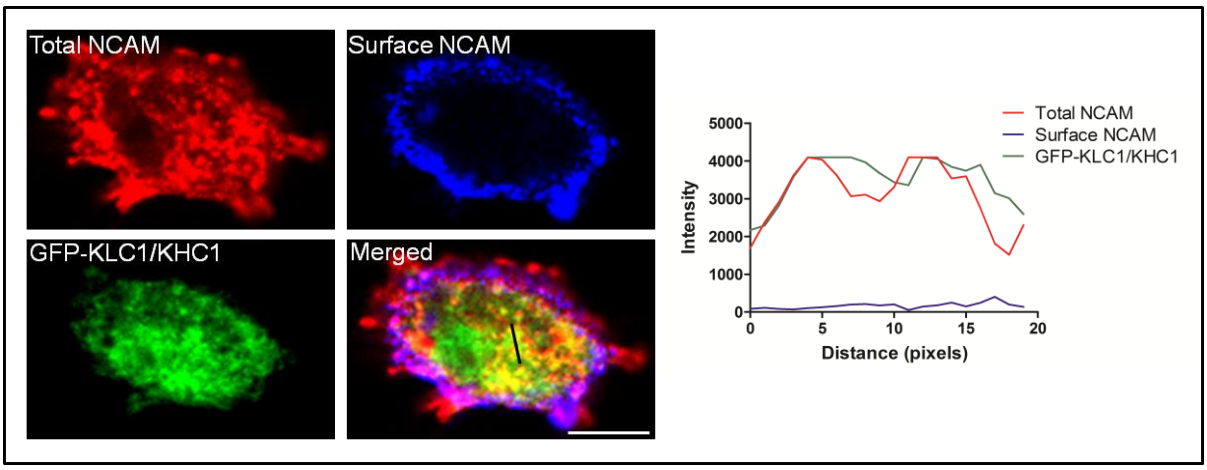

Fig. 7: Immunofluorescence analysis of a CHO cell overexpressing NCAM and GFP-KLC1/KHC1

Cells were transiently co-transfected with cDNAs of NCAM and GFP-KLC1/KHC1 and labeled with ERIC 1 antibody and anti-mouse-CY5-conjugated secondary antibodies applied before fixation to label surface NCAM. Total NCAM was labeled after fixation and permeabilization of the cells with ERIC 1 antibody and anti-mouse-CY3-conjugated secondary antibodies. The graph shows immunofluorescence intensity profiles along the corresponding line in the merged image. Scale bar, 10 µm. NCAM: hNCAM180.

4.2.1.3. Co-localization of endogenous NCAM and KLC1 or KIF5A in primary hippocampal neurons

After having detected the overlap of co-overexpressed NCAM and kinesin-1 in CHO cells, the co-localization of endogenous NCAM with KLC1 and KIF5A, respectively, was investigated in primary hippocampal neurons. As described above, KLC1 binds to a group of KIF5 proteins, as for example KIF5A, to compose the functional motor kinesin-1 (Hirokawa, 1998). In this regard, co-localization of NCAM and KIF5A was also investigated. Hippocampal neurons were isolated from postnatal day 2 mice. After 1 DIV, neurons were fixed and permeabilized. After blocking, NCAM-ED specific antibody H28 with KLC1 or KIF5A antibodies were applied, followed by secondary antibodies. In Fig. 8, confocal images of the NCAM and KLC1 (A) or NCAM and KIF5A (B) staining are shown separately and merged. Examples of co-localized NCAM and KLC1 or KIF5A are numbered and shown by

arrows on higher magnification images. Graphs show immunofluorescence intensity profiles along the corresponding numbered lines, where the concomitant peak of the intensity confirms the co-localization of both proteins. Co-localizations appearing as yellow signals of NCAM and KLC1 were easily detectable and occurred relatively widespread in the somata and in growth cones where both proteins were enriched in accordance with previous records (Sytnyk *et al.*, 2002; Morfini *et al.*, 2001). The co-localization of NCAM and KIF5A appeared less frequently and was therefore counted. Quantification revealed that 15 neurons out of 33 exhibited 17 distinct yellow dots in the somata and growth cones being presumably NCAM-containing vesicles co-localizing with KIF5A.

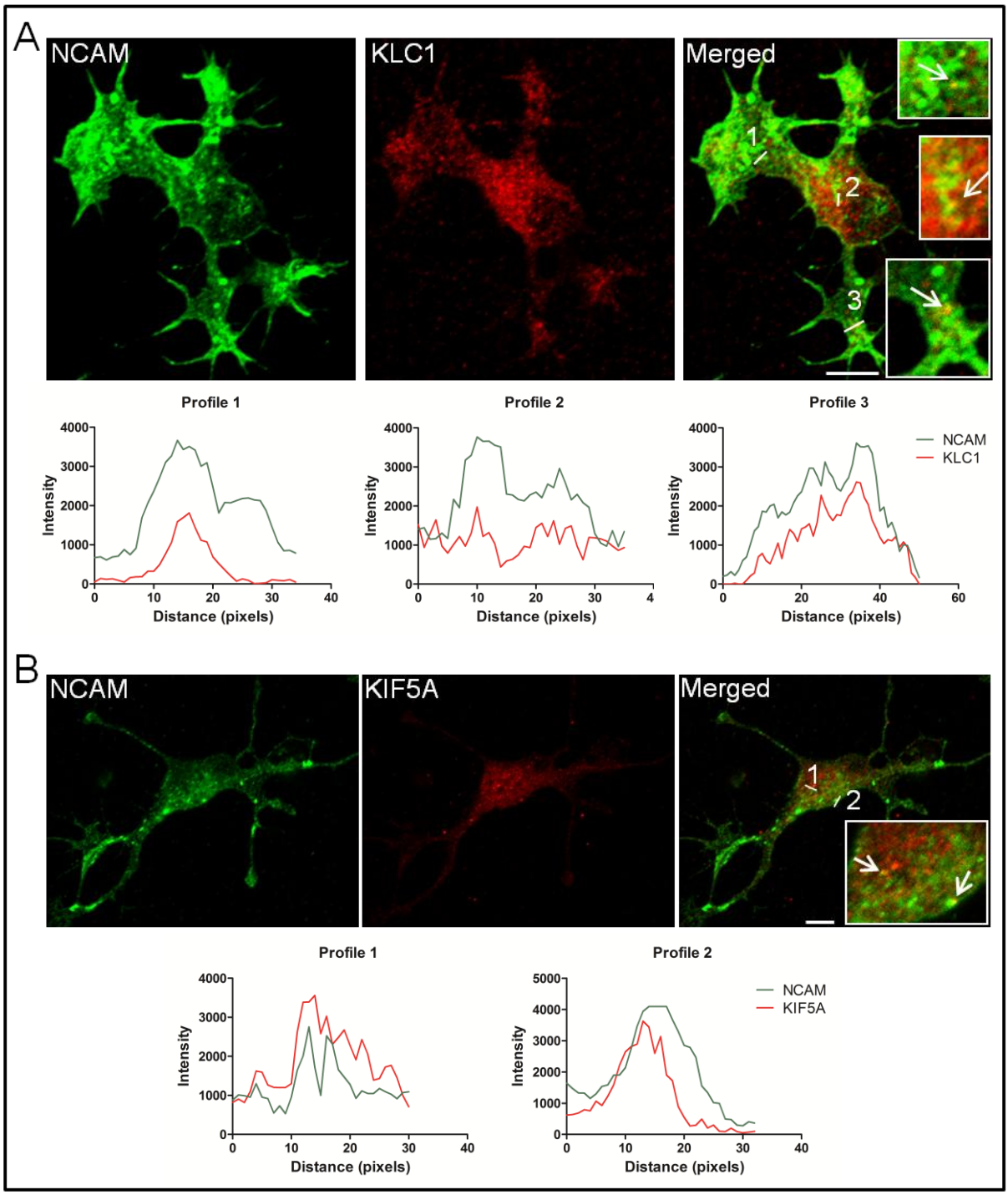

Fig. 8: Immunofluorescence analysis of a hippocampal neuron co-labeled with antibodies against NCAM and KLC1 or KIF5A

Examples of endogenous co-localized NCAM and KLC1 **(A)** or KIF5A **(B)** are numbered and shown by arrows on high magnification images. Graphs show immunofluorescence intensity profiles along the corresponding numbered line in merged images. Scale bar, 5 µm.

4.2.2. Investigation of the presence of NCAM and kinesin-1 in TGN organelles

Proteins, which need to be transported from the Golgi to various locations of the cell, *e.g.* the plasma membrane, are mainly packed into TGN organelles (Stephens & Pepperkok, 2001; Polishchuk *et al.*, 2000; Nakata *et al.*, 1998). The transport of these carriers to their final

destination is facilitated by molecular motors, such as kinesin-1 (Nakata & Hirokawa, 2003; Allan *et al.*, 2002; Hirokawa, 1998). To analyze whether kinesin-1 may be involved in the transport of NCAM-containing TGN organelles, the presence and co-localization of KIF5A, KLC1 and NCAM in TGN organelles was determined.

4.2.2.1. Detection of NCAM, KLC1, and KIF5A in mouse brain TGN organelles by Western blot

First, the presence of KIF5A, KLC1, and NCAM in TGN organelles was investigated by Western blot. Brains from 1 to 3 day old mice were homogenized and centrifuged. The supernatant was collected and TGN organelles isolated by sucrose gradient centrifugation. The brain homogenate (BH) and fractions of soluble proteins (cytosol), TGN organelles, and Golgi stacks were applied onto an SDS-PAGE and analyzed by Western blot with H28 antibody and KIF5A, KLC1, and TGN38 antibodies (Fig. 9). KIF5A was present in the BH and enriched TGN fractions, and less in the cytosolic and Golgi fractions. Interestingly, KIF5A antibodies detected a double band with the upper band being more prominent in BH and TGN and the lower band in the cytosol. In the Golgi fraction, both bands appeared similarly intensive. KLC1 and NCAM were enriched in the TGN organelles, supporting the likelihood of kinesin-1 being involved in transporting NCAM-containing TGN organelles. Staining with TGN marker TGN38 served as control for a successful TGN isolation. Only very weak TGN38 signals appeared in the BH and cytosolic fraction, respectively, whereas TGN38 was clearly enriched in the TGN and Golgi fractions, respectively. Therefore, the separation of the subcellular fractions and TGN isolation was satisfying.

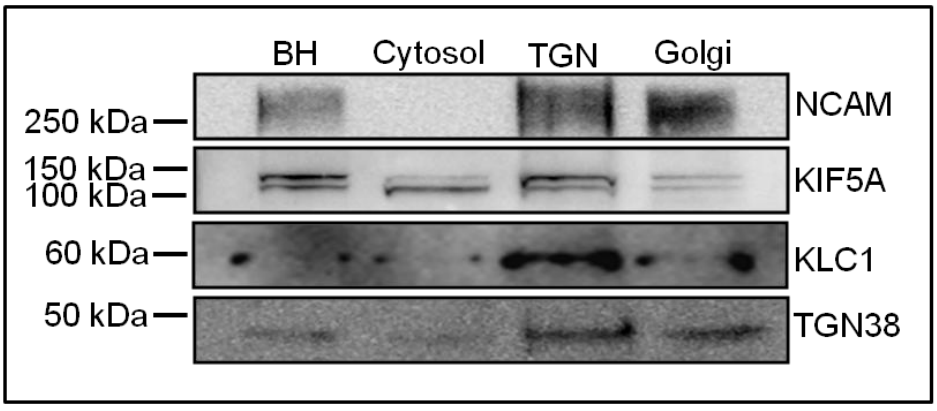

Fig. 9: Western blot analysis of brain homogenate (BH), soluble proteins (cytosol), *trans*-Golgi network (TGN) organelles, and Golgi membranes for NCAM, KIF5A, KLC1, and TGN38

Fractions were isolated from 1 to 3 day old mice brains by sucrose gradient centrifugation, separated by SDS-PAGE followed by Western blot and probing with H28, KIF5A, KLC1, and TGN38 antibodies.

This experiment indicated that NCAM-containing TGN organelles may be bound to kinesin-1, although it did not provide evidence for the presence of NCAM and kinesin-1 at or in exactly

the same organelle, as many TGN organelles were investigated simultaneously. To specify the concomitant presence of NCAM and kinesin-1, it was tried to immunoisolate TGN organelles with an NCAM-ID antibody from the TGN fraction. Subsequent Western blotting and immunolabeling for NCAM showed that immunoisolation was not successful under these conditions. Using more young mice brains for TGN isolation and KLC1 antibodies for immunoisolation, organelles were clearly precipitated, but the staining for NCAM was not quite satisfying (data not shown). Ideally, the experiment should have been repeated, but as 20 mice brains were used for this experiment, the idea was abandoned.

4.2.2.2. Detection of co-localization of NCAM and KIF5A in TGN organelles in primary hippocampal neurons

The possibility of NCAM-containing vesicles being transported by kinesin-1 was further investigated by co-localization studies in neurons. Therefore, a triple immunofluorescence staining of cultured 1 day old hippocampal neurons was performed. Neurons were fixed, permeabilized, and stained with NCAM-ID specific antibody p61, KIF5A and γ-adaptin antibodies, which is a marker protein of TGN organelles. In Fig. 10, images of the staining for NCAM, KIF5A, and γ-adaptin are shown. The high magnification image shows an example of an NCAM-containing γ-adaptin and KIF5A positive vesicle as white dot (arrow) and the graph shows the immunofluorescence intensity profile along the line in the merged image. The analysis of the confocal sections of neuronal somata showed that NCAM and KIF5A indeed co-localized with γ-adaptin positive organelles albeit out of 34 neurons only 12 showed minimal (1 spot) co-localization.

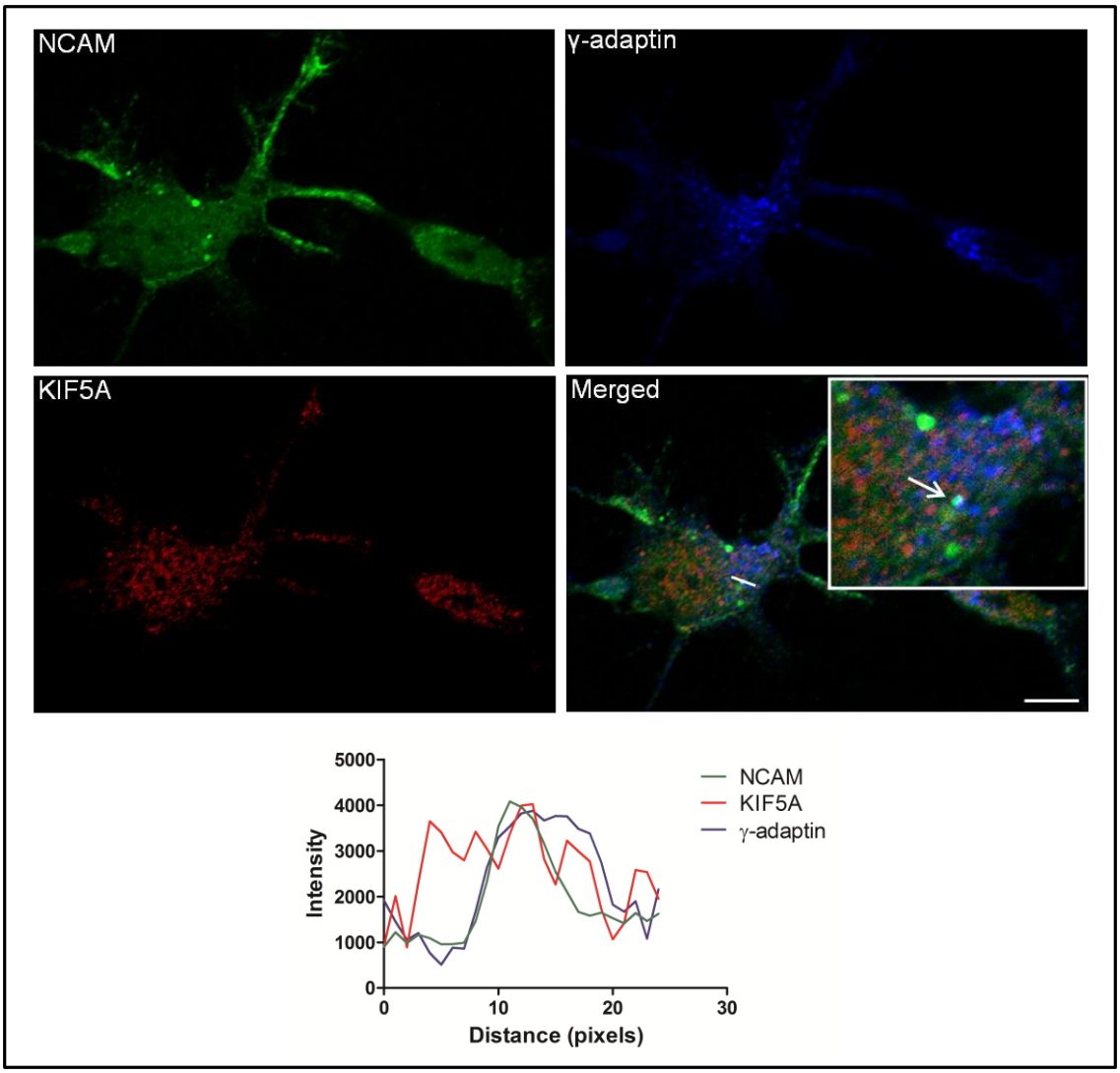

Fig. 10: Immunofluorescence analysis of a hippocampal neuron co-labeled with antibodies against NCAM, KIF5A, and γ-adaptin

The high magnification insert shows an example of an NCAM-containing γ-adaptin and KIF5A positive vesicle (arrow). The immunofluorescence intensity profile along the line in the merged image is shown in the graph. Scale bar, 5 µm.

4.2.3. Functional studies

After having gained strong indications for the interaction of NCAM and KLC1 by co-IP and co-localization studies, functional analyzes were performed to investigate whether kinesin-1 could indeed be involved in the transport of NCAM to the cell surface.

4.2.3.1. Influence of kinesin-1 on the delivery of NCAM to the cell surface in CHO cells

First, the influence of kinesin-1 on the delivery of NCAM to the cell surface was investigated in CHO cells. CHO cells were plated on glass coverslips and transiently co-transfected with cDNAs coding for hNCAM180 and either GFP-KLC1 (KLC1) alone, GFP-KLC1/KHC1 (= motor subunits) or GFP as control. Approximately 40 hours later, cell surface hNCAM180 in transfected cells was labeled with ERIC 1 antibody applied on ice to living cells followed by

anti-mouse-CY5-conjugated secondary antibodies and fixation. After embedding of the coverslips in FluorPreserve™, images were taken using a confocal laser scanning microscope. The mean intensities of the fluorescent signals were quantified by means of ImageJ software. In Fig. 11A, representative fluorescence images of hNCAM180 and GFP signals of three cells of each transfection experiment (KLC1 + NCAM, Motor + NCAM, GFP + NCAM) are shown. The dotted hNCAM180 labeling is due to the application of multivalent antibodies against cell surface antigens to living cells, which typically results in clustering of antigens and therefore a dotted staining (Leshchyns'ka *et al.*, 2003). Immunofluorescence quantification showed that levels of hNCAM180 at the cell surface of KLC1 or motor co-transfected cells were approximately two fold higher when compared to hNCAM180 levels at the cell surface of GFP transfected cells.

At the individual cell level, immunofluorescence intensities of cell surface hNCAM180 correlated positively with the levels of expression of KLC1 ($r = 0.69$; $p < 0.0001$) and the motor ($r = 0.86$; $p < 0.0001$) as measured by antibody staining and GFP fluorescence, respectively. In contrast, cell surface levels of hNCAM180 weakly correlated with GFP levels ($r = 0.35$; $p = 0.004$) in control GFP transfected cells (Fig. 11 B). As an increased expression of kinesin-1 results in increased hNCAM180 levels at the cell surface, these experiments provide evidence of NCAM being delivered to the cell surface in dependency on kinesin-1.

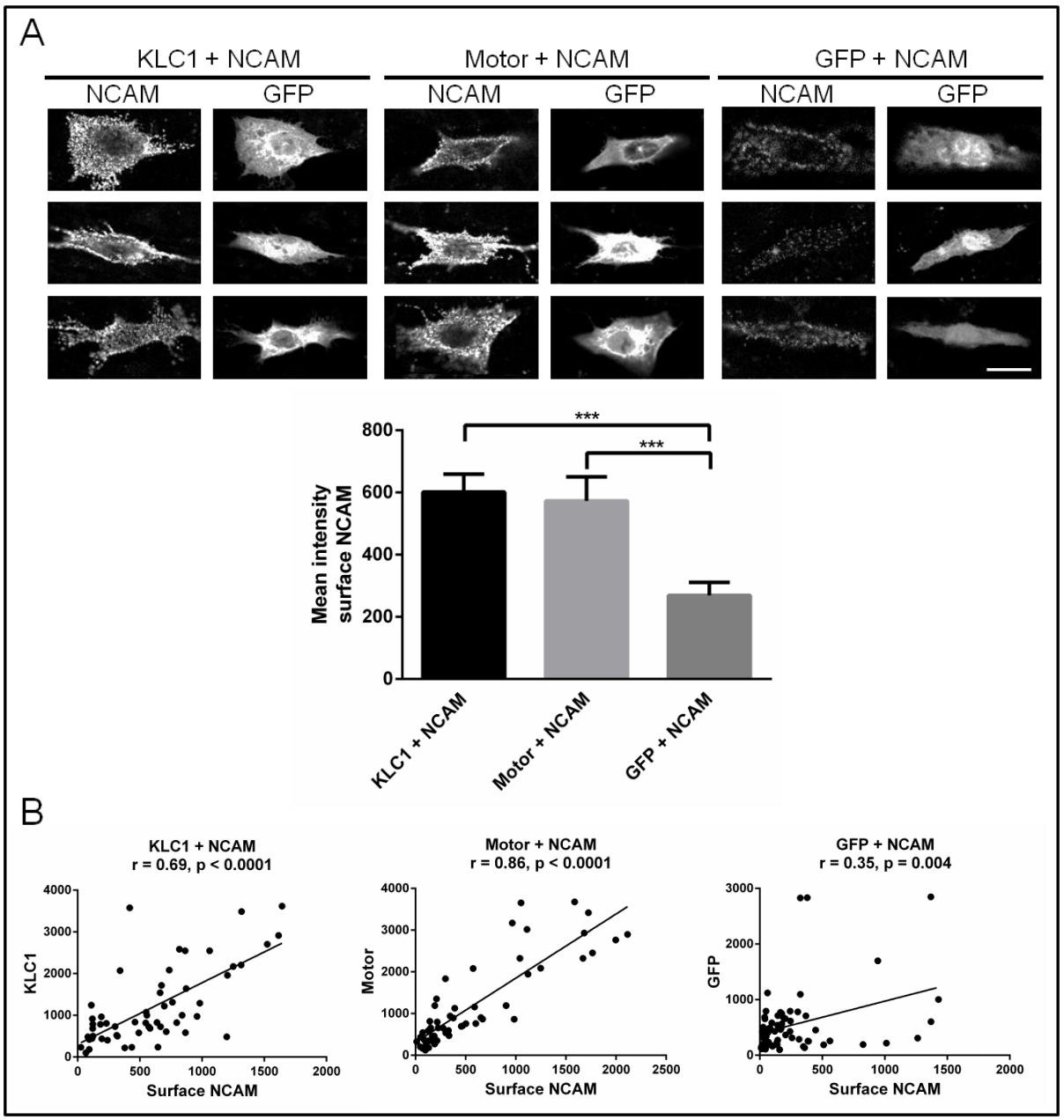

Fig. 11: Functional analysis of the influence of kinesin-1 on the delivery of NCAM to the cell surface in CHO cells

(A) Images of CHO cells co-transfected with cDNAs of NCAM and either KLC1 (KLC1 + NCAM), motor subunits (Motor + NCAM) or GFP (GFP + NCAM), respectively. Cell surface NCAM was labeled on ice with ERIC 1 antibody and anti-mouse-CY5-conjugated secondary antibodies applied before fixation. Shown are three cells for each transfection mode. Scale bar, 10 µm. Graph shows mean + SEM levels of cell surface NCAM. *** $p < 0.001$ (one-way ANOVA, $n \geq 55$). Similar results were obtained in five independent experiments. **(B)** Graphs show the correlation between the expression levels of cell surface NCAM and intracellular KLC1, motor, or GFP, respectively, measured by antibody staining or GFP fluorescence, for the same transfected cells investigated in (A) of the figure. r: Pearson's correlation coefficient. NCAM: hNCAM180.

4.2.3.2. Influence of kinesin-1 on the delivery of NCAMΔCT to the cell surface in CHO cells

Further investigations were carried out to analyze whether the ID of NCAM is required for kinesin-1 dependent delivery of NCAM to the cell surface. CHO cells were transiently co-

transfected with cDNAs of either full-length hNCAM180 or a truncated construct of transfected with cDNAs of either full-length hNCAM180 or a truncated construct of hNCAM180 with a deleted ID (hNCAMΔCT) and motor subunits or GFP, respectively. hNCAMΔCT has been shown to be able to interact extracellularly with its physiological binding partners and to become PSA-modified (Boutin *et al.*, 2009). Cell surface hNCAM180 was labeled on ice with ERIC 1 and anti-mouse-CY5-conjugated secondary antibodies approximately 40 hours after transfection before cells were fixed and images were taken with a confocal microscope. Quantification of the mean intensity of cell surface hNCAM180 showed that the deletion of the ID of NCAM did neither abolish nor increase its transport to the cell surface (Fig. 12 A). The level of hNCAMΔCT at the cell surface was rather similar in CHO cells co-transfected with motor subuntis (Motor + NCAMΔCT) or GFP (GFP + NCAMΔCT). Interestingly, the level of cell surface hNCAMΔCT showed a significant weak correlation with the expression level of the motor (r = 0.3; p = 0.0099) in individual cells (Fig. 12 B) and was similar to the correlation of the surface levels of full-length hNCAM180 and GFP expression (r = 0.35, Fig. 11 B). This indicates that the delivery of hNCAMΔCT is not dependent on kinesin-1. Nonetheless, the cell surface expression level of hNCAMΔCT was similar to that of full-length hNCAM180 co-transfected with motor subunits. Therefore, it is conceivable that hNCAMΔCT is transported to the cell surface by a kinesin-1 independent mechanism.

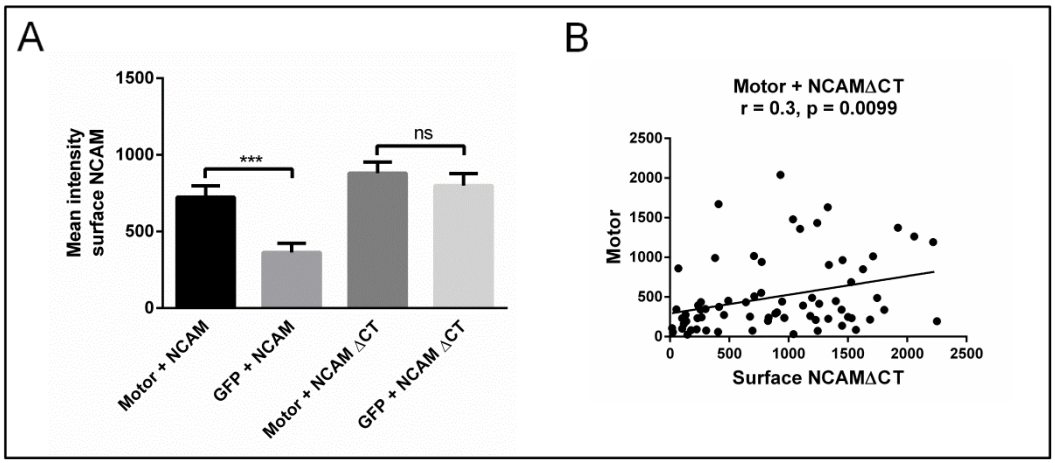

Fig. 12: Functional analysis of the influence of kinesin-1 on the delivery of NCAMΔCT to the cell surface in CHO cells

(A) Graph shows mean + SEM levels of cell surface NCAM in CHO cells co-transfected with cDNAs of NCAM or NCAMΔCT and either motor subunits (Motor + NCAM, Motor + NCAMΔCT) or GFP (GFP + NCAM, GFP + NCAMΔCT), respectively. Cell surface NCAM was labeled with ERIC 1 and anti-mouse-CY5-conjugated secondary antibodies applied on ice before fixation of the cells. ***p < 0.001, ns: not significant (unpaired t-test, $n \geq 68$). Similar results were obtained in three independent experiments. **(B)** Graph shows the correlation between expression levels of cell surface NCAMΔCT and of the motor, measured by antibody staining and GFP fluorescence, respectively, of the same cells investigated in (B) of the figure. r: Pearson's correlation coefficient. NCAM: hNCAM180, NCAMΔCT: hNCAMΔCT.

4.2.3.3. Influence of peptides derived from NCAM-ID on the kinesin-1 dependent delivery of NCAM to the cell surface in CHO cells

Since deletion of the ID of NCAM did not abolish its delivery to the cell surface, but most likely resulted in kinesin-1 independent transport mechanisms for hNCAMΔCT, the influence of inhibition of the interaction between NCAM-ID and kinesin-1 was investigated by performing a competition assay. Additionally, the KLC1-binding region within NCAM could possibly have been narrowed down by using truncated peptides of different length of NCAM-ID. CHO cells were co-transfected with cDNAs corresponding to hNCAM180 and GFP or hNCAM180 and motor subunits together with cDNA constructs coding for NCAM-ID or its fragments covering amino acid sequences 729-750 (NCAM-$ID_{729-750}$), 748-777 (NCAM-$ID_{748-777}$), and 777-810 (NCAM-$ID_{777-810}$) of NCAM140/180 (Fig. 13 A). Cells were stained on ice with ERIC 1 and anti-mouse-CY5-conjugated secondary antibodies approximately 40 hours after transfection, followed by fixation. In Fig. 13 B, the hNCAM180 and GFP signals of two cells per group are shown as an example. Immunofluorescence analysis revealed that after co-transfection with motor subunits together with peptide NCAM-ID, expression level of cell surface hNCAM180 was reduced approximately to the level observed in GFP co-transfected cells. This indicates that the NCAM-ID peptide may interfere with the delivery of hNCAM180 to the cell surface most likely by competing with hNCAM180 for binding to KLC1. Interestingly, CHO cells co-transfected with cDNA of hNCAM180 and motor subunits with NCAM-$ID_{729-750}$, NCAM-$ID_{748-777}$ or NCAM-$ID_{777-810}$, respectively, all showed a reduced level of cell surface hNCAM180, most likely also interfering at other steps of NCAM's cell surface delivery. For this reason no additional information about the KLC1-binding region within NCAM-ID was gained. The experiment was only performed once and afterwards the ELISA technique using synthetic peptides (see 4.2.4.1) was chosen as a more suitable approach to narrow down the KLC1-binding region within NCAM.

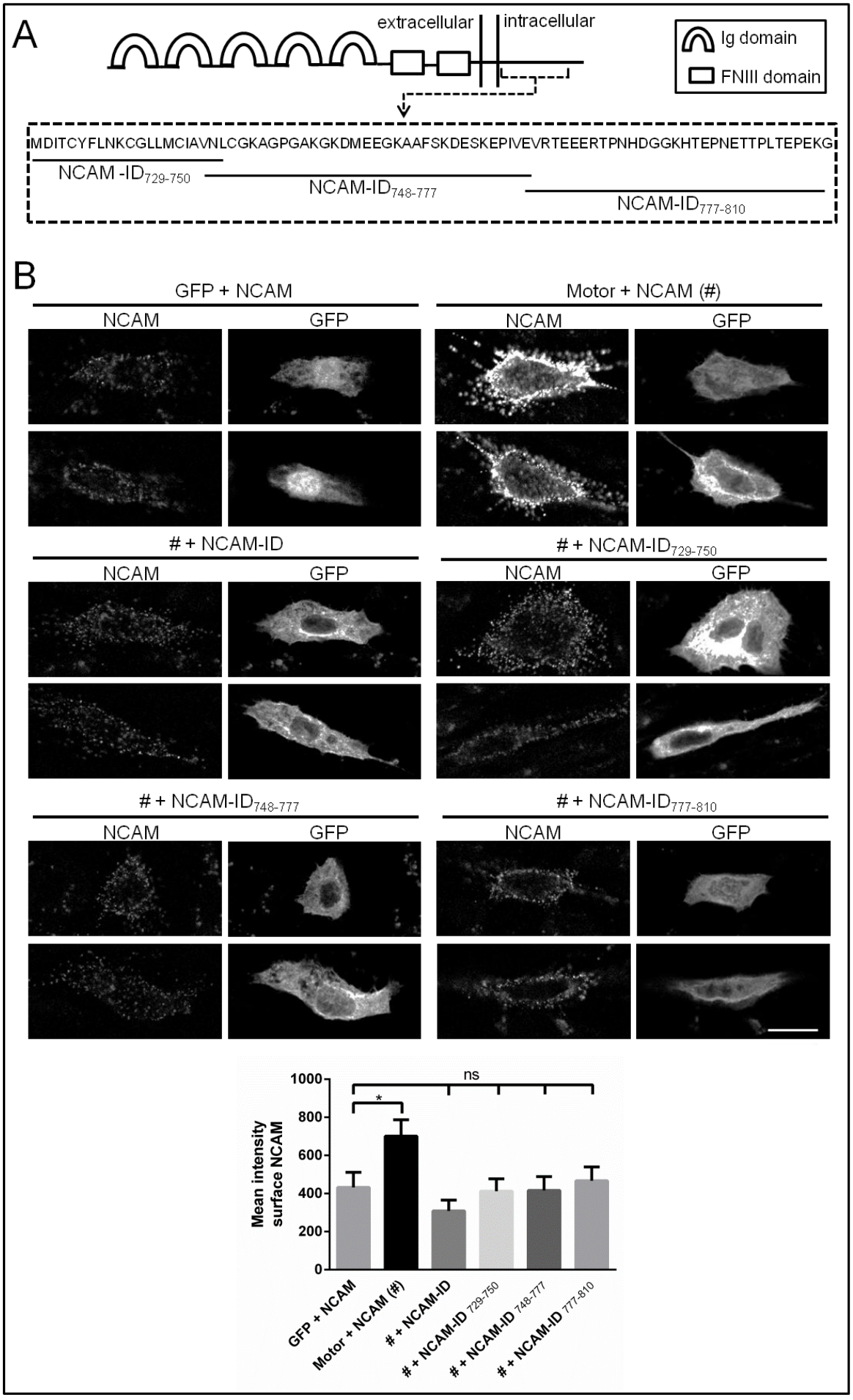
A
extracellular
intracellular
Ig domain
FNIII domain
MDITCYFLNKCGLLMCIAVNLCGKAGPGAKGKDMEEGKAAFSKDESKEPIVEVRTEEERTPNHDGGKHTEPNETTPLTEPEKG
NCAM -ID729-750
NCAM-ID748-777
NCAM-ID777-810
B
GFP + NCAM
Motor + NCAM (#)
NCAM
GFP
+ NCAM-ID
+ NCAM-ID729-750
+ NCAM-ID748-777
+ NCAM-ID777-810
Mean intensity surface NCAM
1000
800
600
400
200
0
ns
*
GFP + NCAM
Motor + NCAM (#)
+ NCAM-ID
+ NCAM-ID 729-750
+ NCAM-ID 748-777
+ NCAM-ID 777-810

Fig. 13: Functional analysis of the influence of peptides derived from NCAM-ID on the kinesin-1 dependent delivery of NCAM to the cell surface in CHO cells

(A) Schematic drawing illustrating full-length rat NCAM140, NCAM-ID, and fragments of NCAM-ID corresponding to amino acids 729-750 (NCAM-$ID_{729-750}$), 748-777 (NCAM-$ID_{748-777}$), and 777-810 (NCAM-$ID_{777-810}$). **(B)** Images of CHO cells co-transfected with cDNAs of NCAM and either GFP (GFP + NCAM) or motor subunits (Motor + NCAM, = #). When indicated, cells were additionally co-transfected with cDNA expressing NCAM-ID or the peptides NCAM-$ID_{729-750}$, NCAM-ID_{748-}777, and NCAM-$ID_{777-810}$, respectively. Cell surface NCAM was labeled on ice with ERIC 1 antibody and anti-mouse-CY5-conjugated secondary antibodies applied before fixation. Shown are two cells per group. Scale bar, 10 µm. Graph shows mean + SEM levels of cell surface NCAM. *$p < 0.05$, ns: not significant (one-way ANOVA, $n \geq 50$). NCAM: hNCAM180.

4.2.3.4. Investigation of the functional role of kinesin-1 in the delivery of NCAM to the cell surface in primary cortical neurons

The functional relationship between NCAM and kinesin-1 should have been verified in primary cortical neurons as a less artificial system. Neurons were isolated from postnatal day 2 mice and directly co-transfected with cDNAs encoding hNCAM180 and KLC1 or GFP, respectively. After 1 DIV, neurons were fixed and cell surface hNCAM180 labeled with ERIC 1 antibody and anti-mouse-CY3-conjugated secondary antibodies. Analysis of cell surface hNCAM180 levels showed no significant differences (Fig. 14 A).

Therefore, another approach was tested. Incubation of living cells with NCAM-ED antibodies (NCAM-triggering) is known to mimic homophilic and heterophilic binding of NCAM which leads to NCAM endocytosis and NCAM-dependent signal transduction and neurite outgrowth (Diestel *et al.*, 2007; Miñana *et al.*, 2001; Schmid *et al.*, 1999). Keeping the CHO cells on ice during the incubation time of the ERIC 1 antibody prevented NCAM endocytosis. In contrast, neurons were incubated at 37°C with ERIC 1 antibodies for NCAM-triggering after 1 DIV and co-transfection with cDNAs for hNCAM180 and KLC1 or motor subunits. Neurons were fixed before labeling with anti-mouse-CY3-conjugated secondary antibodies to stain cell surface hNCAM180. After permeabilization, anti-mouse-CY5-conjugated secondary antibodies were applied for staining of cell surface hNCAM180 and hNCAM180 internalized over the incubation time. After embedding of the coverslips in FluorPreserve™, images were taken using a confocal laser scanning microscope and ImageJ software for the quantification of the antibody stainings and fluorescent signals. The data in Fig. 14 B show a significantly increased mean intensity of surface hNCAM180 when co-transfected with KLC1 (KLC1 + NCAM) or motor subunits (Motor + NCAM), compared to the control (GFP + NCAM). At the individual cell level, expression levels of cell surface hNCAM180 and KLC1 or the motor correlated positively ($r = 0.53$, $p = 0.0002$ or $r = 0.55$, $p < 0.0001$; Fig. 14 C), even though differences to correlation levels of the GFP group ($r = 0.43$, $p < 0.0001$) were less distinct than in CHO cells (Fig. 11 B). Additionally, as in CHO cells, no significant differences in the surface level of hNCAMΔCT were observed in neurons

overexpressing hNCAMΔCT and KLC1 (KLC1 + NCAMΔCT) or GFP (GFP + NCAMΔCT; Fig. 14 B), respectively, and levels of surface hNCAMΔCT and expression levels of KLC1 correlated very weakly (r = 0.2, ns; data not shown). This indicates that hNCAMΔCT is transported kinesin-1 independent also in cortical neurons. Interestingly, in contrast to CHO cells, NCAM-triggering seems to be obligatory for the kinesin-1 dependent transport of hNCAM180 in neurons.

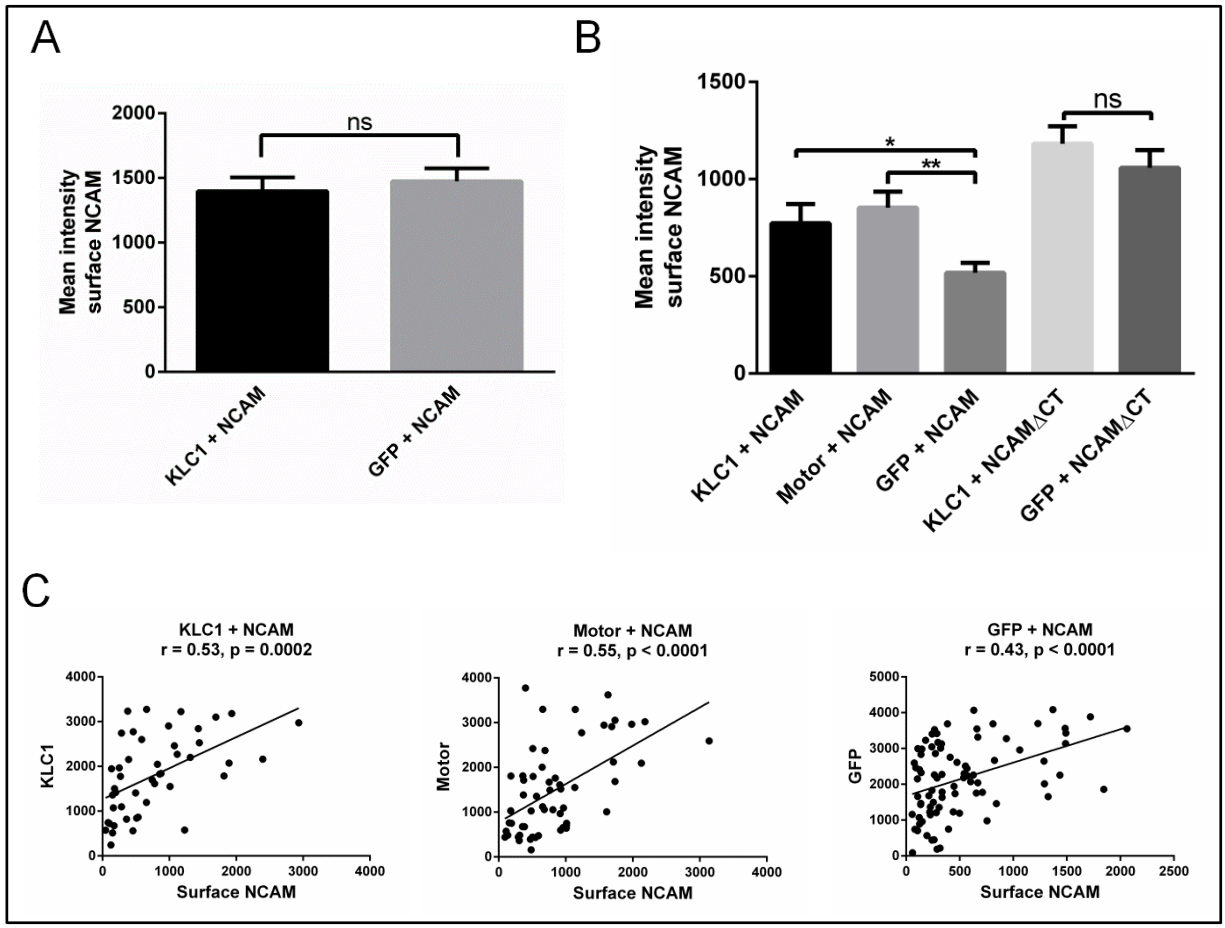

Fig. 14: Functional analysis of the influence of KLC1 or kinesin-1 on the delivery of NCAM and NCAMΔCT to the cell surface in primary cortical neurons

(A) Graph shows mean + SEM levels of cell surface NCAM in primary cortical neurons co-transfected with cDNAs for NCAM and KLC1 (KLC1 + NCAM) or GFP (GFP + NCAM), respectively. Cell surface NCAM was labeled with ERIC 1 antibody and anti-mouse-CY3-conjugated secondary antibodies applied after fixation (no NCAM-triggering). ns: not significant (unpaired t-test, $n \geq 99$ from two independent experiments). **(B)** Graph shows mean + SEM levels of cell surface NCAM in primary cortical neurons co-transfected with cDNAs corresponding to full-length NCAM or NCAMΔCT and either KLC1 (KLC1 + NCAM, KLC1 + NCAMΔCT), motor subunits (Motor + NCAM) or GFP (GFP + NCAM, GFP + NCAMΔCT), respectively. Living neurons were incubated for 1 h at 37°C with ERIC 1 antibody (NCAM-triggering) and, after fixation, cell surface NCAM was labeled with anti-mouse-CY3-conjugated secondary antibodies. *p < 0.05 and **p < 0.01 (one-way ANOVA, $n \geq 46$ from three independent experiments), ns: not significant (unpaired t-test, $n \geq 44$ from three independent experiments). **(C)** Graphs show the correlation between the levels of cell surface NCAM and expression levels of KLC1, the motor or GFP, respectively, for the same neurons investigated in (B) of the figure. r: Pearson's correlation coefficient. NCAM: hNCAM180, NCAMΔCT: hNCAMΔCT.

The transfected primary cortical neurons quantified in Fig. 14 B were further analyzed to observe if exclusively internalized hNCAM180 co-localizes with KLC1 after NCAM-triggering. In Fig. 15 surface hNCAM180 labeling and labeling of internalized hNCAM180 together with surface hNCAM180 of two exemplary neurons are shown. In the merged images co-localization of internalized hNCAM180 and KLC1 appears clearly in the soma (A) and growth cone (B).

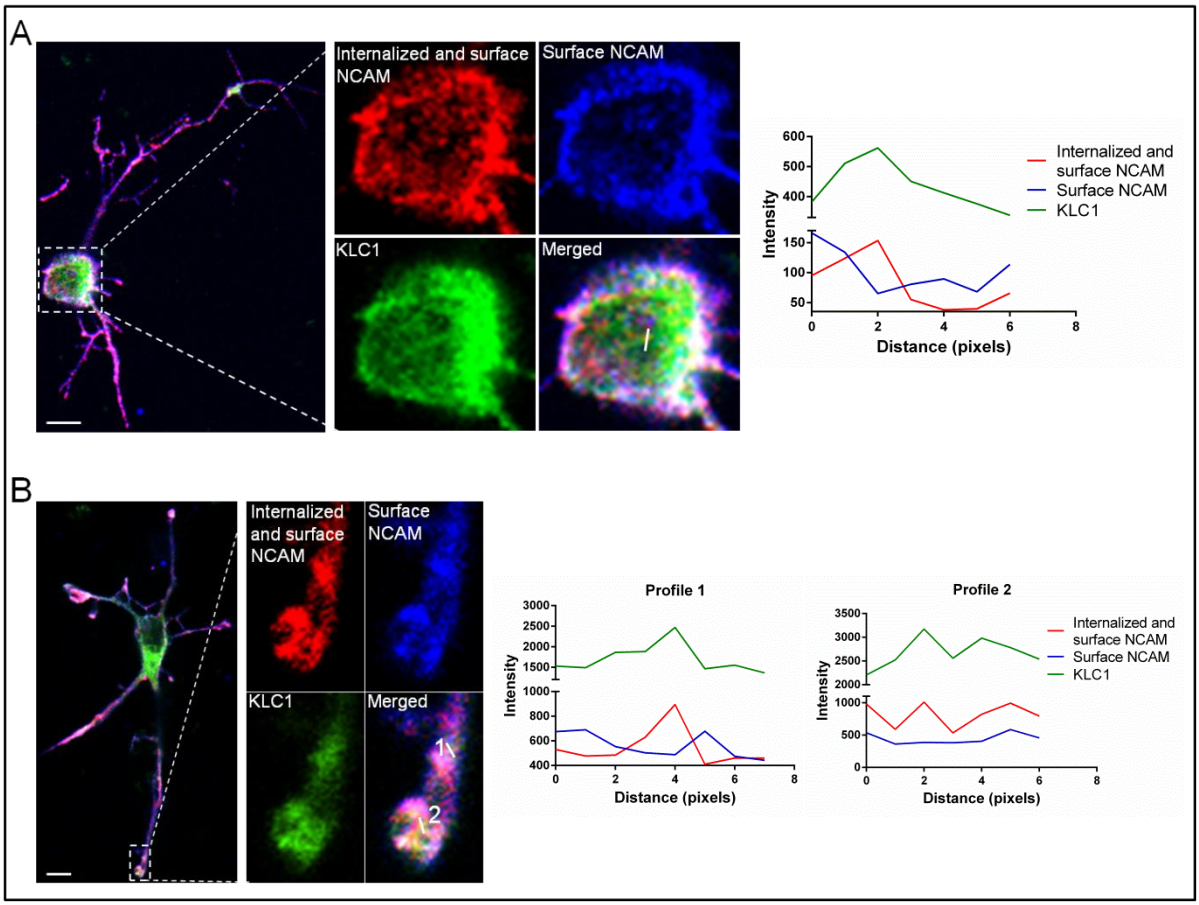

Fig. 15: Immunofluorescence analysis of cortical neurons overexpressing NCAM and KLC1 and detection of internalized and surface NCAM after NCAM-triggering

Transiently with cDNAs of NCAM and KLC1 co-transfected living neurons were incubated with ERIC 1 antibody for NCAM-triggering, fixed, and cell surface NCAM was detected with anti-mouse-CY3-conjugated secondary antibodies. After permeabilization, internalized hNCAM180 and cell surface hNCAM180 were stained with anti-mouse-CY5-conjugated secondary antibodies. Images show exemplary neurons exhibiting co-localized internalized NCAM and KLC1 in the soma **(A)** or growth cone **(B)**. Graphs show immunofluorescence intensity profiles along the corresponding lines in the merged images. Scale bar, 5 µm. NCAM: hNCAM180.

4.2.4. Localization of the KLC1-binding site within the NCAM-sequence and investigation of potential competition partners

The interaction of NCAM and KLC1 was further investigated in more detail by analyzing the KLC1-binding site within the NCAM-sequence that is required for the interaction. Furthermore, a first insight into the mechanisms underlying the interaction of NCAM with KLC1 was gained by identifying a competition partner for the KLC1-binding site.

4.2.4.1. Identification of the KLC1-binding site within NCAM by ELISA

The interaction of KLC1 with chemically synthesized, biotinylated peptides derived from NCAM-ID was investigated in an ELISA. The peptides cover the sequence of NCAM-ID$_{748-777}$ which was used in the competition assay in CHO cells (Fig. 13 A), and were chosen as this region was predicted to contain a potential binding site as described in the discussion (see 5.3). KLC1 antibodies were adsorbed onto the surface of ELISA wells which were incubated after blocking with the soluble fraction of mouse brain tissue to enrich and immobilize KLC1. Subsequently, wells were incubated with increasing concentrations of chemically synthesized biotinylated peptides corresponding to amino acid sequences 748-763 (NCAM-ID$_{748-763}$), 764-777 (NCAM-ID$_{764-777}$), and 756-770 (NCAM-ID$_{756-770}$) of mouse NCAM-ID (Fig. 16 A). Bound biotinylated peptides were detected by POD-conjugated NeutrAvidin and an induced peroxidase reaction. Peptide NCAM140-ID$_{748-763}$ bound to KLC1 in a dose dependent manner, whereas peptides NCAM140-ID$_{764-777}$ and NCAM140-ID$_{756-770}$ did not bind (Fig. 16 B and Tab. 12, Experiment 1).

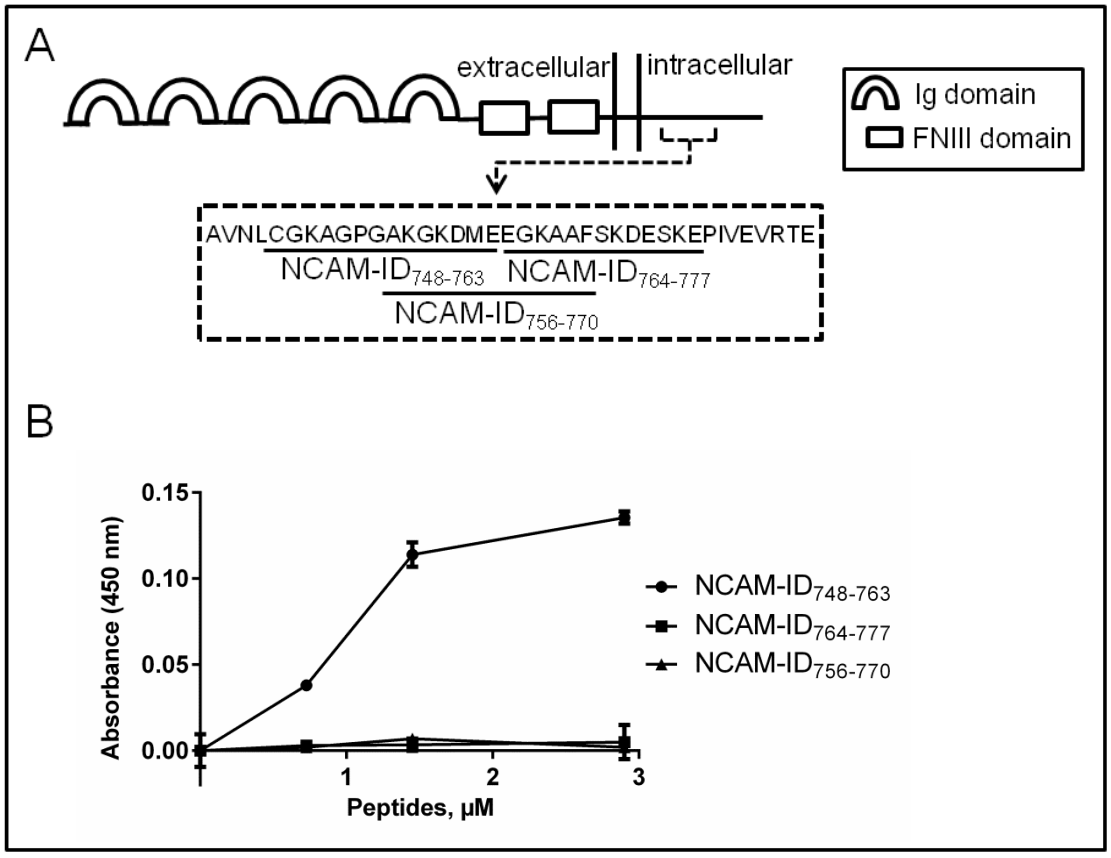

Fig. 16: Identification of the KLC1-binding site within NCAM by ELISA

(A) Schematic drawing illustrating full-length mouse NCAM140 and peptides covering amino acid sequences 748-763 (NCAM-ID$_{748-763}$), 764-777 (NCAM-ID$_{764-777}$), and 756-770 (NCAM-ID$_{756-770}$). **(B)** Binding of biotinylated NCAM peptides NCAM-ID$_{748-763}$, NCAM-ID$_{764-}$777, and NCAM-ID$_{756-770}$ to KLC1 analyzed by ELISA. KLC1 from mouse brain lysate was enriched by binding to KLC1 specific antibodies coated in ELISA wells. NCAM-peptides bound to KLC1 were detected with peroxidase (POD)-conjugated NeutrAvidin followed by a peroxidase-dependent color reaction. Graph shows mean + SD levels of absorbencies from a representative experiment (*n* = 1 or 2 wells).

The exact values of two ELISA experiments are given in Tab. 12. As peptide NCAM140-ID$_{748-763}$ and NCAM140-ID$_{756-770}$ exhibit an overlapping region, the exclusive 8 amino acid region (CGKAGPGA) within NCAM140-ID$_{748-763}$ is likely to be required for the binding of KLC1.

Tab. 12: Absorbance values of ELISA experiments investigating the KLC1-binding site within NCAM

Experiment	Peptides [µM]	Absorbance at 450 nm					
		NCAM-ID$_{748-763}$		NCAM-ID$_{764-777}$		NCAM-ID$_{756-770}$	
1	0	0		0		0	
	0.725	0.038		0.003		0.002	
	1.45	0.047	0.057	0.006	0.001	0.009	0.005
	2.9	0.133	0.138	-0.002	0.012	0.003	0.001
2	0	0		0		0	
	2.9	0.254	0.235	0	0.011	0	

Biotinylated NCAM peptides NCAM-ID$_{748-763}$, NCAM-ID$_{764-}$777, and NCAM-ID$_{756-770}$ were incubated with KLC1 from mouse brain lysate that was immobilized in ELISA wells to coated KLC1 antibodies. Bound peptides were detected with a color reaction of peroxidase conjugated to NeutrAvidin. Shown are the absorbance values at 450 nm of two independent experiments. Peptides were incubated in increasing concentrations once or in duplicates. Blanks (buffer without peptides) were subtracted from the data.

Thereupon, a hNCAM180 construct missing the 8 amino acids CGKAGPGA (hNCAM180Δ747-754) was created by overlap extension polymerase chain reaction (PCR). Primary cortical neurons were co-transfected with cDNAs encoding hNCAM180 and motor subunits or hNCAM180Δ747-754 and motor subunits, and after 1 DIV the cell surface expression of hNCAM180/hNCAM180Δ747-754 was investigated after NCAM-triggering with ERIC 1 antibody and staining with anti-mouse-CY3-conjugated secondary antibodies. Quantification showed that significantly less hNCAM180Δ747-754 than full-length hNCAM180 was delivered to the cell surface in presence of kinesin-1. This result supports the view that these amino acids are required for the binding of NCAM to KLC1 since their deletion seems indeed to abolish the kinesin-1 dependent delivery of NCAM to the cell surface. However, these data are considered as preliminary results and are in need of further verification.

4.2.4.2. Investigation of a potential competition between KLC1 and PAK1 for binding to NCAM by pull-down assay

The amino acid sequence within NCAM-ID required for its binding to KLC1 overlaps with a recently identified binding site for the serine/threonine kinase PAK1 (Li *et al.*, 2013), suggesting that PAK1 and KLC1 may compete with each other for binding to NCAM-ID. To test this hypothesis, a pull-down assay with KLC1 immunopurified from mouse brain was

performed. Beads with immobilized KLC1 were incubated with the chemically synthesized biotinylated peptides NCAM-ID$_{748-763}$, NCAM-ID$_{764-}$777, and NCAM-ID$_{756-770}$, respectively, or NCAM-ID$_{748-763}$ together with PAK1 immunopurified from mouse brain. Slot blot analysis of the pull-downs with POD-conjugated NeutrAvidin showed that only NCAM-ID$_{748-763}$ clearly bound to KLC1 (23 % of the input; Fig. 17) confirming the ELISA result (Fig. 16). The binding of NCAM-ID$_{748-763}$ to KLC1 was abolished in presence of PAK1, giving evidence that KLC1 and PAK1 indeed compete for the binding to NCAM-ID$_{748-763}$.

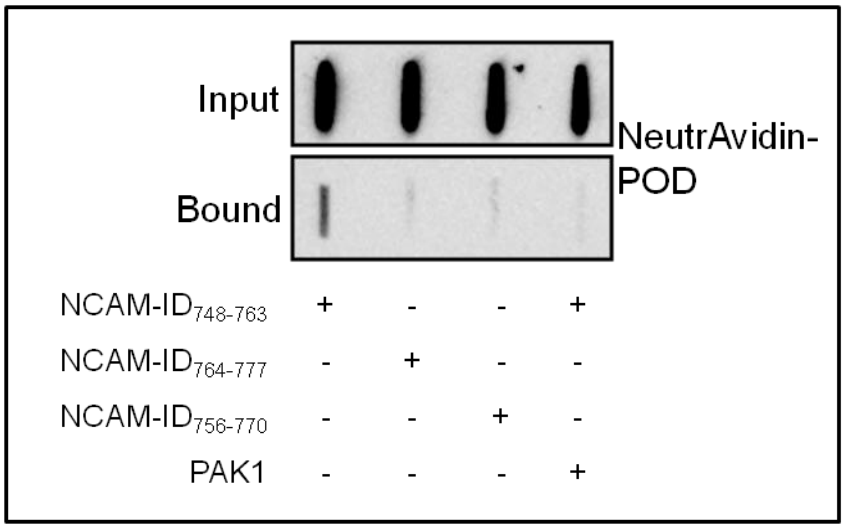

Fig. 17: Investigation of a potential competition between KLC1 and PAK1 for binding to NCAM by pull-down assay

KLC1 was immunopurified from mouse brain, immobilized on agarose beads, and used for a pull-down assay. The beads were incubated with peptides covering NCAM-ID amino acids 748-763 (NCAM-ID$_{748-763}$), 764-777 (NCAM-ID$_{764-777}$), and 756-770 (NCAM-ID$_{756-770}$), respectively, or NCAM-ID$_{748-763}$ together with PAK1. Input material (peptides diluted 1/2000 in buffer) and bound peptides were analyzed by Slot blot using POD-conjugated NeutrAvidin. Similar results were obtained in three independent experiments.

5. Discussion

5.1. Identification of potential interaction partners by protein macroarray

For the identification of novel potential interaction partners of NCAM's intracellular domains a protein macroarray screening was applied. Consisting of 24000 expression clones of human fetal brain proteins, the macroarray presents a high-throughput approach to get first indications of possible protein-protein interactions.

5.1.1. Evaluation of the reliability of the protein macroarray results based on the quality of hNCAM180ID and hNCAM140ID probes

For protein macroarray screening, hNCAM180ID and hNCAM140ID were recombinantly expressed and purified by ligand affinity chromatography. The hNCAM180ID concentrate comprised the complete hNCAM180ID and two lower bands in Western blot (Fig. 4 B). These lower bands most likely represented degradation products of hNCAM180ID as the bands were recognized by 5B8 antibody. The silver staining of the concentrate also revealed some additional minor bands with a molecular weight lower than hNCAM180ID. These additional proteins may also have been degradation products of hNCAM180ID missing the binding site for the NCAM antibody, as the bands were not detected by Western blotting. Generally, it could not be excluded that these bands may have been contaminating host bacterial proteins containing multiple His-residues which could have bound to the Ni-NTA resin, especially as in the E2 fraction some bands beneath the hNCAM180ID signal were detected with tetra-His antibody in Western blot (data not shown).

Although hNCAM140ID concentrate was also not entirely pure (Fig. 5 B), hNCAM180ID and hNCAM140ID concentrates were used for protein macroarray screening, as it was performed solely to gain a first hint of novel potential interaction partners of NCAM which were in any case to be verified by further analyzes.

For the evaluation of the results of the macroarray obtained with hNCAM180ID and hNCAM140ID, it must be considered that both proteins used for the macroarray were tagged. The hNCAM180ID tag of 8 His is relatively small compared to the protein itself that is composed of 386 amino acids. In contrast, the GST-tag comprising 220 amino acids is even bigger than hNCAM140ID (119 amino acids). Therefore, it may have led to false positive signals by interacting with spotted proteins or hinder putative interactions of NCAM with spotted proteins through blocking binding sites given by its 3D structure and/or modification of the structure of hNCAM140ID. Ideally, the GST-tag should have been removed from hNCAM140ID before macroarray performance. The construct contained a thrombin cleavage site to remove GST, however, under various conditions GST was only removable from a

subset of the purified hNCAM140ID, maybe due to folding of the protein which may have obscured the thrombin cleavage site. Finally, the GST-tagged hNCAM140ID was used for macroarray performance. Another way to exclude false positive signals would have been to perform the macroarray with purified free GST as a negative control. Proteins specifically interacting with GST could thus have been excluded from the macroarray results of GST-tagged hNCAM140ID. Free GST was successfully expressed and purified, but after protein macroarray screening with GST-tagged hNCAM140ID, this protein was not removable from the membranes even by repeated stringent stripping treatment. It was not reasonable and affordable to purchase a second macroarray membrane just to perform the negative control Therefore, macroarray results of GST-tagged hNCAM140ID should be regarded with care, except for interaction partners of both isoforms which must be NCAM-specific because the binding occurred with differently tagged isoforms.
In spite of this limitation, first evidence for interesting potential hNCAM-ID interaction partners gained by the macroarray could be verified using other techniques: this applies for UCH-L1 (Wobst *et al.*, 2012), Ufc1 (Homrich *et al.*, 2014) and KLC1 (manuscript in preparation).

5.1.2. Interpretation of the protein macroarray results

Several already known interaction partners of hNCAM-ID were identified by the macroarray, such as spectrin (Pollerberg *et al.*, 1986), PLCγ, and PP2A (Büttner *et al.*, 2005; Tab. 11), suggesting that it may be a reliable tool for the identification of potential hNCAM-ID interaction partners. Functional spectrin exists either as heterodimer composed of two different subunits, namely α- and β-spectrin, or of two equal subunits resulting in a homodimer (Bloch & Morrow, 1989). Using ELISA-based protein ligand-binding assays with NCAM180ID and NCAM140ID, both NCAM isoforms were shown to interact with the α- and β-subunit (Leshchyns'ka *et al.*, 2003). The results of the macroarray showed an interaction of hNCAM180ID and hNCAM140ID with 50 % and 16 %, respectively, of all β-spectrin spots, but only hNCAM140ID interacted with α-spectrin (16 % binding coverage). In addition, exclusively hNCAM140ID did interact with 52 % of the PP2A spots and only hNCAM180ID with PLCγ (33 % binding coverage), although both proteins were described to interact with both transmembrane NCAM isoforms (Büttner *et al.*, 2005).

Calculation of the binding coverage may give additional information about the specificity and affinity of the interaction. Whereas hNCAM180ID only bound to 3 % of all UCH-L1 clones, each spotted Ufc1 protein was detected as interaction partner for hNCAM180ID and hNCAM140ID, respectively, suggesting a high affinity interaction. Uba5 was exclusively spotted on part 9 of the protein macroarray, which was only incubated with hNCAM140ID and bound to 66 % of the spotted Uba5. In a previous work, no interaction between hNCAM180ID and Uba5 was detected on part 8 of the macroarray (Sekulla, 2010).

Approximately 33 % of all KLC1 spots were detected by hNCAM180ID and 36 % by hNCAM140ID.

It should be considered that not all proteins may have been expressed by the spotted bacterial clones on the macroarray membranes therefore contributing to negative results although being taken into account for the calculation of the binding coverage. Additionally, proteins may not have been exposed to NCAM due to incomplete lysis of the bacterial colonies or insufficient removal of bacterial traces. The expression strength should have been tested by labeling of the spotted His-tagged proteins. This consideration was only taken into account for hNCAM180ID as the spotted proteins appeared to be relatively homogenously expressed. As proper control for the expression status of a protein, proteins not labeled with Anti-His IRDye™ 800-antibodies should have been identified and excluded from the total number of spotted proteins. This procedure would have been a disproportionate effort considering that the macroarray should only provide a first hint for the interaction between two proteins. Additionally, as the His-tag is located at the N-terminus of the spotted proteins (Source Bioscience ImaGenes, 2010), no information about the completeness of the expression can be obtained. Taken together, these arguments demonstrate the limitations of the macroarray on one hand, but on the other, its usefulness to get a first impression of potential interactions between proteins which require, however, further verification.

5.2. Investigation of the interaction of NCAM and KLC1

5.2.1. Confirmation of the interaction of NCAM and KLC1 by co-IP

The macroarray screenings indicated a direct binding between hNCAM180ID and hNCAM140ID with KLC1, which was verified and further studied using different methods. First, the interaction was confirmed by co-IP from mice brain tissue (Fig. 6). Using KLC1 antibodies for precipitation, bound NCAM was successfully detected by Western blotting. The appearance of the NCAM signal as a broad smear in Western blot due to polysialylation (Hoffman *et al.*, 1982; Rothbard *et al.*, 1982), did not permit a differentiation between NCAM isoforms. Due to steric hindrance or an unsuitable NCAM antibody the inverse approach, the precipitation of NCAM and subsequent detection of KLC1 in Western blot, was not successful.

5.2.2. Interaction domains of NCAM and KLC1

Using NCAM-ID peptides of different length in an ELISA and a pull-down assay, an 8 amino acid sequence -CGKAGPGA- which is present in NCAM180ID and NCAM140ID was identified as being sufficient for the binding of KLC1 (Fig. 16 and Fig. 17). Initially published

binding regions for KLC1 showed the aromatic amino acid tryptophan being crucial for the interaction of binding partners with KLC1, as shown for Calsyntenin-1/Alcadein (Araki *et al.*, 2007; Konecna *et al.* 2006), Caytaxin (Aoyama *et al.*, 2009; Hayakawa *et al.*, 2007), Vaccina Virus A36 (Dodding *et al.*, 2011), Gamma-A1-adaptin and kinesin interactor (Gadkin; Schmidt *et al.*, 2009), and SifA and kinesin-interacting protein (SKIP; Rosa-Ferreira & Munro, 2011).

Additionally, novel binding motifs not sharing any sequence homology with other KLC1-binding proteins, although also containing an aromatic residue, were discovered successively. For example, the binding of Kidins220/ARMS and JIP-1, respectively, is dependent on a tyrosine within the diverse identified KLC1-interacting motives of both proteins (Bracale *et al.*, 2007; Verhey *et al.*, 2001). As the 8 amino acid sequence of NCAM responsible for the binding to KLC1 does not contain any aromatic amino acid, it represents a new, yet unknown binding motif for KLC1. The peptides of NCAM-ID used for the identification of the KLC1 binding site only covered a region between amino acids 748 and 777. Therefore, it cannot be excluded that other regions within the full-length ID of NCAM are also able to bind to KLC1 by yet unknown sequences. However, the NCAM-ID does not contain further sequences similar to the here identified or any other already published KLC1-binding domain.

KLC1 is composed of N-terminal heptad repeats which are required for the association with KHC and 6 TPR motifs within its C-terminus (Diefenbach *et al.*, 1998; Gindhart & Goldstein, 1996). The ubiquitous TPR motifs mediate protein-protein interactions between the TPR motif of one protein and one or more non-TPR protein(s) in many functionally and structurally unrelated proteins (Blatch & Lässle, 1999). The consensus sequence of TPRs exhibit 34 amino acids and although the TPR motifs of KLC1 comprise 42 amino acids, *i.e.* are longer, the consensus sequence is maintained between its 4th and 37th residue (Zhu *et al.*, 2012).

Many kinesin-1 cargo molecules bind directly to the TPR regions of KLC1, amongst these APP (Kamal *et al.*, 2000), Calsyntenin-1/Alcadein (Araki *et al.*, 2007; Konecna *et al.*, 2006), Caytaxin (Aoyama 2009), Collapsin response mediator protein-2 (CRMP-2; Kimura *et al.*, 2005), and Huntingtin-associated protein-1 (McGuire *et al.*, 2006). The close homologue of L1 (CHL1) is also a cell adhesion molecule of the Ig superfamily. Analysis of local similarity of both sequences revealed that the ID of human CHL1 shares 44 % identity with hNCAM180ID (analyzed by Basic Local Alignment Search Tool, BLAST®; Altschul *et al.*, 1990) and does also not contain a tryptophan, but tyrosines. As the ID of CHL1 is known to bind to TPR regions (Andreyeva *et al.*, 2010), it might be conceivable that the binding between NCAM and KLC1 is also mediated by the TPR motifs of KLC1.

Investigation of the crystal structure of the three TPRs of protein phosphatase 5 revealed that tandemly arranged TPR motifs are organized into a regular right-handed superhelix that is capable of accommodating multiple ligands (Das *et al.*, 1998). Konecna and coworkers quantified the interaction between the cytoplasmic domain of Calsyntenin-1/Alcadein and KLC1 showing a saturation of KLC1 to Calsyntenin-1/Alcadein binding at a molar ratio of 0.5, indicating that indeed one KLC1 binds two cytoplasmic domains of Calsyntenin-1/Alcadein (Konecna *et al.*, 2006), which has been confirmed later by Zhu *et al.* (Zhu *et al.*, 2012). Therefore, one kinesin-1 motor with two KLC1 might bind and transport four Calsyntenin-1/Alcadein simultaneously.

A similar mechanism might be considered for NCAM, especially as NCAM interacts *cis*-homophilically with other NCAM molecules (see 1.1.5.1 for details), which may form a stabilized binding complex for the interaction with KLC1. Interestingly, increasing evidence suggests that motor proteins are not randomly spread over the surface of the cargo, but organized in clusters of two or more. Clustering seems to increase the run length of the motor proteins and is therefore most likely relevant for the long distance transport along microtubule performed by kinesins and dyneins, rather than by myosins, which move along short distances of actin filaments (Erickson *et al.*, 2011; Gross *et al.*, 2007). Accumulations of *cis*-homophilically bound NCAM molecules could therefore bind to clusters of kinesin-1, exhibiting binding sites for several NCAM molecules at each kinesin-1 motor and thereby stabilizing the interaction.

5.2.3. Co-localization studies in CHO cells and primary neurons

Co-localization of NCAM with kinesin-1 or parts of the motor (KLC1 or KIF5A) were confirmed in CHO cells and primary hippocampal and cortical neurons. Whereas the co-localization of intracellular hNCAM180 and the motor was widespread and easily detectable in CHO cells co-transfected with cDNAs of hNCAM180 and motor subunits (Fig. 7) as well as endogenous NCAM and KLC1 in hippocampal neurons (Fig. 8 A), an overlap of endogenous NCAM and KIF5A staining appeared less frequently in hippocampal neurons (Fig. 8 B). By staining of NCAM and KIF5A, co-localization could only be detected where KIF5A associated with KLC1, as KLC2, KLC3, and KLC4 do not bind NCAM according to the macroarray results. NCAM may also be bound to KIF5B and KIF5C associated KLC1, which was not analyzed in this experimental setup. This might explain the relatively rare occurrence of co-localized NCAM and KIF5A.

Interestingly, after stimulation of NCAM endocytosis in cortical neurons overexpressing hNCAM180 and KLC1, internalized hNCAM180 co-localized with KLC1 in the soma and growth cone (Fig. 15). The staining could have been improved by saturation of all membrane

associated antibodies with immunoglobulins for exclusive staining of internalized hNCAM180 without concomitant staining of cell surface hNCAM180. Additionally, for more detailed growth cone analysis higher resolution imaging would be preferable.

5.2.4. Investigation of the presence of NCAM and kinesin-1 in TGN organelles

TGN organelles, the main carriers of proteins synthesized in the ER, were enriched from mouse brain and the concomitant presence of NCAM, KLC1, and KIF5A in TGN organelles confirmed by Western blot (Fig. 9). Interestingly, polyclonal antibodies against KIF5A detected two bands in close proximity to each other at approximately 120 kDa, as shown in other publications (Sun *et al.*, 2011; Xia *et al.*, 2003). Potentially, one of the bands may have represented an unspecific binding of the antibodies, as shown for polyclonal KIF5C antibodies, which recognize an unidentified protein with a molecular weight slightly below KIF5C (Pierce-antibodies, 2014). Another explanation could have been a mobility shift of KIF5A due to posttranslational modifications as for example phosphorylation. Phosphorylation can result in a slower migration of the protein in SDS-PAGE and therefore in an increased apparent molecular weight. This phenomenon is not explainable by the mass of the phosphate of 0.08 kDa, but phosphorylation may alter the SDS coating of the protein in dependence on the local charge of neighboring proteins (Peck, 2006). The KHCs have been described as being phosphorylated (DeBerg et al., 2013; Morfini et al., 2002; Hollenbeck, 1993) which contributes to fine tuning of their functions and/or activity levels.

The co-localization of endogenous NCAM and KIF5A in γ-adaptin positive organelles was also investigated in primary hippocampal neurons to further strengthen the hypothesis of kinesin-1 transporting NCAM packed in TGN organelles. At most one spot per neuron was identified showing co-localization of NCAM, KIF5A, and γ-adaptin (Fig. 10). The rare occurrence may be due to the variability in the composition of the heterotetrameric kinesin-1, as described above for the co-localization of NCAM and KIF5A (see 5.2.3). Possibly, more overlap could have been detected by co-staining KLC1 instead of KIF5A. Interestingly, other groups did not use TGN organelle markers to investigate the co-localization of proteins with kinesin-1 and the transported organelle, instead, co-localization of proteins with already known cargoes of kinesin-1 is often investigated (Aoyama *et al.*, 2009; Bracale *et al.*, 2007), maybe providing a better tool. It might also be conceivable that the low amount of NCAM-containing transport organelles co-localizing with KIF5A could be compensated by a transport of multiple NCAM's by a single kinesin-1 in neurons, as discussed above (see 5.2.2). However, this result also raises the question, whether kinesin-1 is only involved in the transport of NCAM packed in TGN organelles or is additionally functioning in a different trafficking pathway of NCAM in neurons as discussed below (see 5.4.1).

5.3. Functional studies in CHO cells and primary cortical neurons

In the progress of this work, the interaction of NCAM and KLC1 has been verified by co-IP, co-localization studies, ELISA and pull-down assay. To analyze the possible involvement of kinesin-1 in the transport of NCAM to the cell surface, functional studies were carried out. Transfection of CHO cells showed that significantly more hNCAM180 was delivered to the cell surface in dependency on the expression level of motor components (KLC1 or both motor subunits; Fig. 11). Interestingly, the amount of cell surface hNCAM180 was not significantly different in CHO cells co-transfected with cDNAs of hNCAM180 and KLC1 or both motor subunits, respectively, suggesting that endogenous KHC1, which is present in CHO cells (Hammond *et al.*, 2012: Kif5a, Kif5b, and Kif5c genes present), forms a functional motor with exogenous KLC1 as already shown in another publication (Araki *et al.*, 2007), being sufficient for NCAM delivery to the cell surface. The results were confirmed in primary cortical neurons after stimulation of NCAM endocytosis (Fig. 14 B and C), providing more evidence for a kinesin-1 mediated transport of NCAM in neurons.

The KLC1-binding region lies within the ID of NCAM; therefore the effect of kinesin-1 on hNCAM∆CT was tested by co-overexpression of KLC1 or the motor and hNCAM∆CT, respectively, in CHO cells and primary cortical neurons. Quantification of cell surface hNCAM∆CT and correlation analysis revealed that the delivery of hNCAM∆CT to the cell surface occurs most likely independent of kinesin-1 in both cell models (Fig. 12 and Fig. 14 B). The structure of hNCAM∆CT is similar to NCAM120, which is anchored to the membrane via GPI and does not exhibit an ID (Fig. 1). NCAM120 is mainly localized in lipid rafts in oligodendrocytes (Krämer *et al.*, 1999) and has already been shown to be transported by a different mechanism than NCAM180 and NCAM140 (Garner *et al.*, 1986; Nybroe *et al.*, 1986). It would be conceivable that NCAM120 might be transported by a lipid dependent mechanism, which might also be speculated for hNCAM∆CT. But as the GPI anchor has been shown to be obligatory for the localization of NCAM120 into lipid rafts (Krämer *et al.*, 1999), this hypothesis must be rejected. Additionally, NCAM120 is mainly expressed in glia cells (Krämer *et al.*, 1999; Noble *et al.*, 1985). For these reasons the trafficking of hNCAM∆CT is most likely different from NCAM120 as well as neuronal expressed NCAM, as discussed below (see 5.4.1).

Furthermore, NCAM180 and NCAM140 are localized in lipid raft and non-lipid raft fractions in neurons. In case of the transmembrane isoforms, palmitoylation of at least two cysteines has been shown to be responsible for the lipid raft localization (Little *et al.*, 1998). Niethammer and coworkers showed in hippocampal neurons that an NCAM140 construct missing the four palmitoylation sides by replacing the cysteines with serines is exluded from lipid rafts (Niethammer *et al.*, 2002), again confirming that hNCAM∆CT is not likely to be transported

by involvement of lipids. A possible accumulation of hNCAMΔCT within the cell due to altered endocytosis of the construct can also be excluded (Diestel, unpublished data, Institute of Nutrition and Food Science, Department of Human Metabolomics, University of Bonn, Germany). In conclusion, neither a kinesin-1 nor lipid dependent transport mechanism seems to be responsible for the trafficking of hNCAMΔCT.

To further verify the transport of NCAM by kinesin-1 via binding of its ID to KLC1, a competition assay was performed in CHO cells with cDNAs covering NCAM-ID and several shorter peptide sequences thereof (Fig. 13), which were used for triple-transfection together with the cDNAs of hNCAM180 and the motor subunits. Excess of NCAM-ID is predicted to have a dominant-negative effect by binding to KLC1, thereby blocking the interaction of KLC1 with full-length hNCAM180 and inhibiting NCAM's delivery to the cell surface. Indeed, significantly less hNCAM180 was delivered to the cell surface when co-transfected with cDNA coding for NCAM-ID in hNCAM180 and motor overexpressing cells ($p < 0.01$, one-way ANOVA, not shown in graph). Interestingly, even shorter peptides derived from NCAM-ID inhibited the transport of hNCAM180 to the cell surface, showing that a sequence of NCAM-ID is required for the delivery to the cell surface by kinesin-1. Chernyshova and coworkers showed that the exocyst subunit exo70 binds within the amino acids 729-750 of NCAM140ID and sec8 within the amino acids 777-810 (Chernyshova *et al.*, 2011). The exocyst is a protein complex essential for exocytosis *e.g.* in neurite outgrowth, which includes secretion of vesicle content into the extracellular space or integration of intracellular proteins into the plasma membrane (Hsu *et al.*, 2004). Although the binding of exo70 and sec8 did not occur with NCAM180 in that study, NCAM180 is likely to interact with the exocyst subunits, as NCAM180 also contains the required binding regions (Chernyshova *et al.*, 2011). The transfection of the peptides NCAM-$ID_{729-750}$ and NCAM-$ID_{777-810}$ could therefore block the binding of the exocyst subunits and inhibit the exocytosis of hNCAM180 at the plasma membrane. The peptide NCAM-$ID_{748-777}$ contains the binding region for KLC1, which was identified by ELISA (Fig. 16), and was most likely due to that blocking the delivery of hNCAM180 to the cell surface.

5.4. Potential transport mechanisms of NCAM by kinesin-1

5.4.1. Kinesin-1 may influence the transport of newly synthesized and endocytosed NCAM

Studies in CHO cells and primary cortical neurons showed that co-overexpression of hNCAM180 with KLC1 or the motor significantly increases the amount of hNCAM180 at the cell surface compared to control (Fig. 11 and Fig. 14 B), suggesting a kinesin-1 dependent transport of NCAM. The staining of cell surface hNCAM180 was performed on living CHO

cells, which were kept on ice for the incubation time of the antibodies and washing steps (50 min in total) before cells were fixed. The experiment was repeated with primary cortical neurons, which were either fixed before primary antibody incubation (Fig. 14 A) or the antibody was applied to living cells for 1 h at 37°C (Fig. 14 B), before the staining procedure was performed. Interestingly, only neurons which were stained alive - which stimulates NCAM endocytosis - showed an increased delivery of hNCAM180 to the cell surface in presence of kinesin-1. Keeping CHO cells on ice during antibody application inhibits NCAM's endocytosis. However, CHO cells show the same effect on kinesin-1 dependent NCAM delivery without stimulation of NCAM endocytosis as NCAM-triggered neurons. The differences might be explainable by the different cell types used. Sampo *et al.* and Wisco *et al.* even described different trafficking routes of the same protein within different neuronal cell types (Sampo *et al.* 2003; Wisco *et al.*, 2003). Additionally, also other authors noted the possibility that the same protein could use multiple tracks depending on various factors, such as cell type, density of the cells, and stage of maturation (Winckler, 2004; Kamiguchi & Yoshihara, 2001).

As a conclusion of the experiments in CHO cells and neurons, two hypotheses on the transport of NCAM by kinesin-1 are conceivable: The direct transport of newly synthesized NCAM and an indirect transport via the soma plasma membrane and subsequent NCAM endocytosis to its final destination on neurites, for example, the axonal plasma membrane (Fig. 18).

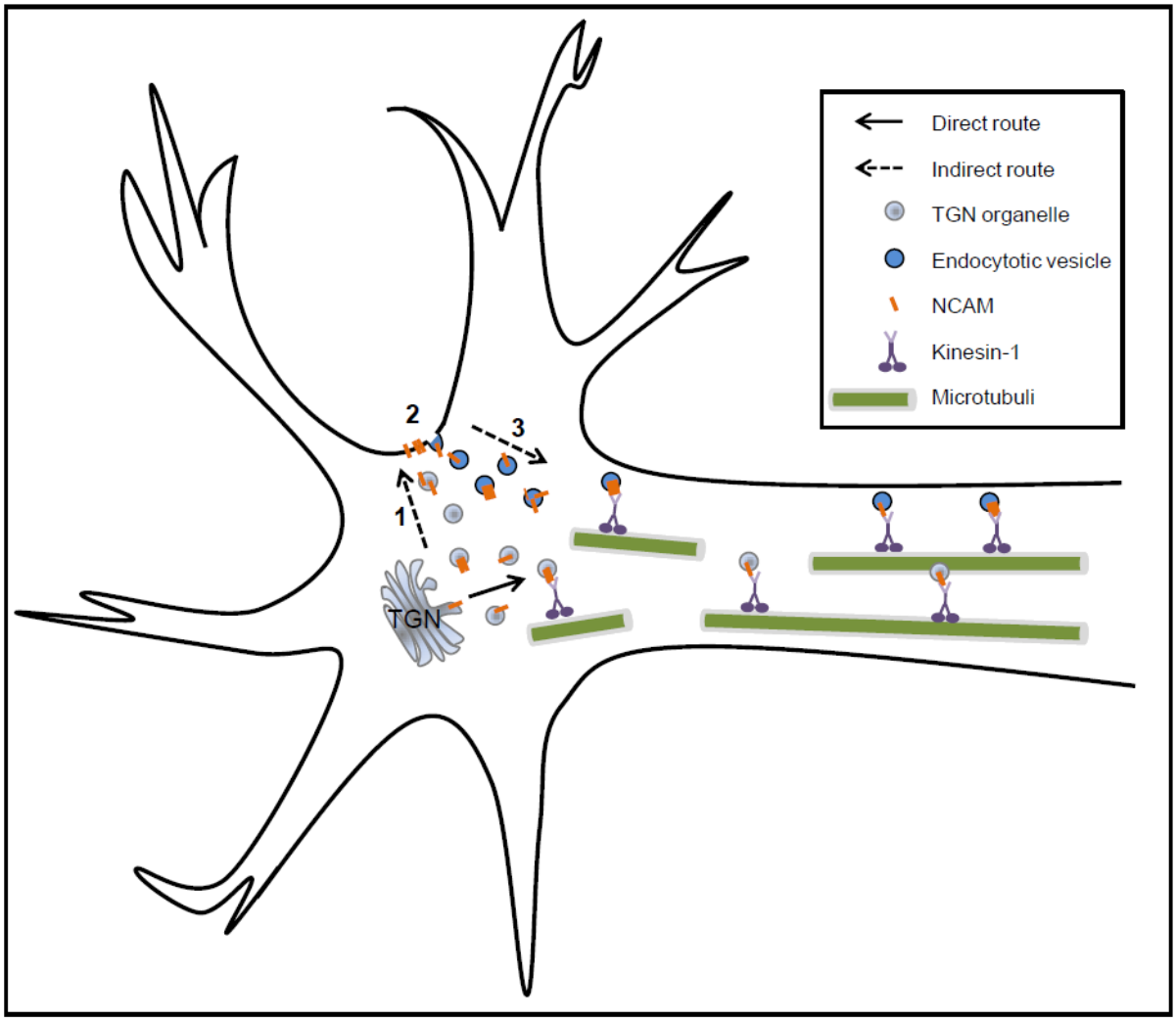

Fig. 18: Schematic model illustrating potential transport mechanisms of NCAM by kinesin-1

NCAM might be transported on a direct route from the *trans*-Golgi network (TGN) to neurites by binding to kinesin-1, which travels along microtubuli. Alternatively, NCAM might be transported on an indirect route, which at least consists of three steps: (1) TGN to soma plasma membrane, (2) soma plasma membrane to endocytotic vesicles in dependence on NCAM endocytosis, and (3) endocytotic vesicles to plasma membrane of neurites along microtubuli by binding to kinesin-1.

Already decades ago NCAM180 and NCAM140 have been shown to be transported by the fast axonal transport in chick retinal ganglion (Garner *et al.*, 1986; Nybroe *et al.*, 1986). Later on, the NCAM related neuron-glia cell adhesion molecule (NgCAM; the chick homologue of L1) of the IgCAM superfamily has been described to be packed into specific transport organelles and being mainly transported to axonal membranes by motor proteins independent of its endocytosis in mature hippocampal neurons (Sampo *et al.*, 2003; Jareb & Banker *et al.*, 1998; Vogt *et al.*, 1996). Also Peretti and coworkers provided evidence for the involvement of a kinesin-like protein, KIF4, in the direct anterograde transport of L1-containing vesicles in rat brain tissue (Peretti *et al.*, 2000). KIF4 has been shown to transport membranous organelles in juvenile tissues and being expressed in a developmentally

regulated manner (Sekine *et al.*, 1994), indicating that other motor proteins may be involved in L1 trafficking in mature individuals.

In contrast, Wisco and coworkers showed that downregulation of endocytosis inhibited axonal polarization of NgCAM in hippocampal neurons. They postulated a trafficking pathway of NgCAM in neurons similar to transcytosis in epithelia, where some membrane proteins are transported from one plasma membrane domain to a different location by the endocytotic system (Wisco *et al.*, 2003), and which has also been demonstrated for a limited number of membrane proteins in neurons, such as APP (Simons *et al.*, 1995; Yamazaki *et al.*, 1995), and the type 1 cannabinoid receptor (Leterrier *et al.*, 2006). Dependent on an intact cytoplasmic domain of NgCAM, the protein was initially inserted in the somatodendritic domain, subsequently endocytosed, and transported to the axon. Interestingly, even a single point mutation (tyrosine to alanine) within the ID of NgCAM changed the trafficking to a direct axonal pathway starting from the TGN. Therefore it was postulated that direct and indirect transport mechanisms exist in polarized neurons and the somatodendritic delivery is domain-specific and signal mediated (Wisco *et al.*, 2003).

The group of Lemmon and coworkers showed in chick dorsal root ganglia that NgCAM is being internalized by clathrin-mediated endocytosis at the central domain of growth cones, sorted into early endosomes and reinserted into the plasma membrane at the leading edge of the growth cones (Kamiguchi & Lemmon, 2000; Kamiguchi *et al.*, 1998). Their studies revealed that NgCAM-containing endocytotic vesicles are positioned along microtubules and their transport is dependent on dynamic microtubules at the leading edge of growth cones (Kamiguchi & Lemmon, 2000), strongly suggesting a transport of these vesicles by the microtubule based anterograde motor kinesin. These observations further underline the presence of multiple pathways for protein transport in different cell types at different stages of maturation.

Endocytosis of NCAM takes place in somata, neurites, and growth cones of cortical neurons in a developmentally regulated way (Diestel *et al.*, 2007). Additionally, NCAM180 and NCAM140 have been shown to be present in rat sarcoma (Ras)-related proteins in brain (Rab)5-, Rab4- and Rab11-positive organelles (Diestel *et al.*, 2007), illustrating NCAM's trafficking through early and recycling endosomes. Several groups showed kinesin-1 transporting Rab5- and Rab4-positive vesicles or other markers associated with early endosomes using various approaches (Loubéry *et al.*, 2008; Nath *et al.*, 2007; Bananis *et al.*, 2004), revealing the possibility of NCAM being transported after endocytosis in early and/or recycling endosomes by kinesin-1. This might also explain the poor co-localization of NCAM and KIF5A in γ-adaptin positive organelles (Fig. 10 and discussed above 5.2.3). Compared to that, the co-localization of internalized hNCAM180 and KLC1 in cortical neurons was more

striking (Fig. 15), supporting the hypothesis of kinesin-1 transporting endocytosed NCAM. Nonetheless, a comparison between transfected and untransfected neurons as well as between hippocampal and cortical neurons might be difficult due to the above mentioned arguments regarding the transport of proteins in different cell types and even different types of neurons.

Endocytosis and recycling of NCAM have been speculated to be important for relocation of the protein at the cell surface and therewith regulating NCAM's functions in neuronal processes such as cell migration, growth cone mobility, and synaptic plasticity. Recently, it has been shown in a human cancer cell line that the ratio between PSA-NCAM and non-PSA-NCAM is not only dependent on the expression and/or activity of the polysialyltransferases ST8SiaIV and ST8SiaII, but also on NCAM's internalization and turnover (Monzo *et al.*, 2013). A small amount of PSA-NCAM was detected to co-localize with Rab5 after endocytosis stimulation (Monzo *et al.*, 2013) and Miñana and coworkers showed a high degree of PSA-NCAM co-localizing with clathrin (Miñana *et al.*, 2001). Inside the endosomes, the PSA is thought to be degraded due to the acidic environment (Monzo *et al.*, 2013; Manzi *et al.*, 1994). As kinesin-1 has been shown to transport various types of endosomes (see above), it could be involved in the relocation of NCAM, concomitant with the change of NCAM from a plasticity-promoting to a stability-promoting protein.

5.4.2. How could kinesin-1 increase the amount of cell surface NCAM?

In case of a direct transport of newly synthesized NCAM from the Golgi to the axonal plasma membrane mediated by kinesin-1, co-overexpression of both proteins would lead to an increased amount of cell surface NCAM compared to the control. However, the question arises how this effect is mediated on endocytosed NCAM by kinesin-1, as kinesin-1 is not likely to influence NCAM's endocytosis rate and not more NCAM vesicles to be present. It is to be expectable that the excessive kinesin-1 in the motor transfected group accelerates NCAM's transport resulting in an increased amount of cell surface NCAM within the investigated time period (Fig. 19 B), while in the control group the NCAM-containing vesicles would be transported relatively slowly by a limited number of endogenous kinesin-1 (Fig. 19 A). In neurons co-transfected with cDNAs encoding hNCAM180 and KLC1, endogenous KHC1 would be the limiting factor to form functional kinesin-1, as described before (see 5.3).

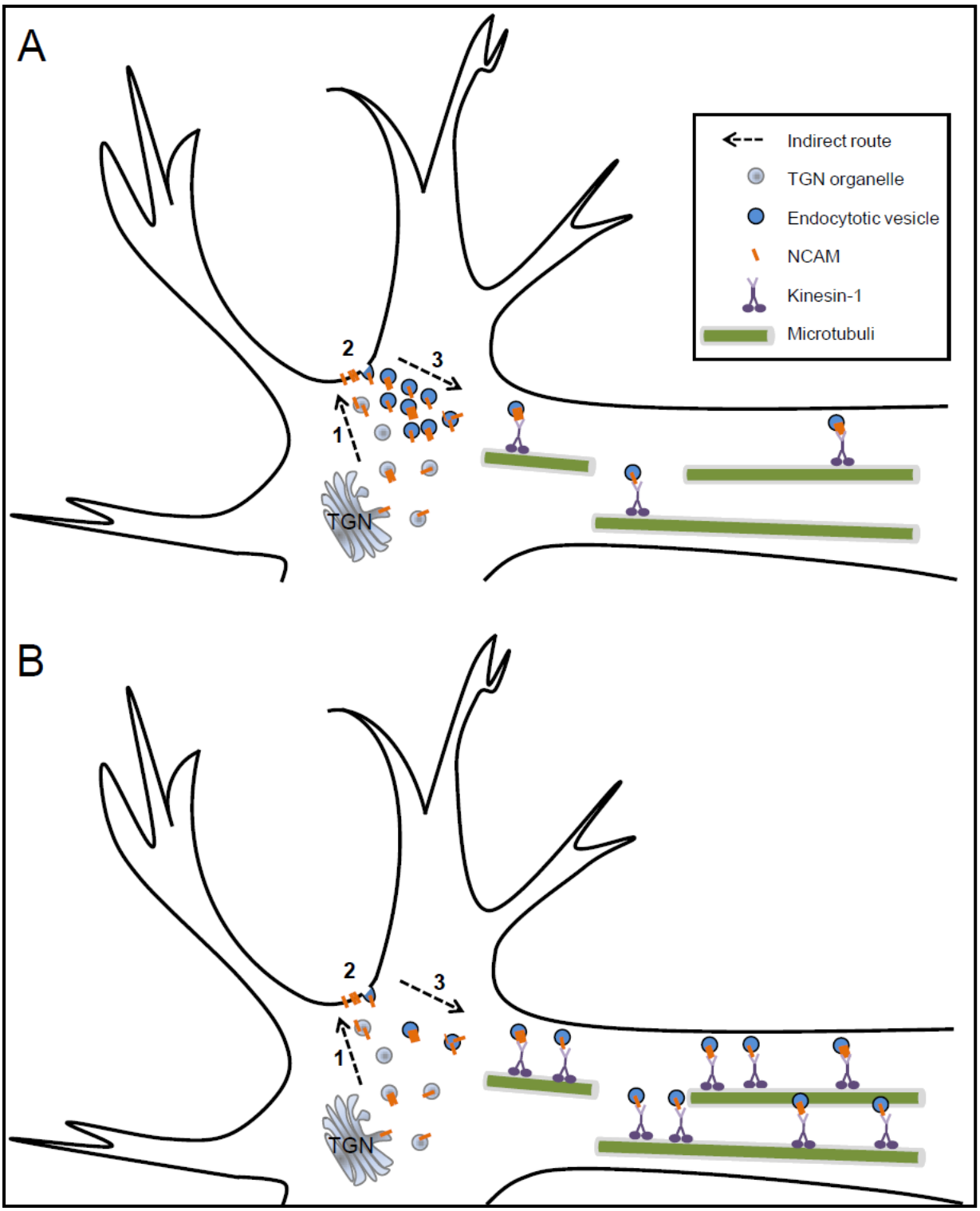

Fig. 19: Schematic model of a hypothesized transport mechanism of NCAM by kinesin-1 after NCAM endocytosis

(1) NCAM is transported from the *trans*-Golgi network (TGN) to the soma plasma membrane by an unknown mechanism, (2) NCAM is endocytosed and packed into vesicles at the plasma membrane, and (3) transport of NCAM endocytotic vesicles to the plasma membrane of neurites along microtubuli is enabled by endogenous kinesin-1 **(A)** or accelerated by overexpressed kinesin-1 **(B)**.

Another explanation might be given by a changed relation of the motor proteins, kinesin, dynein, and myosin, which could lead to the differences of cell surface NCAM levels within

the control and the motor co-transfected group after NCAM-triggering. Transport vesicles have been suggested to be bound not only to one type of motor proteins, but to several different (Hendricks *et al.*, 2010, Gross *et al.*, 2002). Depending on the surrounding effectors (*i.e.* phosphorylation, binding partners), one or the other motor protein(s) could be active, transporting the cargo either anterograde or retrograde along microtubules, or even changing the track from microtubuli to actin filaments driven by myosin, or vice versa (Blasius *et al.*, 2007; Mesngon *et al.*, 2006; Lindesmith *et al.*, 1997). In contrast to the hypothesis of effectors regulating the motor engagement, the number of bound motors of one type to the vesicle was postulated to battle in a so called “tug of war” for the direction of the movement while the motors are simultaneously active (Fu & Holzbaur, 2014; Gross *et al.*, 2007). Later on, the “tug of war” hypothesis gained more evidence and emphasized the importance of the ratio of plus- end minus-end directed motors on the trafficking direction unaffected by other regulatory factors (Hendricks *et al.*, 2010).

NCAM endocytosis is hypothesized by Diestel *et al.* to serve also as pathway for the removal of NCAM interacting molecules from the cell surface (Diestel *et al.*, 2007). At least, it is likely that NCAM interacting molecules or other proteins would also be present in NCAM-containing vesicles and could thereby provide more potential binding sites for motor proteins. Additionally, potential involvement of other motor proteins in NCAM’s transport is reasonable. Recently, an interaction between NCAM180 and dynein has been described (Perlson *et al.*, 2013). Dynein binds to NCAM isoform 180 specific amino acids near its C-termini. Although this paper focused on the ability of NCAM180 bound dynein to tether dynamic microtubules at the actin-rich layer of cytoplasm underlying the plasma membrane (cell cortex), the interaction may also be relevant for NCAM’s transport within the cell. Interestingly, dynein heavy chain 1 was detected on the protein macroarray as potential interaction partner for hNCAM140ID (14 % binding coverage). Furthermore, Polo-Parada and coworkers described a conserved motif at the very end of NCAM’s C-terminus that may signal via myosin light chain kinase to regulate myosin-driven synaptic vesicle trafficking at the presynaptic terminal (Polo-Parada *et al.*, 2005). In case of co-overexpressed kinesin-1 the motor could bind to the ID of NCAM exposed on the vesicle and fulfill its function in anterogradely transporting the increased amount of NCAM to its final destination at the plasma membrane of neurites. If exclusively NCAM is overexpressed, other motor proteins could dominate the transport and relocate NCAM to other destinations within the cell or remarkably slow-down the kinesin-1 dependent transport to the plasma membrane within the investigated time period. However, only detailed analysis could clarify the exact transport mechanism of NCAM within neurons and other cell types.

5.4.3. Potential regulatory mechanisms mediating detachment of NCAM from kinesin-1

Recently, PAK1 has been identified as new interaction partner for NCAM that binds to the same 8 amino acid sequence within NCAM-ID as KLC1 (Li *et al.*, 2013). Therefore, it was suggested that PAK1 and KLC1 may compete with each other for binding to NCAM-ID. This hypothesis was confirmed in a pull-down assay, where the binding of the NCAM-peptide comprising the 8 amino acids to KLC1 was abolished in presence of PAK1 (Fig. 17). Therefore, PAK1 may be involved in the regulation of kinesin-1 dependent transport of NCAM.

PAK1 is a member of the PAK family of serine/threonine kinases, which are key regulators of cytoskeleton dynamics in neurons (Kreis & Barnier, 2009; Bokoch, 2003). PAK1 is targeted to the plasma membrane, influencing the activity of the protein (Daniels *et al.*, 1998; Lu *et al.*, 1997). NCAM and PAK1 have been shown to strikingly co-localize in growth cones of hippocampal neurons (Li *et al.*, 2013). When kinesin-1 and its cargo reach their destination, such as the growth cone plasma membrane, a signal leading to detachment of the cargo from kinesin-1 is required. PAK1 may be involved in detachment of NCAM from kinesin-1 by competing with KLC1 for the same binding site within NCAM-ID. Other NCAM interactions were suspected to be regulated in an analogous way. FGFR and ATP were shown to bind to the same FNIII domains within NCAM (Kiselyov *et al.*, 2003). As ATP has been shown to inhibit the NCAM-FGFR interaction, ATP seems to have a regulatory role on that interaction and thereby indirectly modulates NCAM-mediated cell adhesion and axonal outgrowth (Bork *et al.*, 2013; Kiselyov *et al.*, 2003; Skladchikova *et al.*, 1999). A similar mechanism involving motor protein mediated transport has been described for Calsyntenin-1/Alcadein, JIP1 and APP. Arakit *et al.* showed that Calsyntenin-1/Alcadein inhibits the JIP1 mediated transport of vesicles containing APP, whereas JIP1 disrupts the binding between kinesin-1 and Calsyntenin-1/Alcadein-containing vesicles (Araki *et al.*, 2007). Interestingly, the binding and trafficking of Calsyntenin-1/Alcadein by kinesin-1 has later been shown to be also regulated by phosphorylation of KLC1 (Vagnoni *et al.*, 2011), giving evidence that competition for binding and phosphorylation may potentially simultaneously coordinate the binding between motor proteins and cargoes.

Therefore, another possibility how PAK1 could possibly influence the binding between NCAM-ID and KLC1 might be given by PAK1's kinase activity. Interestingly, a regulatory role of PAK1 on motor proteins by phosphorylation has already been described. It has been shown that PAK1 is able to phosphorylate the light chain 1 of dynein (Vadlamudi *et al.*, 2004). Furthermore, also myosin light chains have been shown to be phosphorylated by PAK1 in HeLa cells and neuronal cells accounting for the stabilization of the localized actin network (Zhang *et al.*, 2005; Brzeska *et al.*, 2004). Finally, Pakala and coworkers showed

that mitotic centromere-associated kinesin (MCAK), a kinesin-13 (formerly KIF2), is phophorylated at two serines *in vitro* and *in vivo* by PAK1 (Pakala *et al.*, 2012).

Phosphorylation has been shown to interrupt the interaction between motor and cargo. For example, Glycogen synthase kinase 3 has been shown to phosphorylate KLCs, which seems to induce the release of kinesin cargo from specific subcellular domains (Morfini *et al.*, 2002). Similarly, the phosphorylation of the dynein light intermediate chain detaches cytoplasmic dynein from membranes (Addinall *et al.*, 2001) and phosphorylation of the C-terminal tail region of myosin-V resulted in detachment of the motor from organelles (Karcher *et al.*, 2001). Guillaud and coworkers showed that the interaction between a member of the kinesin-2 family (formerly KIF17) and the scaffolding protein Mint1 is disrupted by the calcium-calmodulin-dependent protein kinase II (CaMKII) mediated phosphorylation of KIF17 (Guillaud *et al.*, 2007).

In conclusion, these data may underline the possibility that not solely the competition for the NCAM binding site between KLC1 and PAK1 may regulate the interaction, but also the kinase function of PAK1. It is tempting to speculate a connection between the transport of NCAM by kinesin-1 and subsequent PAK1 activation, which as important regulator of the cytoskeletal dynamics may reorganize the cytoskeleton to enable neurite outgrowth.

5.5. Conclusion and future studies

In this thesis, new potential interaction partners of NCAM-ID were identified by a protein macroarray screening with the investigation of NCAM's interaction with KLC1 being in the focus of this work After confirmation of the interaction by several approaches and identification of the KLC1-binding site within NCAM-ID, functional analyzes showed that hNCAM180 is being transported by kinesin-1 to the cell surface in CHO cells and primary neurons by a direct transport of newly synthesized hNCAM180 and in dependency on NCAM endocytosis prior to transport. First evidence was gained for a potential mechanism regulating the detachment of NCAM from KLC1 at the cell surface after kinesin-1 dependent transport.

Preliminary results indicated that deletion of the KLC1-binding site within hNCAM180 (hNCAM180Δ747-754) indeed abrogated the kinesin-1 dependent delivery of hNCAM180 to the cell surface in cortical neurons. In this context, the internalization rates of full-length hNCAM180 and hNCAM180Δ747-754 were also investigated, and revealed no differences. However, results need to be verified and studies are repeated at the moment.

In this thesis, cDNA of hNCAM180ID was used for transfection studies. As the KLC1-binding region within NCAM is also present in hNCAM140ID, a hNCAM180-similar transport

mechanism of hNCAM140 by kinesin-1 is conceivable. Nonetheless, investigation of similarities and differences between the transport mechanisms of hNCAM180 and hNCAM140 would be interesting, especially in regard to their isoforms-specific functions.

Furthermore, it would be interesting to investigate the co-localization of NCAM and kinesin-1 in Rab-positive vesicles in neurons to strengthen the hypothesis of endocytosed NCAM being transported in early and/or recycling endosomes by kinesin-1. Regarding the functional role, clarification if the kinesin-1 dependent transport of NCAM is involved in the progressive replacement of PSA-NCAM by non-PSA-NCAM at the cell surface could be involved in further experiments.

In motor protein dependent trafficking, life cell imaging is a commonly used tool to monitor real-time events in the cells. First experiments to investigate the route of hNCAM180 throughout CHO cells by using different fluorescent timers that change color over the time in the cell (Subach *et al.*, 2009) unfortunately failed. However, fluorescent timers provide a valuable tool and could answer the question about the exact trafficking of NCAM in CHO cells and neurons in future studies.

Moreover, the exact mechanism of PAK1 influencing the interaction of NCAM and KLC1 should be further investigated to identify regulatory parameters for attachment or detachment of NCAM to KLC1 and of the kinesin-1 dependent transport of NCAM with the aim to better understand the role of this transport for the functioning of neurons.

6. Summary

The aim of the thesis was the identification of novel intracellular interaction partners of the neural cell adhesion molecule (NCAM) to gain further knowledge about the molecular mechanisms responsible for NCAM functions during brain development and in adult brain. The intracellular domains (ID) of human NCAM180 and NCAM140 (hNCAM180ID/140ID), respectively, were recombinantly expressed in *E. coli* BL21 (DE3) and purified by ligand affinity chromatography. Fluorescently labeled purified proteins were applied onto a protein macroarray comprising 24000 expression clones of human fetal brain. Besides already known interaction partners, several yet unknown potential interaction partners for NCAM were identified and further verified, namely ubiquitin carboxyl-terminal hydrolase isozyme L1, ubiquitin-fold modifier-conjugating enzyme 1, and kinesin light chain 1 (KLC1).

KLC1 is part of the heterotetrameric motor protein kinesin-1, which is composed of two KLCs and two kinesin heavy chains (KHCs, *e.g.* KIF5A) that transports cargoes towards the plus end of microtubules in neurons.

The interaction of NCAM and KLC1 was verified by co-immunoprecipitation from young mouse brain tissue. Subsequently, co-localization of intracellular NCAM and the motor was detected in Chinese hamster ovary (CHO) cells overexpressing NCAM and kinesin-1. In primary hippocampal neurons, a co-localization of endogenous NCAM with KLC1 or KIF5A was observed. As further indication for NCAM-containing vesicles being bound to kinesin-1, *trans*-Golgi network (TGN) organelles were isolated from mice brains and the presence of NCAM, KIF5A, and KLC1 confirmed in Western blot. Subsequent co-localization studies in primary hippocampal neurons did indicate that only a small amount of NCAM and KIF5A co-localized in TGN organelles.

Functional studies in transiently co-transfected CHO cells showed an increased amount of cell surface NCAM in dependence on the expression level of KLC1 or kinesin-1, indicating that kinesin-1 is involved in the trafficking of NCAM to the cell surface. Excess of free intracellular NCAM-ID as well as several shorter peptides thereof reduced the amount of delivered NCAM, showing that the ID of NCAM is required for NCAM's transport to the cell surface. Complete deletion of the ID of NCAM resulted in kinesin-1 independent delivery of NCAM to the cell surface, suggesting existence of alternative routes.

Primary cortical neurons overexpressing NCAM and KLC1 or NCAM and kinesin-1 were used as another cell model to unravel the role of kinesin-1 in NCAM's trafficking. Interestingly, increased delivery of NCAM to the cell surface was only observed after stimulation of NCAM endocytosis. Detection of co-localized NCAM and KLC1 in the soma and growth cone further indicated that endocytosed NCAM is being transported by kinesin-1

in neurons. These results showed that NCAM may be transported via two distinct routes, depending on *e.g.* the cell type: a direct route from the TGN to the plasma membrane and an indirect route including delivery of NCAM to the soma plasma membrane, endocytosis of NCAM, and subsequent transport to its ultimate destination, *e.g.* the axonal plasma membrane.

Using several NCAM-ID peptides in an ELISA, an 8 amino acid sequence within NCAM-ID was identified as being sufficient for the interaction with KLC1. Preliminary experiments using a construct with deleted KLC1-binding region showed an abrogated delivery of NCAM, and will be followed up in future studies. As p21-activated kinase 1 (PAK1) has been described to bind to the same domain of NCAM as KLC1, a competition between PAK1 and KLC1 for the binding to NCAM was investigated and confirmed in a pull-down assay. This observation gives first insights into possible regulatory mechanisms being potentially involved in the detachment of NCAM from KLC1 at NCAM's final destination. Further investigations will have to be carried out to support this interesting hypothesis.

References

Addinall SG, Mayr PS, Doyle S, Sheehan JK, Woodman PG, Allan VJ (2001): Phosphorylation by cdc2-CyclinB1 kinase releases cytoplasmic dynein from membranes. J. Biol. Chem. 276: 15939–15944.

Albach C, Damoc E, Denzinger T, Schachner M, Przybylski M, Schmitz B (2004): Identification of N-glycosylation sites of the murine neural cell adhesion molecule NCAM by MALDI-TOF and MALDI-FTICR mass spectrometry. Anal Bioanal Chem 378: 1129–1135.

Allan VJ, Thompson HM, McNiven MA (2002): Motoring around the Golgi. Review. Nat. Cell Biol. 4: E236-42.

Altschul SF, Gish W, Miller W, Myers EW, Lipman DJ (1990): Basic local alignment search tool. J. Mol. Biol. 215: 403–410.

Andersson AM, Olsen M, Zhernosekov D, Gaardsvoll H, Krog L, Linnemann D, Bock E (1993): Age-related changes in expression of the neural cell adhesion molecule in skeletal muscle: a comparative study of newborn, adult and aged rats. Biochem. J. 290 (Pt 3): 641–648.

Andreyeva A, Leshchyns'ka I, Knepper M, Betzel C, Redecke L, Sytnyk V, Schachner M (2010): CHL1 is a selective organizer of the presynaptic machinery chaperoning the SNARE complex. PLoS ONE 5: e12018.

Angata K, Suzuki M, Fukuda M (1998): Differential and cooperative polysialylation of the neural cell adhesion molecule by two polysialyltransferases, PST and STX. J. Biol. Chem. 273: 28524–28532.

Angst BD, Marcozzi C, Magee AI (2001): The cadherin superfamily: diversity in form and function. Review. J. Cell. Sci. 114: 629–641.

Aoyama T, Hata S, Nakao T, Tanigawa Y, Oka C, Kawaichi M (2009): Cayman ataxia protein caytaxin is transported by kinesin along neurites through binding to kinesin light chains. J. Cell. Sci. 122: 4177–4185.

Araki Y, Kawano T, Taru H, Saito Y, Wada S, Miyamoto K, Kobayashi H, Ishikawa HO, Ohsugi Y, Yamamoto T, Matsuno K, Kinjo M, Suzuki T (2007): The novel cargo Alcadein induces vesicle association of kinesin-1 motor components and activates axonal transport. EMBO J. 26: 1475–1486.

Atkins AR, Chung J, Deechongkit S, Little EB, Edelman GM, Wright PE, Cunningham BA, Dyson HJ (2001): Solution structure of the third immunoglobulin domain of the neural cell adhesion molecule N-CAM: can solution studies define the mechanism of homophilic binding? J. Mol. Biol. 311: 161–172.

Atkins AR, Osborne MJ, Lashuel HA, Edelman GM, Wright PE, Cunningham BA, Dyson HJ (1999): Association between the first two immunoglobulin-like domains of the neural cell adhesion molecule N-CAM. FEBS Lett. 451: 162–168.

Bananis E, Nath S, Gordon K, Satir P, Stockert RJ, Murray JW, Wolkoff AW (2004): Microtubule-dependent movement of late endocytic vesicles in vitro: requirements for Dynein and Kinesin. Mol. Biol. Cell 15: 3688–3697.

Barclay AN (2003): Membrane proteins with immunoglobulin-like domains--a master superfamily of interaction molecules. Review. Semin. Immunol. 15: 215–223.

Beggs HE, Baragona SC, Hemperly JJ, Maness PF (1997): NCAM140 interacts with the focal adhesion kinase p125(fak) and the SRC-related tyrosine kinase p59(fyn). J. Biol. Chem. 272: 8310–8319.

Blasius TL, Cai D, Jih GT, Toret CP, Verhey KJ (2007): Two binding partners cooperate to activate the molecular motor Kinesin-1. J. Cell Biol. 176: 11–17.

Blatch GL, Lässle M (1999): The tetratricopeptide repeat: a structural motif mediating protein-protein interactions. Review. Bioessays 21: 932–939.

Bloch RJ, Morrow JS (1989): An unusual beta-spectrin associated with clustered acetylcholine receptors. J. Cell Biol. 108: 481–493.

Bock E, Edvardsen K, Gibson A, Linnemann D, Lyles JM, Nybroe O (1987): Characterization of soluble forms of NCAM. FEBS Lett. 225: 33–36.

Bodrikov V, Leshchyns'ka I, Sytnyk V, Overvoorde J, den Hertog J, Schachner M (2005): RPTPalpha is essential for NCAM-mediated p59fyn activation and neurite elongation. J. Cell Biol. 168: 127–139.

Bokoch GM (2003): Biology of the p21-activated kinases. Review. Annu. Rev. Biochem. 72: 743–781.

Bonfanti L, Olive S, Poulain DA, Theodosis DT (1992): Mapping of the distribution of polysialylated neural cell adhesion molecule throughout the central nervous system of the adult rat: an immunohistochemical study. Neuroscience 49: 419–436.

Bork K, Hoffmann M, Horstkorte R (2013): ATP interferes with neural cell adhesion molecule-induced neurite outgrowth. Neuroreport 24: 616–619.

Boutin C, Schmitz B, Cremer H, Diestel S (2009): NCAM expression induces neurogenesis in vivo. EUR J NEUROSCI 30: 1209–1218.

Bracale A, Cesca F, Neubrand VE, Newsome TP, Way M, Schiavo G (2007): Kidins220/ARMS is transported by a kinesin-1-based mechanism likely to be involved in neuronal differentiation. Mol. Biol. Cell 18: 142–152.

Brady ST (1985): A novel brain ATPase with properties expected for the fast axonal transport motor. Nature 317: 73–75.

Brümmendorf T, Lemmon V (2001): Immunoglobulin superfamily receptors: cis-interactions, intracellular adapters and alternative splicing regulate adhesion. Review. Curr. Opin. Cell Biol. 13: 611–618.

Brzeska H, Szczepanowska J, Matsumura F, Korn ED (2004): Rac-induced increase of phosphorylation of myosin regulatory light chain in HeLa cells. Cell Motil. Cytoskeleton 58: 186–199.

Butterworth MB, Edinger RS, Ovaa H, Burg D, Johnson JP, Frizzell RA (2007): The deubiquitinating enzyme UCH-L3 regulates the apical membrane recycling of the epithelial sodium channel. J. Biol. Chem. 282: 37885–37893.

Büttner B, Kannicht C, Reutter W, Horstkorte R (2003): The neural cell adhesion molecule is associated with major components of the cytoskeleton. Biochem. Biophys. Res. Commun. 310: 967–971.

Büttner B, Kannicht C, Reutter W, Horstkorte R (2005): Novel cytosolic binding partners of the neural cell adhesion molecule: mapping the binding domains of PLC gamma, LANP, TOAD-64, syndapin, PP1, and PP2A. Biochemistry 44: 6938–6947.

Cabeza-Arvelaiz Y, Shih LC, Hardman N, Asselbergs F, Bilbe G, Schmitz A, White B, Siciliano MJ, Lachman LB (1993): Cloning and genetic characterization of the human kinesin light-chain (KLC) gene. DNA Cell Biol. 12: 881–892.

Campodónico PB, de Kier Joffé, Elisa D Bal, Urtreger AJ, Lauria LS, Lastiri JM, Puricelli LI, Todaro LB (2010): The neural cell adhesion molecule is involved in the metastatic capacity in a murine model of lung cancer. Mol. Carcinog. 49: 386–397.

Cavallaro U, Dejana E (2011): Adhesion molecule signalling: not always a sticky business. Review. Nat Rev Mol Cell Biol 12: 189–197.

Chazal G, Durbec P, Jankovski A, Rougon G, Cremer H (2000): Consequences of neural cell adhesion molecule deficiency on cell migration in the rostral migratory stream of the mouse. J. Neurosci. 20: 1446–1457.

Chen A, Haines S, Maxson K, Akeson RA (1994): VASE exon expression alters NCAM-mediated cell-cell interactions. J. Neurosci. Res. 38: 483–492.

Chernyshova Y, Leshchyns´ka I, Hsu S, Schachner M, Sytnyk V (2011): The neural cell adhesion molecule promotes FGFR-dependent phosphorylation and membrane targeting of the exocyst complex to induce exocytosis in growth cones. J NEUROSCI 31: 3522–3535.

Chevalier-Larsen E, Holzbaur ELF (2006): Axonal transport and neurodegenerative disease. Review. Biochim. Biophys. Acta 1762: 1094–1108.

Chuong CM, Edelman GM (1984): Alterations in neural cell adhesion molecules during development of different regions of the nervous system. J. Neurosci. 4: 2354–2368.

Cole GJ, Glaser L (1986): A heparin-binding domain from N-CAM is involved in neural cell-substratum adhesion. J. Cell Biol. 102: 403–412.

Colwell G, Li B, Forrest D, Brackenbury R (1992): Conserved regulatory elements in the promoter region of the N-CAM gene. Genomics 14: 875–882.

Cremer H, Chazal G, Goridis C, Represa A (1997): NCAM is essential for axonal growth and fasciculation in the hippocampus. Mol. Cell. Neurosci. 8: 323–335.

Cremer H, Lange R, Christoph A, Plomann M, Vopper G, Roes J, Brown R, Baldwin S, Kraemer P, Scheff S (1994): Inactivation of the N-CAM gene in mice results in size reduction of the olfactory bulb and deficits in spatial learning. Nature 367: 455–459.

Cunningham BA, Hemperly JJ, Murray BA, Prediger EA, Brackenbury R, Edelman GM (1987): Neural cell adhesion molecule: structure, immunoglobulin-like domains, cell surface modulation, and alternative RNA splicing. Science 236: 799–806.

Daniels RH, Hall PS, Bokoch GM (1998): Membrane targeting of p21-activated kinase 1 (PAK1) induces neurite outgrowth from PC12 cells. EMBO J. 17: 754–764.

Das AK, Cohen PW, Barford D (1998): The structure of the tetratricopeptide repeats of protein phosphatase 5: implications for TPR-mediated protein-protein interactions. EMBO J. 17: 1192–1199.

DeBerg HA, Blehm BH, Sheung J, Thompson AR, Bookwalter CS, Torabi SF, Schroer TA, Berger CL, Lu Y, Trybus KM, Selvin PR (2013): Motor domain phosphorylation modulates kinesin-1 transport. J. Biol. Chem. 288: 32612–32621.

Diefenbach RJ, Mackay JP, Armati PJ, Cunningham AL (1998): The C-terminal region of the stalk domain of ubiquitous human kinesin heavy chain contains the binding site for kinesin light chain. Biochemistry 37: 16663–16670.

Diestel S, Hinkle C, Schmitz B, Maness PF (2005): NCAM140 stimulates integrin-dependent cell migration by ectodomain shedding. Journal of neurochemistry J NEUROCHEM 95: 1777–1784.

Diestel S, Laurini C, Traub O, Schmitz B (2004): Tyrosine 734 of NCAM180 interferes with FGF receptor-dependent signaling implicated in neurite growth. Biochemical and Biophysical Research Communications 322: 186–196.

Diestel S, Schaefer D, Cremer H, Schmitz B (2007): NCAM is ubiquitylated, endocytosed and recycled in neurons. J. Cell. Sci. 120: 4035–4049.

Dodding MP, Mitter R, Humphries AC, Way M (2011): A kinesin-1 binding motif in vaccinia virus that is widespread throughout the human genome. EMBO J. 30: 4523–4538.

Doherty P, Cohen J, Walsh FS (1990): Neurite outgrowth in response to transfected N-CAM changes during development and is modulated by polysialic acid. Neuron 5: 209–219.

Doherty P, Moolenaar CE, Ashton SV, Michalides RJ, Walsh FS (1992): The VASE exon downregulates the neurite growth-promoting activity of NCAM 140. Nature 356: 791–793.

Dzhandzhugazyan K, Bock E (1997): Demonstration of an extracellular ATP-binding site in NCAM: functional implications of nucleotide binding. Biochemistry 36: 15381–15395.

Erickson RP, Jia Z, Gross SP, Yu CC (2011): How molecular motors are arranged on a cargo is important for vesicular transport. PLoS Comput. Biol. 7: e1002032.

Esni F, Täljedal IB, Perl AK, Cremer H, Christofori G, Semb H (1999): Neural cell adhesion molecule (N-CAM) is required for cell type segregation and normal ultrastructure in pancreatic islets. J. Cell Biol. 144: 325–337.

Faraidun H (2008): Finding New Binding Partners for human cytoplasmic part of Neural Cell Adhesion Molecule. Master thesis.

Fath KR, Burgess DR (1993): Golgi-derived vesicles from developing epithelial cells bind actin filaments and possess myosin-I as a cytoplasmically oriented peripheral membrane protein. J. Cell Biol. 120: 117–127.

Finne J, Finne U, Deagostini-Bazin H, Goridis C (1983): Occurrence of alpha 2-8 linked polysialosyl units in a neural cell adhesion molecule. Biochem. Biophys. Res. Commun. 112: 482–487.

Fogar P, Basso D, Pasquali C, Paoli M de, Sperti C, Roveroni G, Pedrazzoli S, Plebani M (1997): Neural cell adhesion molecule (N-CAM) in gastrointestinal neoplasias. Anticancer Res. 17: 1227–1230.

Fu M, Holzbaur ELF (2014): Integrated regulation of motor-driven organelle transport by scaffolding proteins. Review. Trends Cell Biol.

Gaardsvoll H, Krog L, Zhernosekov D, Andersson AM, Edvardsen K, Olsen M, Bock E, Linnemann D (1993): Age-related changes in expression of neural cell adhesion molecule (NCAM) in heart: a comparative study of newborn, adult and aged rats. Eur. J. Cell Biol. 61: 100–107.

Garner JA, Watanabe M, Rutishauser U (1986): Rapid axonal transport of the neural cell adhesion molecule. J. Neurosci. 6: 3242–3249.

Gindhart JG, Goldstein LS (1996): Tetratrico peptide repeats are present in the kinesin light chain. Trends Biochem. Sci. 21: 52–53.

Gower HJ, Barton CH, Elsom VL, Thompson J, Moore SE, Dickson G, Walsh FS (1988): Alternative splicing generates a secreted form of N-CAM in muscle and brain. Cell 55: 955–964.

Greenwood TA, Light GA, Swerdlow NR, Radant AD, Braff DL (2012): Association analysis of 94 candidate genes and schizophrenia-related endophenotypes. PLoS ONE 7: e29630.

Gross BJ, Kraybill BC, Walker S (2005): Discovery of O-GlcNAc transferase inhibitors. J. Am. Chem. Soc. 127: 14588–14589.

Gross SP, Vershinin M, Shubeita GT (2007): Cargo transport: two motors are sometimes better than one. Review. Curr. Biol. 17: R478-86.

Gross SP, Welte MA, Block SM, Wieschaus EF (2002): Coordination of opposite-polarity microtubule motors. J. Cell Biol. 156: 715–724.

Grumet M, Friedlander DR, Edelman GM (1993): Evidence for the binding of Ng-CAM to laminin. Cell Adhes. Commun. 1: 177–190.

Guillaud L, Wong R, Hirokawa N (2007): Disruption of KIF17–Mint1 interaction by CaMKII-dependent phosphorylation: a molecular model of kinesin–cargo release. Nat Cell Biol 10: 19–29.

Gumbiner BM (1996): Cell adhesion: the molecular basis of tissue architecture and morphogenesis. Review. Cell 84: 345–357.

Hammond S, Kaplarevic M, Borth N, Betenbaugh M, Lee K (2012): Chinese hamster genome database: an online resource for the CHO community at www.CHOgenome.org. Biotechnol Bioeng 109: 1353–1356.

Hansen SM, Berezin V, Bock E (2008): Signaling mechanisms of neurite outgrowth induced by the cell adhesion molecules NCAM and N-cadherin. Review. Cell. Mol. Life Sci. 65: 3809–3821.

Harris, Tony J C, Tepass U (2010): Adherens junctions: from molecules to morphogenesis. Review. Nat. Rev. Mol. Cell Biol. 11: 502–514.

Hayakawa Y, Itoh M, Yamada A, Mitsuda T, Nakagawa T (2007): Expression and localization of Cayman ataxia-related protein, Caytaxin, is regulated in a developmental- and spatial-dependent manner. Brain Res. 1129: 100–109.

He Q, Meiri KF (2002): Isolation and characterization of detergent-resistant microdomains responsive to NCAM-mediated signaling from growth cones. Mol. Cell. Neurosci. 19: 18–31.

Heiland PC, Griffith LS, Lange R, Schachner M, Hertlein B, Traub O, Schmitz B (1998): Tyrosine and serine phosphorylation of the neural cell adhesion molecule L1 is implicated in its oligomannosidic glycan dependent association with NCAM and neurite outgrowth. Eur. J. Cell Biol. 75: 97–106.

Hendricks AG, Perlson E, Ross JL, Schroeder HW, Tokito M, Holzbaur ELF (2010): Motor coordination via a tug-of-war mechanism drives bidirectional vesicle transport. Curr. Biol. 20: 697–702.

Hicke L, Dunn R (2003): Regulation of membrane protein transport by ubiquitin and ubiquitin-binding proteins. Review. Annu. Rev. Cell Dev. Biol. 19: 141–172.

Hinsby AM, Berezin V, Bock E (2004): Molecular mechanisms of NCAM function. Front. Biosci. 9: 2227–2244.

Hirokawa N (1998): Kinesin and dynein superfamily proteins and the mechanism of organelle transport. Review. Science 279: 519–526.

Hirokawa N, Pfister KK, Yorifuji H, Wagner MC, Brady ST, Bloom GS (1989): Submolecular domains of bovine brain kinesin identified by electron microscopy and monoclonal antibody decoration. Cell 56: 867–878.

Hirokawa N, Sato-Yoshitake R, Kobayashi N, Pfister KK, Bloom GS, Brady ST (1991): Kinesin associates with anterogradely transported membranous organelles in vivo. J. Cell Biol. 114: 295–302.

Hirokawa N, Takemura R (2003): Biochemical and molecular characterization of diseases linked to motor proteins. Review. Trends Biochem. Sci. 28: 558–565.

Hirokawa N, Takemura R (2005): Molecular motors and mechanisms of directional transport in neurons. Review. Nat. Rev. Neurosci. 6: 201–214.

Hoffman S, Edelman GM (1983): Kinetics of homophilic binding by embryonic and adult forms of the neural cell adhesion molecule. Proc. Natl. Acad. Sci. U.S.A. 80: 5762–5766.

Hoffman S, Sorkin BC, White PC, Brackenbury R, Mailhammer R, Rutishauser U, Cunningham BA, Edelman GM (1982): Chemical characterization of a neural cell adhesion molecule purified from embryonic brain membranes. J. Biol. Chem. 257: 7720–7729.

Hollenbeck PJ (1993): Phosphorylation of neuronal kinesin heavy and light chains in vivo. J. Neurochem. 60: 2265–2275.

Homrich M, Wobst H, Laurini C, Sabrowski J, Schmitz B, Diestel S (2014): Cytoplasmic domain of NCAM140 interacts with ubiquitin-fold modifier-conjugating enzyme-1 (Ufc1). Exp. Cell Res.

Horstkorte R, Schachner M, Magyar JP, Vorherr T, Schmitz B (1993): The fourth immunoglobulin-like domain of NCAM contains a carbohydrate recognition domain for oligomannosidic glycans implicated in association with L1 and neurite outgrowth. J. Cell Biol. 121: 1409–1421.

Hsu S, TerBush D, Abraham M, Guo W (2004): The exocyst complex in polarized exocytosis. Review. Int. Rev. Cytol. 233: 243–265.

Hynes RO (1992): Integrins: versatility, modulation, and signaling in cell adhesion. Review. Cell 69: 11–25.

Jacque CM, Jørgensen OS, Baumann NA, Bock E (1976): Brain-specific antigens in the Quaking mouse during ontogeny. J. Neurochem. 27: 905–909.

Jareb M, Banker G (1998): The polarized sorting of membrane proteins expressed in cultured hippocampal neurons using viral vectors. Neuron 20: 855–867.

Jeanes A, Gottardi CJ, Yap AS (2008): Cadherins and cancer: how does cadherin dysfunction promote tumor progression? Review. Oncogene 27: 6920–6929.

Jensen PH, Soroka V, Thomsen NK, Ralets I, Berezin V, Bock E, Poulsen FM (1999): Structure and interactions of NCAM modules 1 and 2, basic elements in neural cell adhesion. Nat. Struct. Biol. 6: 486–493.

Jørgensen OS, Bock E (1974): Brain specific synaptosomal membrane proteins demonstrated by crossed immunoelectrophoresis. J. Neurochem. 23: 879–880.

Kamal A, Stokin GB, Yang Z, Xia CH, Goldstein LS (2000): Axonal transport of amyloid precursor protein is mediated by direct binding to the kinesin light chain subunit of kinesin-I. Neuron 28: 449–459.

Kameda K, Shimada H, Ishikawa T, Takimoto A, Momiyama N, Hasegawa S, Misuta K, Nakano A, Nagashima Y, Ichikawa Y (1999): Expression of highly polysialylated neural cell adhesion molecule in pancreatic cancer neural invasive lesion. Cancer Lett. 137: 201–207.

Kamiguchi H, Lemmon V (2000): Recycling of the cell adhesion molecule L1 in axonal growth cones. J. Neurosci. 20: 3676–3686.

Kamiguchi H, Long KE, Pendergast M, Schaefer AW, Rapoport I, Kirchhausen T, Lemmon V (1998): The neural cell adhesion molecule L1 interacts with the AP-2 adaptor and is endocytosed via the clathrin-mediated pathway. J. Neurosci. 18: 5311–5321.

Kamiguchi H, Yoshihara F (2001): The role of endocytic l1 trafficking in polarized adhesion and migration of nerve growth cones. J. Neurosci. 21: 9194–9203.

Kansas GS (1996): Selectins and their ligands: current concepts and controversies. Review. Blood 88: 3259–3287.

Karcher RL, Roland JT, Zappacosta F, Huddleston MJ, Annan RS, Carr SA, Gelfand VI (2001): Cell cycle regulation of myosin-V by calcium/calmodulin-dependent protein kinase II. Science 293: 1317–1320.

Kasper C, Rasmussen H, Kastrup JS, Ikemizu S, Jones EY, Berezin V, Bock E, Larsen IK (2000): Structural basis of cell-cell adhesion by NCAM. Nat. Struct. Biol. 7: 389–393.

Kasper C, Stahlhut M, Berezin V, Maar TE, Edvardsen K, Kiselyov VV, Soroka V, Bock E (1996): Functional characterization of NCAM fibronectin type III domains: demonstration of modulatory effects of the proline-rich sequence encoded by alternatively spliced exons a and AAG. J. Neurosci. Res. 46: 173–186.

Katzmann DJ, Babst M, Emr SD (2001): Ubiquitin-dependent sorting into the multivesicular body pathway requires the function of a conserved endosomal protein sorting complex, ESCRT-I. Cell 106: 145–155.

Kawano T, Araseki M, Araki Y, Kinjo M, Yamamoto T, Suzuki T (2012): A Small Peptide Sequence is Sufficient for Initiating Kinesin-1 Activation Through Part of TPR Region of KLC1. Traffic 13: 834–848.

Kimura T, Watanabe H, Iwamatsu A, Kaibuchi K (2005): Tubulin and CRMP-2 complex is transported via Kinesin-1. J. Neurochem. 93: 1371–1382.

Kiselyov VV, Skladchikova G, Hinsby AM, Jensen PH, Kulahin N, Soroka V, Pedersen N, Tsetlin V, Poulsen FM, Berezin V, Bock E (2003): Structural basis for a direct interaction between FGFR1 and NCAM and evidence for a regulatory role of ATP. Structure 11: 691–701.

Kiselyov VV, Soroka V, Berezin V, Bock E (2005): Structural biology of NCAM homophilic binding and activation of FGFR. Review. Journal of neurochemistry J NEUROCHEM 94: 1169–1179.

Kleene R, Schachner M (2004): Glycans and neural cell interactions. Review. Nat Rev Neurosci 5: 195–208.

Kojima N, Tachida Y, Yoshida Y, Tsuji S (1996): Characterization of mouse ST8Sia II (STX) as a neural cell adhesion molecule-specific polysialic acid synthase. Requirement of core alpha1,6-linked fucose and a polypeptide chain for polysialylation. J. Biol. Chem. 271: 19457–19463.

Kolkova K, Novitskaya V, Pedersen N, Berezin V, Bock E (2000): Neural cell adhesion molecule-stimulated neurite outgrowth depends on activation of protein kinase C and the Ras-mitogen-activated protein kinase pathway. J. Neurosci. 20: 2238–2246.

Komatsu M, Chiba T, Tatsumi K, Iemura S, Tanida I, Okazaki N, Ueno T, Kominami E, Natsume T, Tanaka K (2004): A novel protein-conjugating system for Ufm1, a ubiquitin-fold modifier. EMBO J. 23: 1977–1986.

Konecna A, Frischknecht R, Kinter J, Ludwig A, Steuble M, Meskenaite V, Indermühle M, Engel M, Cen C, Mateos J, Streit P, Sonderegger P (2006): Calsyntenin-1 docks vesicular cargo to kinesin-1. Mol. Biol. Cell 17: 3651–3663.

Korshunova I, Novitskaya V, Kiryushko D, Pedersen N, Kolkova K, Kropotova E, Mosevitsky M, Rayko M, Morrow JS, Ginzburg I, Berezin V, Bock E (2007): GAP-43 regulates NCAM-180-mediated neurite outgrowth. J. Neurochem. 100: 1599–1612.

Krämer EM, Klein C, Koch T, Boytinck M, Trotter J (1999): Compartmentation of Fyn kinase with glycosylphosphatidylinositol-anchored molecules in oligodendrocytes facilitates kinase activation during myelination. J. Biol. Chem. 274: 29042–29049.

Kreis P, Barnier J (2009): PAK signalling in neuronal physiology. Review. Cell. Signal. 21: 384–393.

Lahrtz F, Horstkorte R, Cremer H, Schachner M, Montag D (1997): VASE-encoded peptide modifies NCAM- and L1-mediated neurite outgrowth. J. Neurosci. Res. 50: 62–68.

Lanier LL, Chang C, Azuma M, Ruitenberg JJ, Hemperly JJ, Phillips JH (1991): Molecular and functional analysis of human natural killer cell-associated neural cell adhesion molecule (N-CAM/CD56). J. Immunol. 146: 4421–4426.

Lantuéjoul S, Laverrière MH, Sturm N, Moro D, Frey G, Brambilla C, Brambilla E (2000): NCAM (neural cell adhesion molecules) expression in malignant mesotheliomas. Hum. Pathol. 31: 415–421.

Lantuéjoul S, Moro D, Michalides RJ, Brambilla C, Brambilla E (1998): Neural cell adhesion molecules (NCAM) and NCAM-PSA expression in neuroendocrine lung tumors. Am. J. Surg. Pathol. 22: 1267–1276.

Lazarov O, Morfini GA, Lee EB, Farah MH, Szodorai A, DeBoer SR, Koliatsos VE, Kins S, Lee VM, Wong PC, Price DL, Brady ST, Sisodia SS (2005): Axonal transport, amyloid precursor protein, kinesin-1, and the processing apparatus: revisited. J. Neurosci. 25: 2386–2395.

Lehembre F, Yilmaz M, Wicki A, Schomber T, Strittmatter K, Ziegler D, Kren A, Went P, Derksen, Patrick W B, Berns A, Jonkers J, Christofori G (2008): NCAM-induced focal adhesion assembly: a functional switch upon loss of E-cadherin. EMBO J. 27: 2603–2615.

Leshchyns'ka I, Sytnyk V, Morrow JS, Schachner M (2003): Neural cell adhesion molecule (NCAM) association with PKCbeta2 via betaI spectrin is implicated in NCAM-mediated neurite outgrowth. J. Cell Biol. 161: 625–639.

Leterrier C, Lainé J, Darmon M, Boudin H, Rossier J, Lenkei Z (2006): Constitutive activation drives compartment-selective endocytosis and axonal targeting of type 1 cannabinoid receptors. J. Neurosci. 26: 3141–3153.

Ley K (2003): The role of selectins in inflammation and disease. Review. Trends in Molecular Medicine 9: 263–268.

Li S, Leshchyns'ka I, Chernyshova Y, Schachner M, Sytnyk V (2013): The neural cell adhesion molecule (NCAM) associates with and signals through p21-activated kinase 1 (Pak1). J. Neurosci. 33: 790–803.

Lindesmith L, McIlvain JM, Argon Y, Sheetz MP (1997): Phosphotransferases associated with the regulation of kinesin motor activity. J. Biol. Chem. 272: 22929–22933.

Linnemann D, Lyles JM, Bock E (1985): A developmental study of the biosynthesis of the neural cell adhesion molecule. Dev. Neurosci. 7: 230–238.

Little EB, Crossin KL, Krushel LA, Edelman GM, Cunningham BA (2001): A short segment within the cytoplasmic domain of the neural cell adhesion molecule (N-CAM) is essential for N-CAM-induced NF-kappa B activity in astrocytes. Proc. Natl. Acad. Sci. U.S.A. 98: 2238–2243.

Little EB, Edelman GM, Cunningham BA (1998): Palmitoylation of the cytoplasmic domain of the neural cell adhesion molecule N-CAM serves as an anchor to cellular membranes. Cell Adhes. Commun. 6: 415–430.

Liu L, Haines S, Shew R, Akeson RA (1993): Axon growth is enhanced by NCAM lacking the VASE exon when expressed in either the growth substrate or the growing axon. J. Neurosci. Res. 35: 327–345.

Loubéry S, Wilhelm C, Hurbain I, Neveu S, Louvard D, Coudrier E (2008): Different microtubule motors move early and late endocytic compartments. Traffic 9: 492–509.

Lu W, Katz S, Gupta R, Mayer BJ (1997): Activation of Pak by membrane localization mediated by an SH3 domain from the adaptor protein Nck. Curr. Biol. 7: 85–94.

Luo B, Carman CV, Springer TA (2007): Structural Basis of Integrin Regulation and Signaling. Review. Annu. Rev. Immunol. 25: 619–647.

Lyles JM, Linnemann D, Bock E (1984a): Biosynthesis of the D2-cell adhesion molecule: post-translational modifications, intracellular transport, and developmental changes. J. Cell Biol. 99: 2082–2091.

Lyles JM, Norrild B, Bock E (1984b): Biosynthesis of the D2 cell adhesion molecule: pulse-chase studies in cultured fetal rat neuronal cells. J. Cell Biol. 98: 2077–2081.

Manzi AE, Higa HH, Diaz S, Varki A (1994): Intramolecular self-cleavage of polysialic acid. J. Biol. Chem. 269: 23617–23624.

Margolis RK, Rauch U, Maurel P, Margolis RU (1996): Neurocan and phosphacan: two major nervous tissue-specific chondroitin sulfate proteoglycans. Perspect Dev Neurobiol 3: 273–290.

Matthias S, Horstkorte R (2006): Phosphorylation of the neural cell adhesion molecule on serine or threonine residues is induced by adhesion or nerve growth factor. J. Neurosci. Res. 84: 142–150.

McEver RP (2002): Selectins: lectins that initiate cell adhesion under flow. Review. Curr. Opin. Cell Biol. 14: 581–586.

McGuire JR, Rong J, Li S, Li X (2006): Interaction of Huntingtin-associated protein-1 with kinesin light chain: implications in intracellular trafficking in neurons. J. Biol. Chem. 281: 3552–3559.

Meiri KF, Saffell JL, Walsh FS, Doherty P (1998): Neurite outgrowth stimulated by neural cell adhesion molecules requires growth-associated protein-43 (GAP-43) function and is associated with GAP-43 phosphorylation in growth cones. J. Neurosci. 18: 10429–10437.

Mesngon MT, Tarricone C, Hebbar S, Guillotte AM, Schmitt EW, Lanier L, Musacchio A, King SJ, Smith DS (2006): Regulation of cytoplasmic dynein ATPase by Lis1. J. Neurosci. 26: 2132–2139.

Miñana R, Duran JM, Tomas M, Renau-Piqueras J, Guerri C (2001): Neural cell adhesion molecule is endocytosed via a clathrin-dependent pathway. Eur. J. Neurosci. 13: 749–756.

Monzo HJ, Park, Thomas I H, Dieriks BV, Jansson D, Faull, Richard L M, Dragunow M, Curtis MA (2013): Insulin and IGF1 modulate turnover of polysialylated neural cell adhesion molecule (PSA-NCAM) in a process involving specific extracellular matrix components. J. Neurochem. 126: 758–770.

Morfini G, Szebenyi G, Richards B, Brady ST (2001): Regulation of kinesin: implications for neuronal development. Dev. Neurosci. 23: 364–376.

Morfini G, Szebenyi G, Elluru R, Ratner N, Brady ST (2002): Glycogen synthase kinase 3 phosphorylates kinesin light chains and negatively regulates kinesin-based motility. EMBO J. 21: 281–293.

Mühlenhoff M, Eckhardt M, Bethe A, Frosch M, Gerardy-Schahn R (1996): Polysialylation of NCAM by a single enzyme. Curr. Biol. 6: 1188–1191.

Muller D, Wang C, Skibo G, Toni N, Cremer H, Calaora V, Rougon G, Kiss JZ (1996): PSA-NCAM is required for activity-induced synaptic plasticity. Neuron 17: 413–422.

Nakata T, Terada S, Hirokawa N (1998): Visualization of the dynamics of synaptic vesicle and plasma membrane proteins in living axons. J. Cell Biol. 140: 659–674.

Nakata T, Hirokawa N (2003): Microtubules provide directional cues for polarized axonal transport through interaction with kinesin motor head. J. Cell Biol. 162: 1045–1055.

Nath S, Bananis E, Sarkar S, Stockert RJ, Sperry AO, Murray JW, Wolkoff AW (2007): Kif5B and Kifc1 interact and are required for motility and fission of early endocytic vesicles in mouse liver. Mol. Biol. Cell 18: 1839–1849.

Needham LK, Schnaar RL (1993): The HNK-1 reactive sulfoglucuronyl glycolipids are ligands for L-selectin and P-selectin but not E-selectin. Proc. Natl. Acad. Sci. U.S.A. 90: 1359–1363.

Nelson RW, Bates PA, Rutishauser U (1995): Protein determinants for specific polysialylation of the neural cell adhesion molecule. J. Biol. Chem. 270: 17171–17179.

Niclas J, Navone F, Hom-Booher N, Vale RD (1994): Cloning and localization of a conventional kinesin motor expressed exclusively in neurons. Neuron 12: 1059–1072.

Niethammer P, Delling M, Sytnyk V, Dityatev A, Fukami K, Schachner M (2002): Cosignaling of NCAM via lipid rafts and the FGF receptor is required for neuritogenesis. J. Cell Biol. 157: 521–532.

Noble M, Albrechtsen M, Møller C, Lyles J, Bock E, Goridis C, Watanabe M, Rutishauser U (1985): Glial cells express N-CAM/D2-CAM-like polypeptides in vitro. Nature 316: 725–728.

Novotny JR, Nückel H, Dührsen U (2006): Correlation between expression of CD56/NCAM and severe leukostasis in hyperleukocytic acute myelomonocytic leukaemia. Eur. J. Haematol. 76: 299–308.

Nybroe O, Gibson A, Møller CJ, Rohde H, Dahlin J, Bock E (1986): Expression of N-CAM polypeptides in neurons. Neurochem. Int. 9: 539–544.

Ono K, Tomasiewicz H, Magnuson T, Rutishauser U (1994): N-CAM mutation inhibits tangential neuronal migration and is phenocopied by enzymatic removal of polysialic acid. Neuron 13: 595–609.

Owens GC, Edelman GM, Cunningham BA (1987): Organization of the neural cell adhesion molecule (N-CAM) gene: alternative exon usage as the basis for different membrane-associated domains. Proc. Natl. Acad. Sci. U.S.A. 84: 294–298.

Pakala SB, Nair VS, Reddy SD, Kumar R (2012): Signaling-dependent phosphorylation of mitotic centromere-associated kinesin regulates microtubule depolymerization and its centrosomal localization. J. Biol. Chem. 287: 40560–40569.

Panicker AK, Buhusi M, Thelen K, Maness PF (2003): Cellular signalling mechanisms of neural cell adhesion molecules. Review. Front. Biosci. 8: d900-11.

Paratcha G, Ledda F, Ibáñez CF (2003): The neural cell adhesion molecule NCAM is an alternative signaling receptor for GDNF family ligands. Cell 113: 867–879.

Paschal BM, Vallee RB (1987): Retrograde transport by the microtubule-associated protein MAP 1C. Nature 330: 181–183.

Peck SC (2006): Analysis of protein phosphorylation: methods and strategies for studying kinases and substrates. Plant J. 45: 512–522.

Peretti D, Peris L, Rosso S, Quiroga S, Cáceres A (2000): Evidence for the involvement of KIF4 in the anterograde transport of L1-containing vesicles. J. Cell Biol. 149: 141–152.

Perlson E, Hendricks AG, Lazarus JE, Ben-Yaakov K, Gradus T, Tokito M, Holzbaur ELF (2013): Dynein interacts with the neural cell adhesion molecule (NCAM180) to tether dynamic microtubules and maintain synaptic density in cortical neurons. J. Biol. Chem. 288: 27812–27824.

Persohn E, Pollerberg GE, Schachner M (1989): Immunoelectron-microscopic localization of the 180 kD component of the neural cell adhesion molecule N-CAM in postsynaptic membranes. J. Comp. Neurol. 288: 92–100.

Persohn E, Schachner M (1987): Immunoelectron microscopic localization of the neural cell adhesion molecules L1 and N-CAM during postnatal development of the mouse cerebellum. J. Cell Biol. 105: 569–576.

Pierce-antibodies (2014): Kinesin 5C polyclonal antibody for Western blot - 100 µg (PA1-644). http://www.google.de/imgres?imgurl=http%3A%2F%2Fd27pv9ovxbcf9p.cloudfront.net%2Fimages%2Fprodvalimagenew_200%2FPA1-644_1_07232010.jpg&imgrefurl=http%3A%2F%2Fwww.pierce-antibodies.com%2F1%2F3%2Fkinesin-family-member&h=200&w=200&tbnid=_n5LTZ69bndE-M%3A&zoom=1&docid=WaF9JrGh_J1ouM&itg=1&ei=fuRPU-j7B4GGywO-yoHQBg&tbm=isch&client=firefox-a&iact=rc&uact=3&dur=294&page=2&start=33&ndsp=35&ved=0COsBEK0DMDA (30.07.2014).

Pierre K, Bonhomme R, Dupouy B, Poulain DA, Theodosis DT (2001): The polysialylated neural cell adhesion molecule reaches cell surfaces of hypothalamic neurons and astrocytes via the constitutive pathway. Neuroscience 103: 133–142.

Polishchuk RS, Polishchuk EV, Marra P, Alberti S, Buccione R, Luini A, Mironov AA (2000): Correlative light-electron microscopy reveals the tubular-saccular ultrastructure of carriers operating between Golgi apparatus and plasma membrane. J. Cell Biol. 148: 45–58.

Pollerberg EG, Sadoul R, Goridis C, Schachner M (1985): Selective expression of the 180-kD component of the neural cell adhesion molecule N-CAM during development. J. Cell Biol. 101: 1921–1929.

Pollerberg GE, Burridge K, Krebs KE, Goodman SR, Schachner M (1987): The 180-kD component of the neural cell adhesion molecule N-CAM is involved in cell-cell contacts and cytoskeleton-membrane interactions. Cell Tissue Res. 250: 227–236.

Pollerberg GE, Schachner M, Davoust J (1986): Differentiation state-dependent surface mobilities of two forms of the neural cell adhesion molecule. Nature 324: 462–465.

Pollscheit J, Glaubitz N, Haller H, Horstkorte R, Bork K (2012): Phosphorylation of serine 774 of the neural cell adhesion molecule is necessary for cyclic adenosine monophosphate response element binding protein activation and neurite outgrowth. J. Neurosci. Res. 90: 1577–1582.

Polo-Parada L, Plattner F, Bose C, Landmesser LT (2005): NCAM 180 acting via a conserved C-terminal domain and MLCK is essential for effective transmission with repetitive stimulation. Neuron 46: 917–931.

Poltorak M, Khoja I, Hemperly JJ, Williams JR, el-Mallakh R, Freed WJ (1995): Disturbances in cell recognition molecules (N-CAM and L1 antigen) in the CSF of patients with schizophrenia. Exp. Neurol. 131: 266–272.

Poltorak M, Wright R, Hemperly JJ, Torrey EF, Issa F, Wyatt RJ, Freed WJ (1997): Monozygotic twins discordant for schizophrenia are discordant for N-CAM and L1 in CSF. Brain Res. 751: 152–154.

Probstmeier R, Kühn K, Schachner M (1989): Binding properties of the neural cell adhesion molecule to different components of the extracellular matrix. J. Neurochem. 53: 1794–1801.

Puchkov D, Leshchyns'ka I, Nikonenko AG, Schachner M, Sytnyk V (2011): NCAM/spectrin complex disassembly results in PSD perforation and postsynaptic endocytic zone formation. Cereb. Cortex 21: 2217–2232.

Qiagen (2003): A handbook for high-level expression and purification of 6xHis-tagged proteins. http://www.qiagen.com/resources/resourcedetail?id=79ca2f7d-42fe-4d62-8676-4cfa948c9435&lang=en (30.07.2014).

Qiagen (2009): Glutathione affinity handbook. For purifying and detecting proteins carrying a GST tag. http://www.qiagen.com/resources/resourcedetail?id=8b978045-d0b9-4ba3-ab00-54f2ae9fde4d&lang=en (30.07.2014).

Rahman A, Friedman DS, Goldstein LS (1998): Two kinesin light chain genes in mice. Identification and characterization of the encoded proteins. J. Biol. Chem. 273: 15395–15403.

Ranheim TS, Edelman GM, Cunningham BA (1996): Homophilic adhesion mediated by the neural cell adhesion molecule involves multiple immunoglobulin domains. Proc. Natl. Acad. Sci. U.S.A. 93: 4071–4075.

Rao Y, Wu XF, Gariepy J, Rutishauser U, Siu CH (1992): Identification of a peptide sequence involved in homophilic binding in the neural cell adhesion molecule NCAM. J. Cell Biol. 118: 937–949.

Rao Y, Wu XF, Yip P, Gariepy J, Siu CH (1993): Structural characterization of a homophilic binding site in the neural cell adhesion molecule. J. Biol. Chem. 268: 20630–20638.

Rao Y, Zhao X, Siu CH (1994): Mechanism of homophilic binding mediated by the neural cell adhesion molecule NCAM. Evidence for isologous interaction. J. Biol. Chem. 269: 27540–27548.

Rojas A, Ahmed A (1999): Adhesion Receptors in Health and Disease. Review. Critical Reviews in Oral Biology & Medicine 10: 337–358.

Rønn LC, Berezin V, Bock E (2000): The neural cell adhesion molecule in synaptic plasticity and ageing. Review. Int. J. Dev. Neurosci. 18: 193–199.

Rosa-Ferreira C, Munro S (2011): Arl8 and SKIP act together to link lysosomes to kinesin-1. Dev. Cell 21: 1171–1178.

Rothbard JB, Brackenbury R, Cunningham BA, Edelman GM (1982): Differences in the carbohydrate structures of neural cell-adhesion molecules from adult and embryonic chicken brains. J. Biol. Chem. 257: 11064–11069.

Rougon G, Hobert O (2003): New insights into the diversity and function of neuronal immunoglobulin superfamily molecules. Review. Annu. Rev. Neurosci. 26: 207–238.

Rousselot P, Lois C, Alvarez-Buylla A (1995): Embryonic (PSA) N-CAM reveals chains of migrating neuroblasts between the lateral ventricle and the olfactory bulb of adult mice. J. Comp. Neurol. 351: 51–61.

Rutishauser U, Hoffman S, Edelman GM (1982): Binding properties of a cell adhesion molecule from neural tissue. Proc. Natl. Acad. Sci. U.S.A. 79: 685–689.

Rutishauser U, Thiery JP, Brackenbury R, Sela BA, Edelman GM (1976): Mechanisms of adhesion among cells from neural tissues of the chick embryo. Proc. Natl. Acad. Sci. U.S.A. 73: 577–581.

Sadoul R, Hirn M, Deagostini-Bazin H, Rougon G, Goridis C (1983): Adult and embryonic mouse neural cell adhesion molecules have different binding properties. Nature 304: 347–349.

Saffell JL, Williams EJ, Mason IJ, Walsh FS, Doherty P (1997): Expression of a dominant negative FGF receptor inhibits axonal growth and FGF receptor phosphorylation stimulated by CAMs. Neuron 18: 231–242.

Sakamoto J, Watanabe T, Kito T, Yamamura Y, Kiriyama K, Kannagi R, Ueda R, Takagi H, Takahashi T (1994): Expression of neural cell adhesion molecule in normal gastric mucosa and in gastric carcinoid tumors. Eur Surg Res 26: 230–239.

Salinas S, Bilsland LG, Schiavo G (2008): Molecular landmarks along the axonal route: axonal transport in health and disease. Review. Curr. Opin. Cell Biol. 20: 445–453.

Sampo B, Kaech S, Kunz S, Banker G (2003): Two distinct mechanisms target membrane proteins to the axonal surface. Neuron 37: 611–624.

Santuccione A, Sytnyk V, Leshchyns'ka I, Schachner M (2005): Prion protein recruits its neuronal receptor NCAM to lipid rafts to activate p59fyn and to enhance neurite outgrowth. J. Cell Biol. 169: 341–354.

Sasaki H, Yoshida K, Ikeda E, Asou H, Inaba M, Otani M, Kawase T (1998): Expression of the neural cell adhesion molecule in astrocytic tumors: an inverse correlation with malignancy. Cancer 82: 1921–1931.

Sasaki T, Endo T (1999): Evidence for the presence of N-CAM 180 on astrocytes from rat cerebellum and differences in glycan structures between N-CAM 120 and N-CAM 140. Glia 28: 236–243.

Schizophrenia Working Group of Psychiatric Genomics Consortium (2014): Biological insights from 108 schizophrenia-associated genetic loci. Nature 511: 421–427.

Schmid RS, Graff RD, Schaller MD, Chen S, Schachner M, Hemperly JJ, Maness PF (1999): NCAM stimulates the Ras-MAPK pathway and CREB phosphorylation in neuronal cells. J. Neurobiol. 38: 542–558.

Schmidt MR, Maritzen T, Kukhtina V, Higman VA, Doglio L, Barak NN, Strauss H, Oschkinat H, Dotti CG, Haucke V (2009): Regulation of endosomal membrane traffic by a Gadkin/AP-1/kinesin KIF5 complex. Proc. Natl. Acad. Sci. U.S.A. 106: 15344–15349.

Schroer TA, Steuer ER, Sheetz MP (1989): Cytoplasmic dynein is a minus end-directed motor for membranous organelles. Cell 56: 937–946.

Schwarting GA, Jungalwala FB, Chou DK, Boyer AM, Yamamoto M (1987): Sulfated glucuronic acid-containing glycoconjugates are temporally and spatially regulated antigens in the developing mammalian nervous system. Dev. Biol. 120: 65–76.

Schwarz LA, Patrick GN (2012): Ubiquitin-dependent endocytosis, trafficking and turnover of neuronal membrane proteins. Review. Mol. Cell. Neurosci. 49: 387–393.

Sekine Y, Okada Y, Noda Y, Kondo S, Aizawa H, Takemura R, Hirokawa N (1994): A novel microtubule-based motor protein (KIF4) for organelle transports, whose expression is regulated developmentally. J. Cell Biol. 127: 187–201.

Sekulla A: Identifizierung von NCAM Bindungspartnern mittels des rekombinanten C-Terminus von NCAM im Proteinarray. Diploma thesis.

Simons M, Ikonen E, Tienari PJ, Cid-Arregui A, Mönning U, Beyreuther K, Dotti CG (1995): Intracellular routing of human amyloid protein precursor: axonal delivery followed by transport to the dendrites. J. Neurosci. Res. 41: 121–128.

Skladchikova G, Ronn LC, Berezin V, Bock E (1999): Extracellular adenosine triphosphate affects neural cell adhesion molecule (NCAM)-mediated cell adhesion and neurite outgrowth. J. Neurosci. Res. 57: 207–218.

Small SJ, Akeson R (1990): Expression of the unique NCAM VASE exon is independently regulated in distinct tissues during development. J. Cell Biol. 111: 2089–2096.

Sorkin BC, Hoffman S, Edelman GM, Cunningham BA (1984): Sulfation and phosphorylation of the neural cell adhesion molecule, N-CAM. Science 225: 1476–1478.

Soroka V, Kasper C, Poulsen FM (2010): Structural biology of NCAM. Review. In: Berezin V (ed.), Structure and Function of the Neural Cell Adhesion Molecule NCAM. Springer Sciences, 3–22.

Soroka V, Kolkova K, Kastrup JS, Diederichs K, Breed J, Kiselyov VV, Poulsen FM, Larsen IK, Welte W, Berezin V, Bock E, Kasper C (2003): Structure and interactions of NCAM Ig1-2-3 suggest a novel zipper mechanism for homophilic adhesion. Structure 11: 1291–1301.

Source Bioscience ImaGenes (2010): Protein Macroarrays. Manual. http://www.lifesciences.sourcebioscience.com/media/290406/sbs_ig_manual_proteinarray_v1.pdf (30.07.2014).

Springer TA (1990): Adhesion receptors of the immune system. Review. Nature 346: 425–434.

Stephens DJ, Pepperkok R (2001): Illuminating the secretory pathway: when do we need vesicles? Review. J. Cell. Sci. 114: 1053–1059.

Storms SD, Kim AC, Tran BH, Cole GJ, Murray BA (1996): NCAM-mediated adhesion of transfected cells to agrin. Cell Adhes. Commun. 3: 497–509.

Storms SD, Rutishauser U (1998): A role for polysialic acid in neural cell adhesion molecule heterophilic binding to proteoglycans. J. Biol. Chem. 273: 27124–27129.

Stratagene (2004): XL1-Blue Competent Cells. http://www.chem.agilent.com/library/usermanuals/Public/200249.pdf (29.07.2014).

Studier FW, Moffatt BA (1986): Use of bacteriophage T7 RNA polymerase to direct selective high-level expression of cloned genes. J. Mol. Biol. 189: 113–130.

Subach FV, Subach OM, Gundorov IS, Morozova KS, Piatkevich KD, Cuervo AM, Verkhusha VV (2009): Monomeric fluorescent timers that change color from blue to red report on cellular trafficking. Nat. Chem. Biol. 5: 118–126.

Sun F, Zhu C, Dixit R, Cavalli V (2011): Sunday Driver/JIP3 binds kinesin heavy chain directly and enhances its motility. EMBO J. 30: 3416–3429.

Sytnyk V, Leshchyns'ka I, Delling M, Dityateva G, Dityatev A, Schachner M (2002): Neural cell adhesion molecule promotes accumulation of TGN organelles at sites of neuron-to-neuron contacts. J. Cell Biol. 159: 649–661.

Takada Y, Ye X, Simon S (2007): The integrins. Review. Genome Biol. 8: 215.

Tang J, Rutishauser U, Landmesser L (1994): Polysialic acid regulates growth cone behavior during sorting of motor axons in the plexus region. Neuron 13: 405–414.

Tedder TF, Steeber DA, Chen A, Engel P (1995): The selectins: vascular adhesion molecules. Review. FASEB J. 9: 866–873.

Tessier-Lavigne M, Goodman CS (1996): The molecular biology of axon guidance. Review. Science 274: 1123–1133.

Tezel E, Kawase Y, Takeda S, Oshima K, Nakao A (2001): Expression of neural cell adhesion molecule in pancreatic cancer. Pancreas 22: 122–125.

Theodosis DT, Rougon G, Poulain DA (1991): Retention of embryonic features by an adult neuronal system capable of plasticity: polysialylated neural cell adhesion molecule in the hypothalamo-neurohypophysial system. Proc. Natl. Acad. Sci. U.S.A. 88: 5494–5498.

Thiery JP, Brackenbury R, Rutishauser U, Edelman GM (1977): Adhesion among neural cells of the chick embryo. II. Purification and characterization of a cell adhesion molecule from neural retina. J. Biol. Chem. 252: 6841–6845.

Thoulouze MI, Lafage M, Schachner M, Hartmann U, Cremer H, Lafon M (1998): The neural cell adhesion molecule is a receptor for rabies virus. J. Virol. 72: 7181–7190.

Togashi H, Sakisaka T, Takai Y (2009): Cell adhesion molecules in the central nervous system. Review. Cell Adh Migr 3: 29–35.

Trouillas J, Daniel L, Guigard M, Tong S, Gouvernet J, Jouanneau E, Jan M, Perrin G, Fischer G, Tabarin A, Rougon G, Figarella-Branger D (2003): Polysialylated neural cell adhesion molecules expressed in human pituitary tumors and related to extrasellar invasion. J. Neurosurg. 98: 1084–1093.

Vadlamudi RK, Bagheri-Yarmand R, Yang Z, Balasenthil S, Nguyen D, Sahin AA, den Hollander P, Kumar R (2004): Dynein light chain 1, a p21-activated kinase 1-interacting substrate, promotes cancerous phenotypes. Cancer Cell 5: 575–585.

Vagnoni A, Rodriguez L, Manser C, De Vos, Kurt J, Miller, Christopher C J (2011): Phosphorylation of kinesin light chain 1 at serine 460 modulates binding and trafficking of calsyntenin-1. J. Cell. Sci. 124: 1032–1042.

Vale RD, Reese TS, Sheetz MP (1985): Identification of a novel force-generating protein, kinesin, involved in microtubule-based motility. Cell 42: 39–50.

Vale RD (2003): The molecular motor toolbox for intracellular transport. Review. Cell 112: 467–480.

van Kammen, D P, Poltorak M, Kelley ME, Yao JK, Gurklis JA, Peters JL, Hemperly JJ, Wright RD, Freed WJ (1998): Further studies of elevated cerebrospinal fluid neuronal cell adhesion molecule in schizophrenia. Biol. Psychiatry 43: 680–686.

Vawter MP, Cannon-Spoor HE, Hemperly JJ, Hyde TM, VanderPutten DM, Kleinman JE, Freed WJ (1998): Abnormal expression of cell recognition molecules in schizophrenia. Exp. Neurol. 149: 424–432.

Vawter MP, Frye MA, Hemperly JJ, VanderPutten DM, Usen N, Doherty P, Saffell JL, Issa F, Post RM, Wyatt RJ, Freed WJ (2000): Elevated concentration of N-CAM VASE isoforms in schizophrenia. J Psychiatr Res 34: 25–34.

Vawter MP, Howard AL, Hyde TM, Kleinman JE, Freed WJ (1999): Alterations of hippocampal secreted N-CAM in bipolar disorder and synaptophysin in schizophrenia. Mol. Psychiatry 4: 467–475.

Vawter MP, Usen N, Thatcher L, Ladenheim B, Zhang P, VanderPutten DM, Conant K, Herman MM, van Kammen, D P, Sedvall G, Garver DL, Freed WJ (2001): Characterization of human cleaved N-CAM and association with schizophrenia. Exp. Neurol. 172: 29–46.

Verhey KJ, Lizotte DL, Abramson T, Barenboim L, Schnapp BJ, Rapoport TA (1998): Light chain-dependent regulation of Kinesin's interaction with microtubules. J. Cell Biol. 143: 1053–1066.

Verhey KJ, Meyer D, Deehan R, Blenis J, Schnapp BJ, Rapoport TA, Margolis B (2001): Cargo of kinesin identified as JIP scaffolding proteins and associated signaling molecules. J. Cell Biol. 152: 959–970.

Vogt L, Giger RJ, Ziegler U, Kunz B, Buchstaller A, Hermens WTJMC, Kaplitt MG, Rosenfeld MR, Pfaff DW, Verhaagen J, Sonderegger P (1996): Continuous renewal of the axonal pathway sensor apparatus by insertion of new sensor molecules into the growth cone membrane. Curr. Biol. 6: 1153–1158.

Vutskits L, Djebbara-Hannas Z, Zhang H, Paccaud JP, Durbec P, Rougon G, Muller D, Kiss JZ (2001): PSA-NCAM modulates BDNF-dependent survival and differentiation of cortical neurons. Eur. J. Neurosci. 13: 1391–1402.

Walmod PS, Pedersen MV, Berezin V, Bock E (2007): Cell adhesion molecules of the immungobulin superfamily in the nervous system. Review. In: Lajtha A (ed.), Handbook of Neurochemistry and Molecular Neurobiology. Springer 3. Aufl., 43–151.

Walmod PS, Kolkova K, Berezin V, Bock E (2004): Zippers make signals: NCAM-mediated molecular interactions and signal transduction. Neurochemical Research NEUROCHEM RES 29: 2015–2035.

Walsh FS, Doherty P (1997): Neural cell adhesion molecules of the immunoglobulin superfamily: role in axon growth and guidance. Review. Annu. Rev. Cell Dev. Biol. 13: 425–456.

Walsh FS, Furness J, Moore SE, Ashton S, Doherty P (1992): Use of the neural cell adhesion molecule VASE exon by neurons is associated with a specific down-regulation of neural cell adhesion molecule-dependent neurite outgrowth in the developing cerebellum and hippocampus. J. Neurochem. 59: 1959–1962.

Walsh FS, Parekh RB, Moore SE, Dickson G, Barton CH, Gower HJ, Dwek RA, Rademacher TW (1989): Tissue specific O-linked glycosylation of the neural cell adhesion molecule (N-CAM). Development 105: 803–811.

Weinhold B, Seidenfaden R, Röckle I, Mühlenhoff M, Schertzinger F, Conzelmann S, Marth JD, Gerardy-Schahn R, Hildebrandt H (2005): Genetic ablation of polysialic acid causes severe neurodevelopmental defects rescued by deletion of the neural cell adhesion molecule. J. Biol. Chem. 280: 42971–42977.

Wheelock MJ, Johnson KR (2003): Cadherins as modulators of cellular phenotype. Review. Annu. Rev. Cell Dev. Biol. 19: 207–235.

Wilkinson KD (2000): Ubiquitination and deubiquitination: targeting of proteins for degradation by the proteasome. Review. Semin. Cell Dev. Biol. 11: 141–148.

Williams AF, Barclay AN (1988): The immunoglobulin superfamily--domains for cell surface recognition. Review. Annu. Rev. Immunol. 6: 381–405.

Williams EJ, Furness J, Walsh FS, Doherty P (1994): Activation of the FGF receptor underlies neurite outgrowth stimulated by L1, N-CAM, and N-cadherin. Neuron 13: 583–594.

Winckler B (2004): Scientiae forum / models and speculations pathways for axonal targeting of membrane proteins. Review. Biol. Cell 96: 669–674.

Wisco D, Anderson ED, Chang MC, Norden C, Boiko T, Fölsch H, Winckler B (2003): Uncovering multiple axonal targeting pathways in hippocampal neurons. J. Cell Biol. 162: 1317–1328.

Wobst H, Förster S, Laurini C, Sekulla A, Dreiseidler M, Höhfeld J, Schmitz B, Diestel S (2012): UCHL1 regulates ubiquitination and recycling of the neural cell adhesion molecule NCAM. FEBS J. 279: 4398–4409.

Wood GK, Tomasiewicz H, Rutishauser U, Magnuson T, Quirion R, Rochford J, Srivastava LK (1998): NCAM-180 knockout mice display increased lateral ventricle size and reduced prepulse inhibition of startle. Neuroreport 9: 461–466.

Xia C, Rahman A, Yang Z, Goldstein LS (1998): Chromosomal localization reveals three kinesin heavy chain genes in mouse. Genomics 52: 209–213.

Xia C, Roberts EA, Her L, Liu X, Williams DS, Cleveland DW, Goldstein, Lawrence S B (2003): Abnormal neurofilament transport caused by targeted disruption of neuronal kinesin heavy chain KIF5A. J. Cell Biol. 161: 55–66.

Yamazaki T, Selkoe DJ, Koo EH (1995): Trafficking of cell surface beta-amyloid precursor protein: retrograde and transcytotic transport in cultured neurons. J. Cell Biol. 129: 431–442.

Yang JT, Saxton WM, Stewart RJ, Raff EC, Goldstein LS (1990): Evidence that the head of kinesin is sufficient for force generation and motility in vitro. Science 249: 42–47.

Zecchini S, Cavallaro U (2010): Neural cell adhesion molecule in cancer: expression and mechanisms. Review. In: Berezin V (ed.), Structure and Function of the Neural Cell Adhesion Molecule NCAM. Springer Sciences, 319–333.

Zhang H, Vutskits L, Calaora V, Durbec P, Kiss JZ (2004): A role for the polysialic acid-neural cell adhesion molecule in PDGF-induced chemotaxis of oligodendrocyte precursor cells. J. Cell. Sci. 117: 93–103.

Zhang H, Webb DJ, Asmussen H, Niu S, Horwitz AF (2005): A GIT1/PIX/Rac/PAK signaling module regulates spine morphogenesis and synapse formation through MLC. J. Neurosci. 25: 3379–3388.

Zhou H, Fuks A, Alcaraz G, Bolling TJ, Stanners CP (1993): Homophilic adhesion between Ig superfamily carcinoembryonic antigen molecules involves double reciprocal bonds. J. Cell Biol. 122: 951–960.

Zhu H, Lee HY, Tong Y, Hong B, Kim K, Shen Y, Lim KJ, Mackenzie F, Tempel W, Park H (2012): Crystal structures of the tetratricopeptide repeat domains of kinesin light chains: insight into cargo recognition mechanisms. PLoS ONE 7: e33943.

Appendix

Vector map of pGEX-4T-2/hNCAM140ID

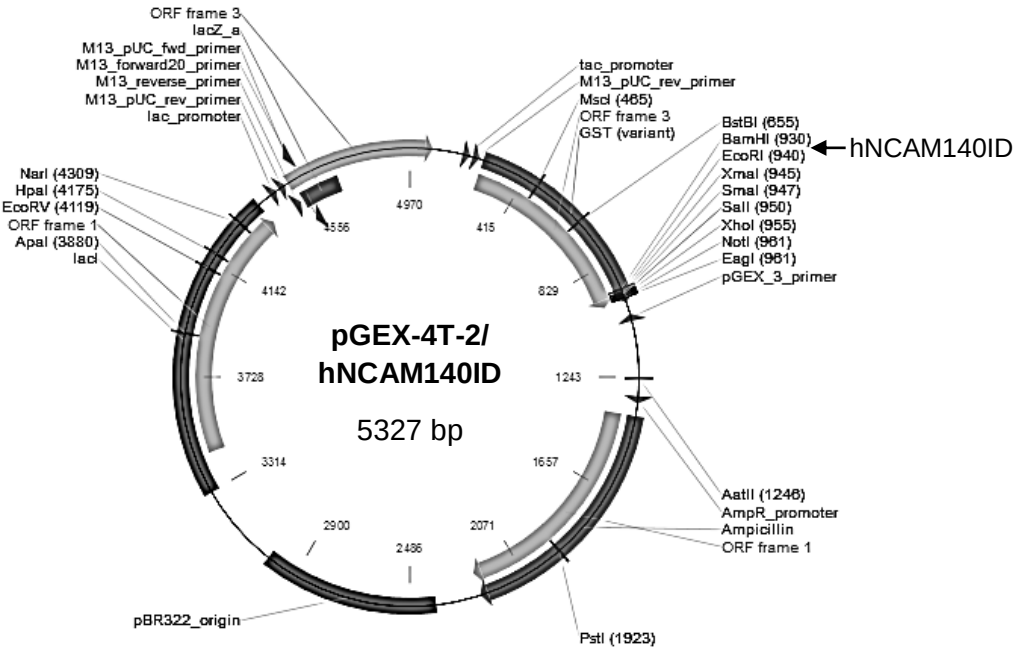

The cDNA of hNCAM140ID was restricted from pcDNA3/hNCAM140ID with *Bam*HI and *EcoRI* and inserted in frame in the pGEX-4T-2 vector.

Danksagung

Bei Frau Professorin Dr. Schmitz bedanke ich mich herzlich für die Überlassung des interessanten Themas, ihre ständige Unterstützung und eine lehrreiche und schöne Zeit in der Biochemie. Herrn Prof. Dr. Höhfeld danke ich für die Übernahme des Zweitgutachtens und die Möglichkeit, den Protein Macroarray in seiner Abteilung durchzuführen. Den weiteren Mitgliedern der Promotionskommission danke ich für die Übernahme ihres Amtes.

Mein besonderer Dank gilt Herrn Dr. Vladimir Sytnyk und Frau Dr. Iryna Leshchyns'ka für die Möglichkeit ein Forschungsjahr in ihrer Abteilung zu verbringen und die ausgezeichnete Betreuung. Für die Finanzierung dieser Zeit danke ich dem DAAD.

Der gesamten Arbeitsgruppe der „alten" Biochemie und heutigen Human Metabolomics danke ich aus vollem Herzen für eine unvergessliche Doktorandenzeit, in der ich nicht nur auf eine herzliche und kollegiale Atmosphäre getroffen bin, sondern auch auf Unterstützung in sämtlichen Lebenslagen. Besonders bedanke ich mich bei Frau PD Dr. Simone Diestel für ihre Hilfsbereitschaft, ihre Geduld und die exzellente, jahrelange Betreuung. Frau Sarah Förster danke ich für all die Antworten auf meine Fragen, den Zusammenhalt und die tolle Stimmung in unserem Büro. Frau Christine Laurini und den „Mastermädels" danke ich für ihre Herzlichkeit und fröhliche Art.

Besonders möchte ich mich bei meinem Freund Uli, bei meiner Familie und insbesondere bei meinen Eltern für ihre Unterstützung in jeglicher Hinsicht bedanken.

Ausschlusserklärung

Hiermit erkläre ich, die vorliegende Arbeit selbstständig verfasst und keine anderen als die hier angegebenen Hilfsmittel benutzt, sowie alle Stellen der Arbeit, die anderen Werken im Wortlaut oder Sinn nach entnommen sind, kenntlich gemacht zu haben.

Bonn, 14.08.2014

Hilke Johanna Wobst